Module 1

Background: Making sounds in the sea

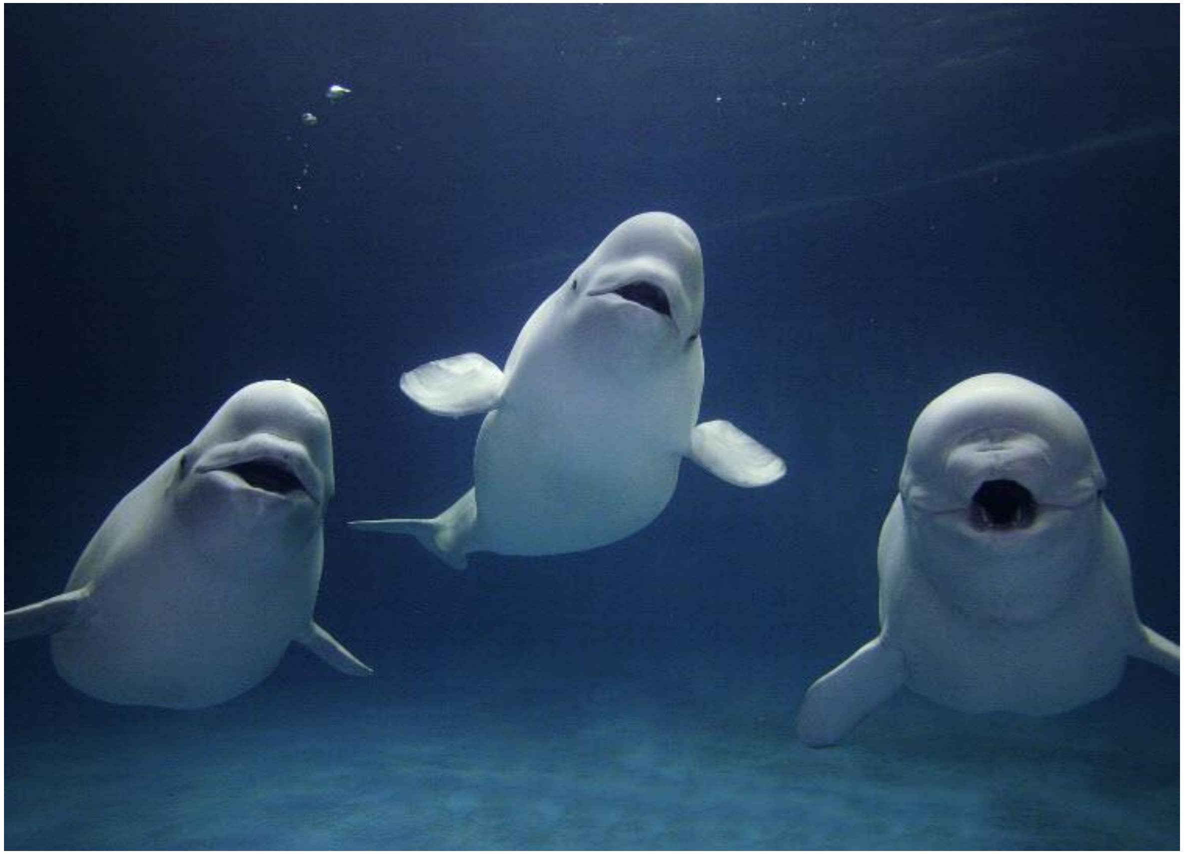

NTNU
Norwegian University of Science and Technology

Martin Landrø and Lasse Amundsen

Air gun – the most common marine seismic source

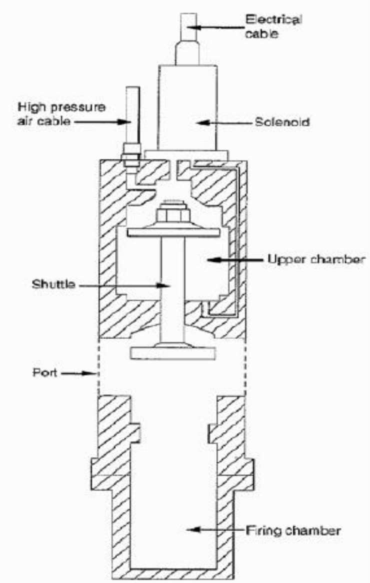

Figur 4.11: Viser bildet av en BOLT luftkanon med luftkammeret nederst og solenoiden på toppen. Stempelet beveger seg hurtig oppover idet kanonen avfyres, slik at lufta slipper ut gjennom de fire portåpningene. Til høyre vises et skjematisk snitt av luftkanonen.

Stephen Chelminski founded Bolt Technology in 1970 and patented the air gun in 1975 – received the Kauffman award in 1975

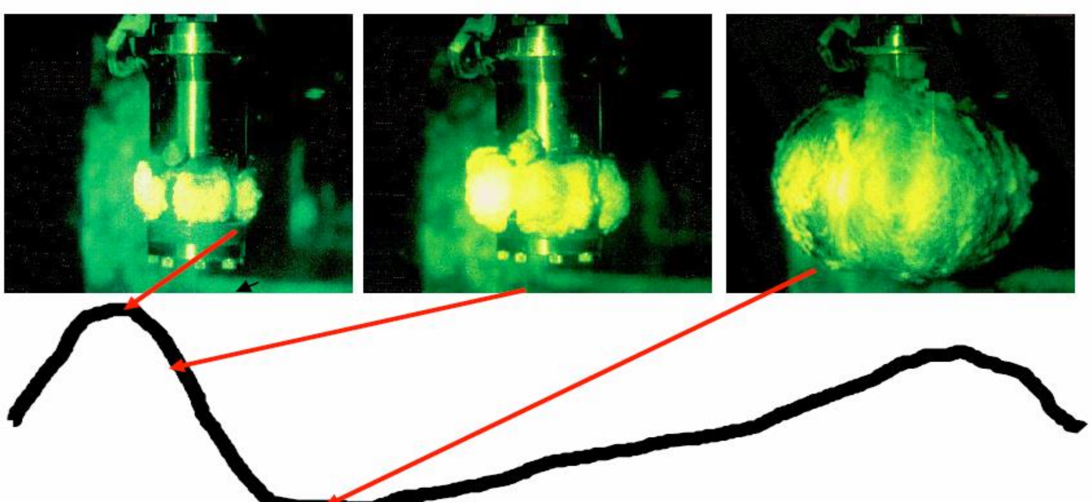

The peak signal is generated when the bubble is small – the bubble oscillates several times before it breakes the water surface – bubble period is dependent on volume, gun depth and firing pressure

Rayleigh's equation (1917)

$$\boxed{R\ddot{R} + \frac{3}{2}\dot{R}^2 = \frac{p - p_\infty}{\rho}}$$

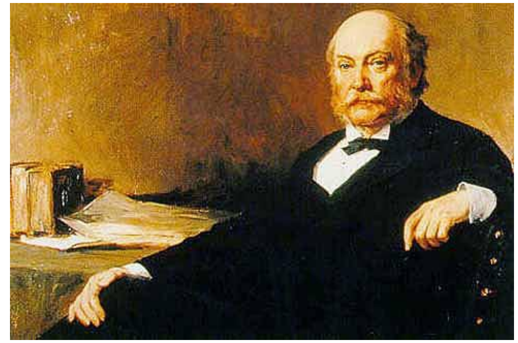

Studied the sound emitted when water is boiling => collapse

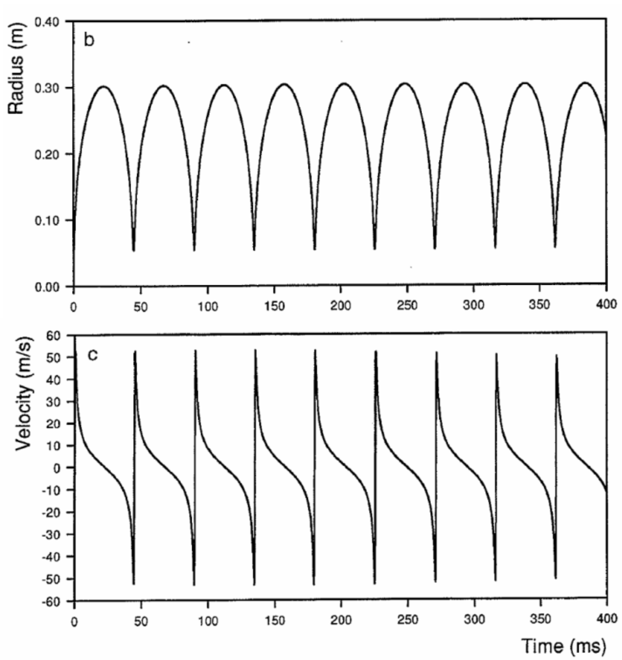

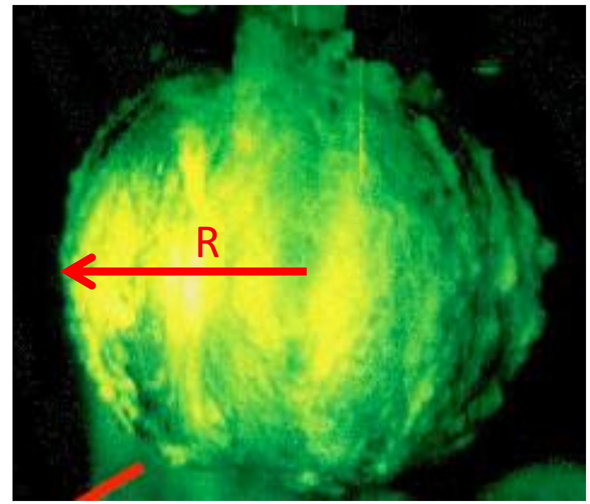

Kirkwood and Bethe (1942)

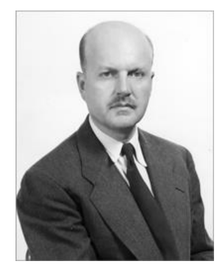

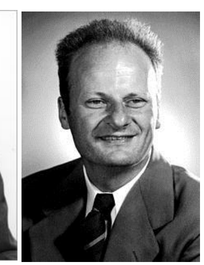

$$\boxed{R\ddot{R}\left(1 - \frac{\dot{R}}{C}\right) + \frac{3}{2}\dot{R}^2\left(1 - \frac{\dot{R}}{3C}\right) = H\left(1 + \frac{\dot{R}}{C}\right) + R\frac{\dot{H}}{C}\left(1 - \frac{\dot{R}}{C}\right)}$$

Rayleigh's paper from Phil. Mag. 34, 1917:

VIII. *On the Pressure developed in a Liquid during the Collapse of a Spherical Cavity.* *By* Lord RAYLEIGH, *O.M., F.R.S.**

WHEN reading O. Reynolds's description of the sounds emitted by water in a kettle as it comes to the boil, and their explanation as due to the partial or complete collapse of bubbles as they rise through cooler water, I proposed to myself a further consideration of the problem thus presented; but I had not gone far when I learned from Sir C. Parsons that he also was interested in the same question in connexion with cavitation behind screw-propellers, and that at his instigation Mr. S. Cook, on the basis of an investigation by Besant, had calculated the pressure developed when the collapse is suddenly arrested by impact against a rigid concentric obstacle. During the collapse the fluid is regarded as incompressible.

Rayleigh studied the collapse and sound generated by water vapor cavities in boiling water

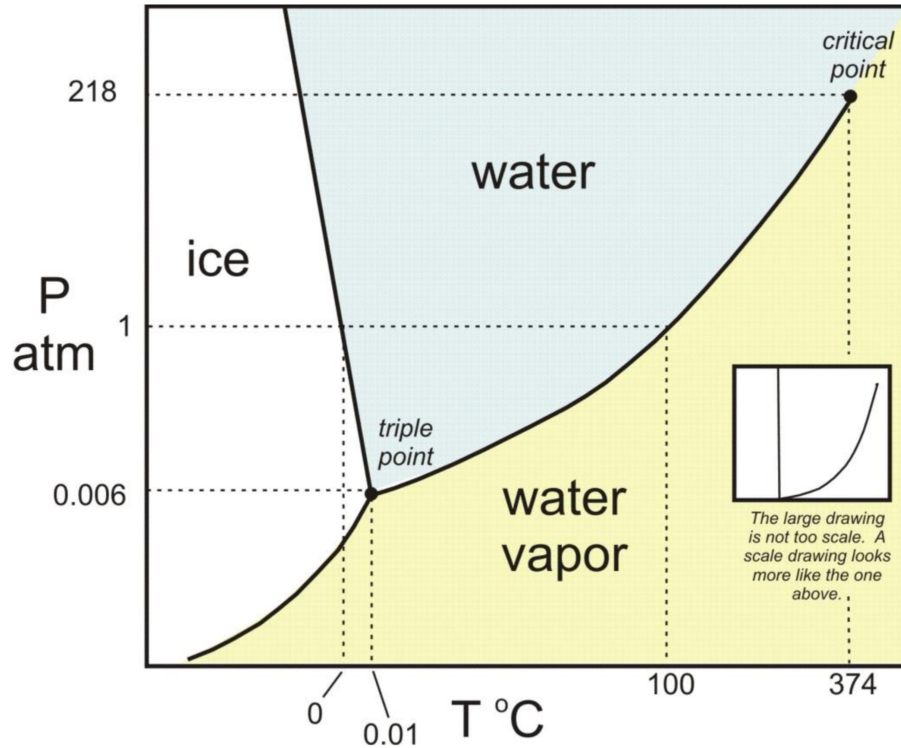

Striking similarity between boiling water and air gun bubbles

$$u/\mathrm{U}=\mathrm{R}^2/r^2; \quad . \quad . \quad . \quad . \quad . \quad . \quad . \qquad (1)$$

and if ρ be the density, the whole kinetic energy of the motion is

$$\tfrac{1}{2}\rho\int_{\mathrm{R}}^{\infty} u^2 \,.\, 4\pi r^2\, dr=2\pi\rho\mathrm{U}^2\mathrm{R}^3. \quad . \quad . \quad . \qquad (2)$$

Again, if P be the pressure at infinity and R_0 the initial value of R, the work done is

$$\frac{4\pi\mathrm{P}}{3}(\mathrm{R}_0{}^3-\mathrm{R}^3). \quad . \quad . \quad . \quad . \quad . \quad . \quad . \qquad (3)$$

When we equate (2) and (3) we get

$$\mathrm{U}^2=\frac{2\mathrm{P}}{3\rho}\left(\frac{\mathrm{R}_0{}^3}{\mathrm{R}^3}-1\right), \quad . \quad . \quad . \quad . \quad . \quad . \quad . \qquad (4)$$

expressing the velocity of the boundary in terms of the radius. Also, since $\mathrm{U}=d\mathrm{R}/dt$,

$$t=\sqrt{\left(\frac{3\rho}{2\mathrm{P}}\right)}\cdot\int_{\mathrm{R}}^{\mathrm{R}_0}\frac{(\mathrm{R}^{3/2}d\mathrm{R}}{(\mathrm{R}_0{}^3-\mathrm{R}^3)^{\frac{1}{2}}}=\mathrm{R}_0\sqrt{\left(\frac{3\rho}{2\mathrm{P}}\right)}\cdot\int_{\beta}^{1}\frac{\beta^{3/2}d\beta}{(1-\beta^3)^{\frac{1}{2}}} \quad . \quad . \quad . \qquad (5)$$

if $\beta=\mathrm{R}/\mathrm{R}_0$. The time of collapse to a given fraction of

Writing $\beta^3 = z$, we have

$$\int_0^1 \frac{\beta^{3/2}\,d\beta}{(1-\beta^3)^{\frac{1}{2}}} = \tfrac{1}{3}\int_0^1 z^{-\frac{1}{6}}(1-z)^{-\frac{1}{2}}\,dz,$$

which may be expressed by means of Γ functions. Thus

$$\tau = \mathrm{R}_0\sqrt{\left(\frac{\rho}{6\mathrm{P}}\right)}\cdot\frac{\Gamma(\frac{5}{6})\,.\,\Gamma(\frac{1}{2})}{\Gamma(\frac{4}{3})} = \cdot 91468\,\mathrm{R}_0\sqrt{(\rho/\mathrm{P})}. \quad . \quad (6)$$

THE JOURNAL OF THE ACOUSTICAL SOCIETY OF AMERICA VOLUME 24, NUMBER 6 NOVEMBER, 1952

An Experimental Study of Single Bubble Cavitation Noise*

MARK HARRISON
David Taylor Model Basin, Department of the Navy, Washington 7, D. C.

(Received May 23, 1952)

An experimental study of the noise produced by a single cavitation bubble has been made. The noise consists principally of a transient pressure pulse associated with the collapse of the bubble. The motion of the bubble has been photographed simultaneously with the measurement of the pressure pulse.

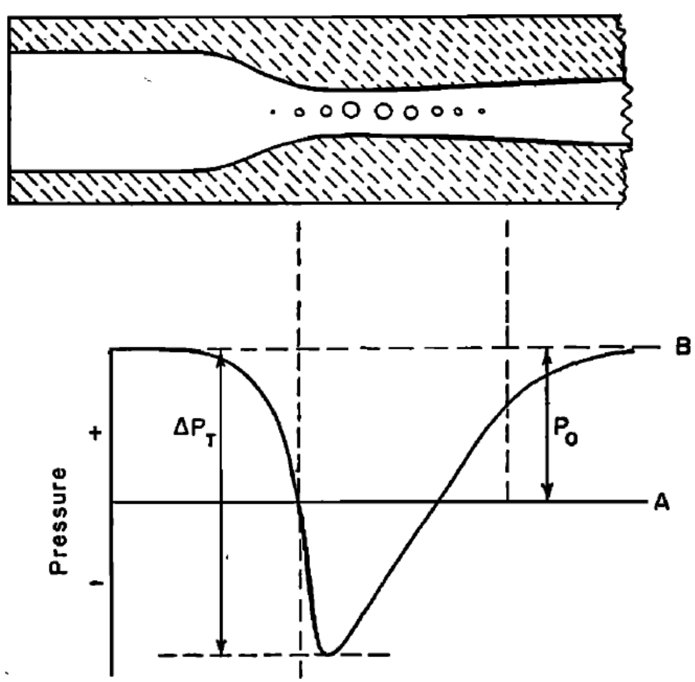

FIG. 3. Sketch of the pressure in the venturi nozzle; the history of a single bubble is illustrated.

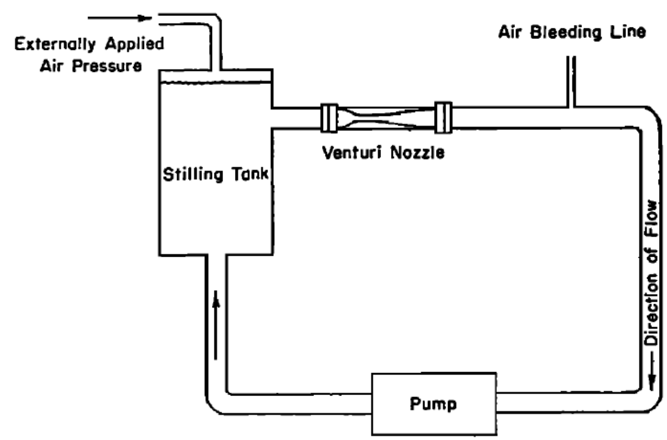

Cavities formed close to air bubbles injected into the water – for small air bubbles (not visible) the vapor cavity collapsed completely =>

Observed cavity and comparison with the Rayleigh formula

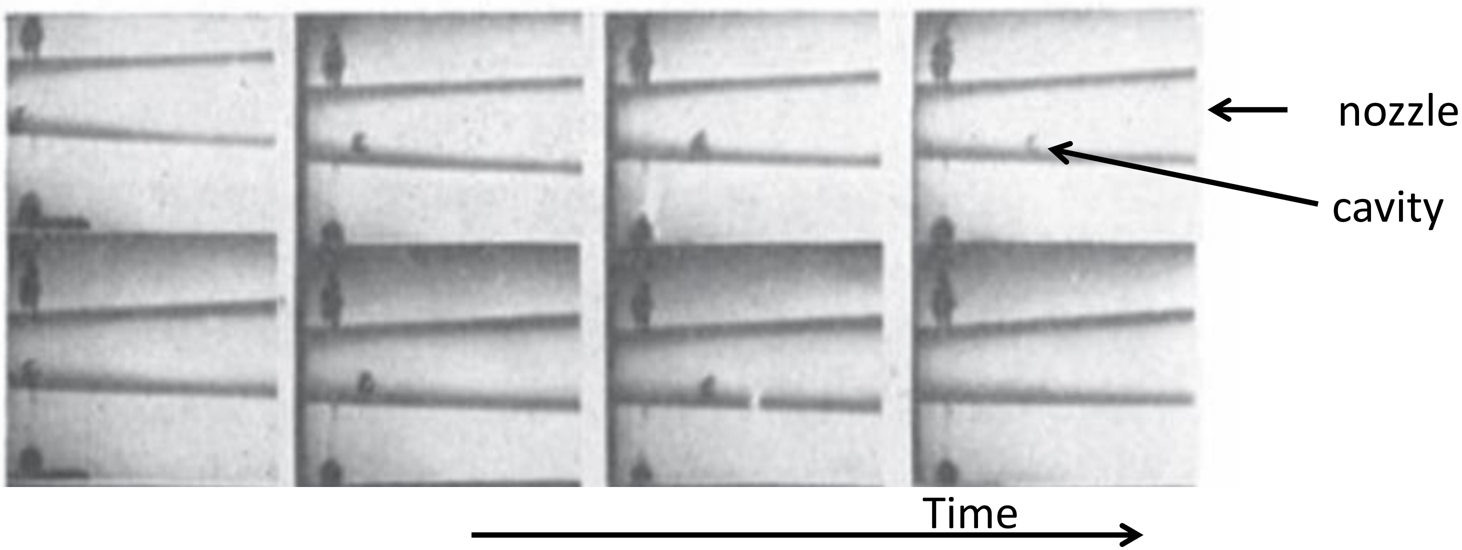

$$t=\sqrt{\left(\frac{3\rho}{2P}\right)}\cdot\int_{R}^{R_0}\frac{(R^{3/2}dR}{(R_0^{3}-R^{3})^{\frac{1}{2}}}=R_0\sqrt{\left(\frac{3\rho}{2P}\right)}\cdot\int_{\beta}^{1}\frac{\beta^{3/2}d\beta}{(1-\beta^{3})^{\frac{1}{2}}}$$

Rayleigh's collapse time formula fits the experimental data

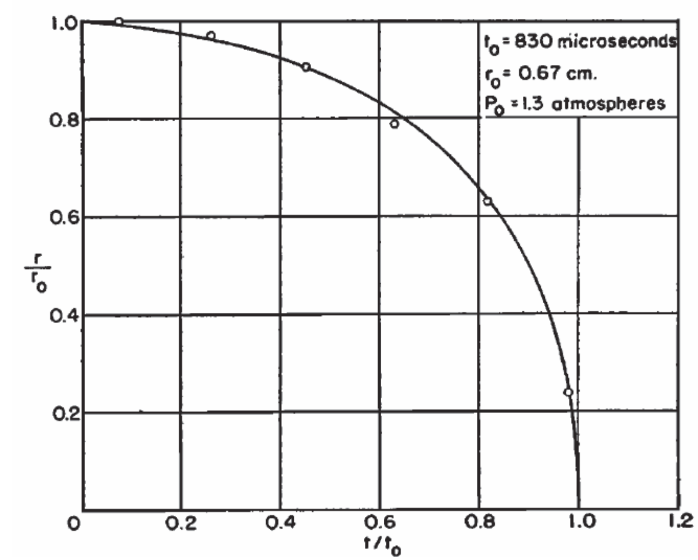

Gilmore (1952):

$$p - p_\infty = \rho_\infty \frac{R}{r}\left(H + \frac{\dot{R}^2}{2}\right)$$

Enthalpy at bubble wall: $$H = \int \frac{dp}{\rho}$$

=> If H and R are known, we can find the relative pressure signal

Anton Ziolkowski (1970) formulated a method for calculating the output pressure waveform from an air gun (Geophys. J. Roy. Astr. Soc., **21**, 137-161)

Milton Plesset teaching on «collapse of cavities»

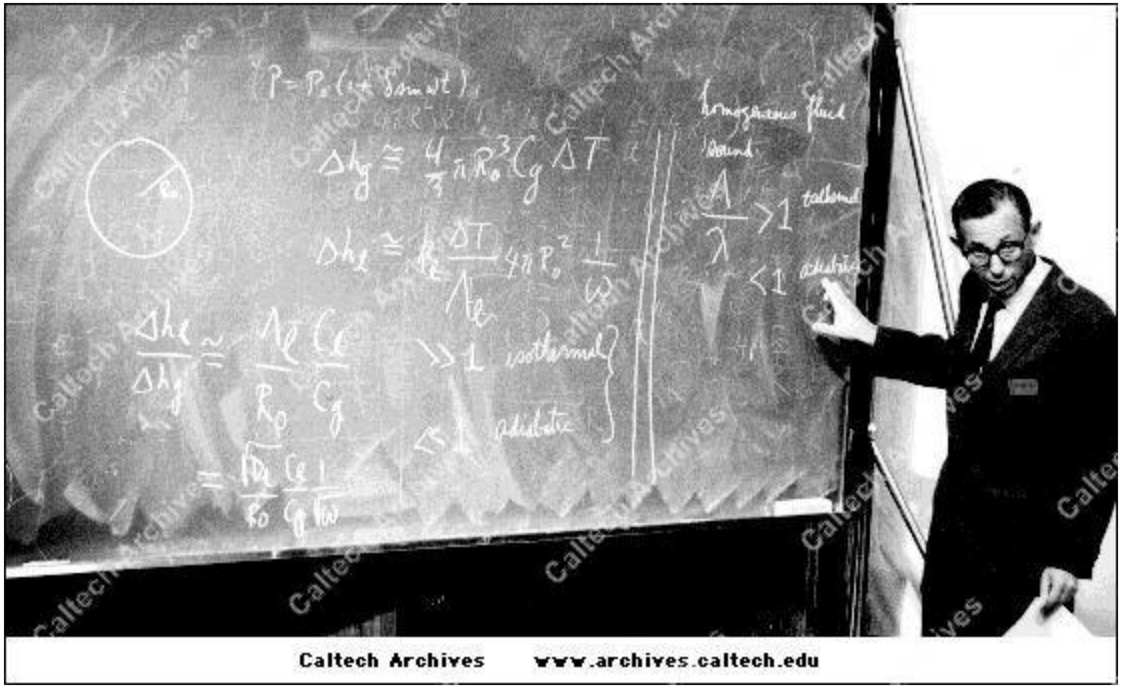

J. Fluid Mech. (1971), *vol.* 47, *part* 2, *pp.* 283–290 283
Printed in Great Britain

Collapse of an initially spherical vapour cavity in the neighbourhood of a solid boundary

By MILTON S. PLESSET AND RICHARD B. CHAPMAN
California Institute of Technology

J. Fluid Mech. (1971), *vol.* 47, *part* 2, *pp.* 283–290
Printed in Great Britain

Collapse of an initially spherical vapour cavity in the neighbourhood of a solid boundary

By MILTON S. PLESSET AND RICHARD B. CHAPMAN
California Institute of Technology

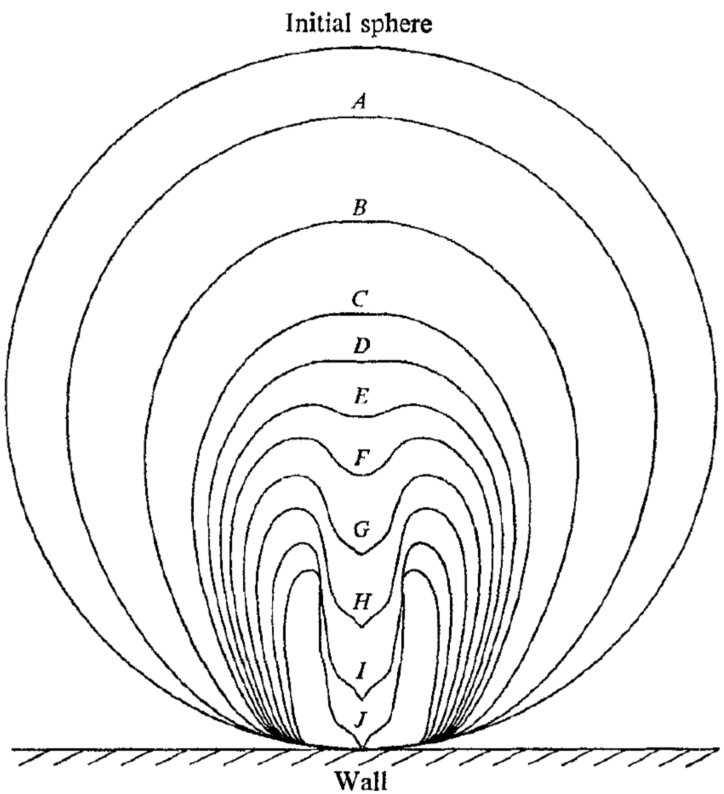

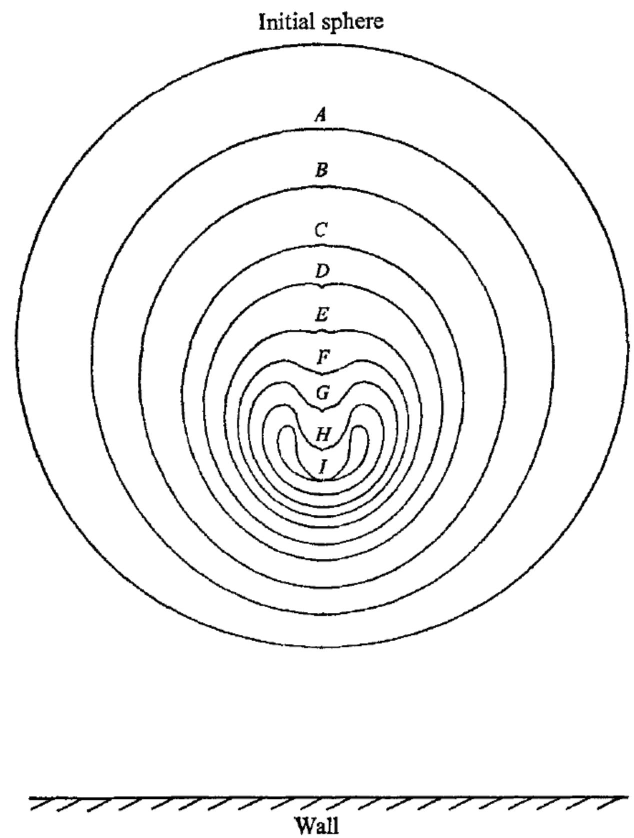

Figure 2. Bubble surfaces from case 2.

Milton Plesset in Copenhagen - 1934

Milton Plesset, Niels Bohr, Fritz Kalckar, Edward Teller and Otto Robert Frisch at the Institute for Theoretical Physics in Denmark, 1934.

Congress in Copenhagen 1934 (?)

N. Bohr, P.A.M. Dirac, W. Heisenberg, P. Ehrenfest, M. Delbruck, L. Meitner

Otto Robert Frisch (1904-1979)

- Lise Meitner was his aunt
- Left to London in **1933**
- 5 years in Copenhagen
- In **1938** Lise got a mail from Otto Hahn reporting that barium was a biproduct if neutrons collided with uranium. Frisch and Meitner interpreted this as splitting of the uranium nucleus. Frisch denoted this as ***fission.***
- At Los Alamos Frisch becomes leader of the «Critical Assemblies group» – to determine the exact amount of enriched uranium which would sustain a nuclear reaction…
- He did this by stacking several 3 cm bars of uranium hydride at a time and measuring rising neutron activity….
- One day he almost caused a runaway reaction – of the corner of his eye he saw the red lamps flickering – realizing what was happening he scattered the bars with his hands. Later he found that this dose was quite harmless, but if he had waited another 2 seconds it would have been fatal….
- This experiment was used to determine the exact mass of uranium required for the Hiroshima bomb.
- Returned to England in **1946**

Otto Robert Frisch

Otto Robert Frisch's wartime Los Alamos ID badge photo.

Born	1 October 1904 Vienna, Austria
Died	22 September 1979 (aged 74)
Nationality	Austrian/British
Fields	physics
Known for	atomic bomb
Influences	Rudolf Peierls
Notable awards	Fellow of the Royal Society

Signature

Lise Meitner (1878-1968)

- Meitner is often mentioned as one of the most glaring examples of women's scientific achievement overlooked by the Nobel committee
- Meitner also first realized that Einstein's famous equation, $E = mc^2$, explained the source of the tremendous releases of energy in nuclear fission, by the conversion of rest mass into kinetic energy, popularly described as the conversion of mass into energy.
- Meitner refused an offer to work on the project at Los Alamos, declaring "I will have nothing to do with a bomb!"[28] Meitner said that Hiroshima had come as a surprise to her, and that she was *"sorry that the bomb had to be invented*."[29]

Nearfield and farfield signatures of a single (40 cu.in.) air gun

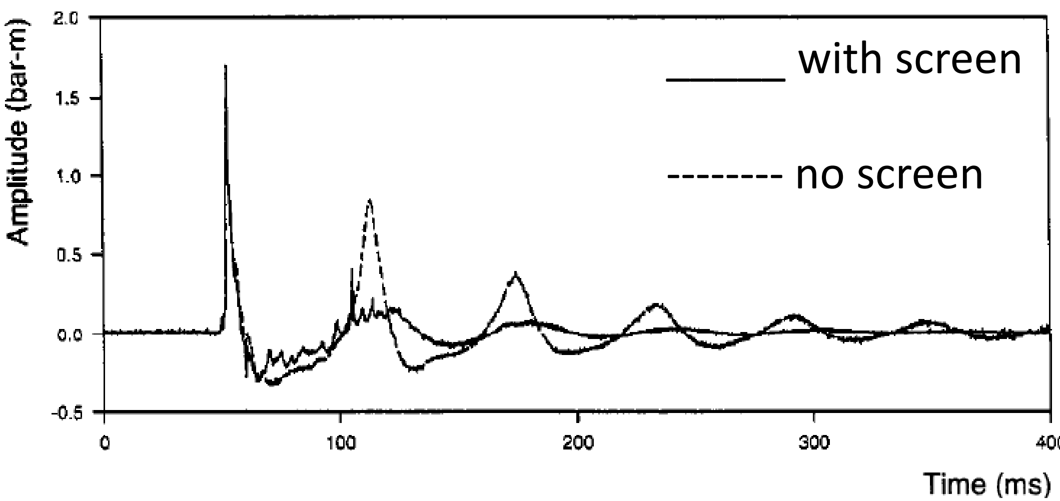

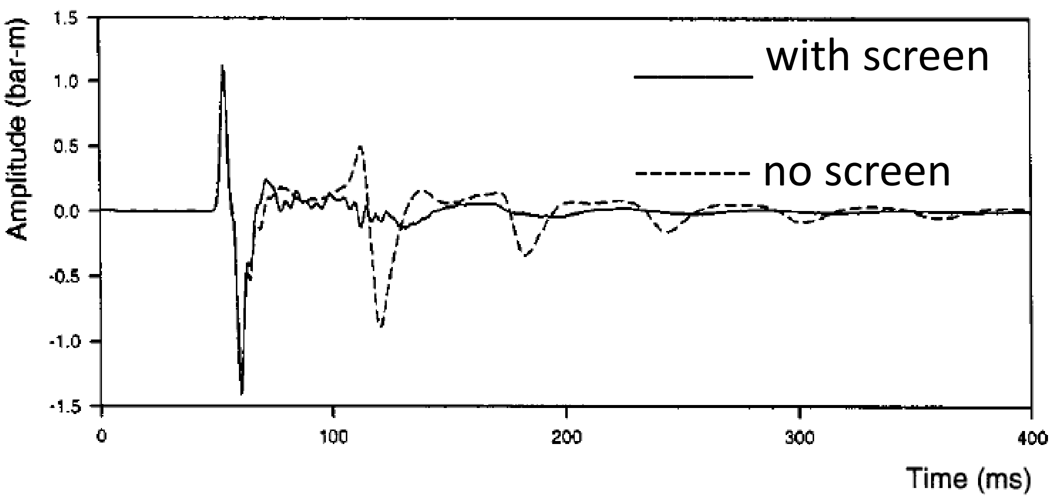

Amplitude damping from primary to first, second and third bubble…

WHY?

- **Irrotational water motion**
- **Temperature effects**
- **Transport of water vapor across the bubble wall**
- **Viscosity**
- **Bubble is gradually loosing air**
- **……**

Characteristics of a far field source signature

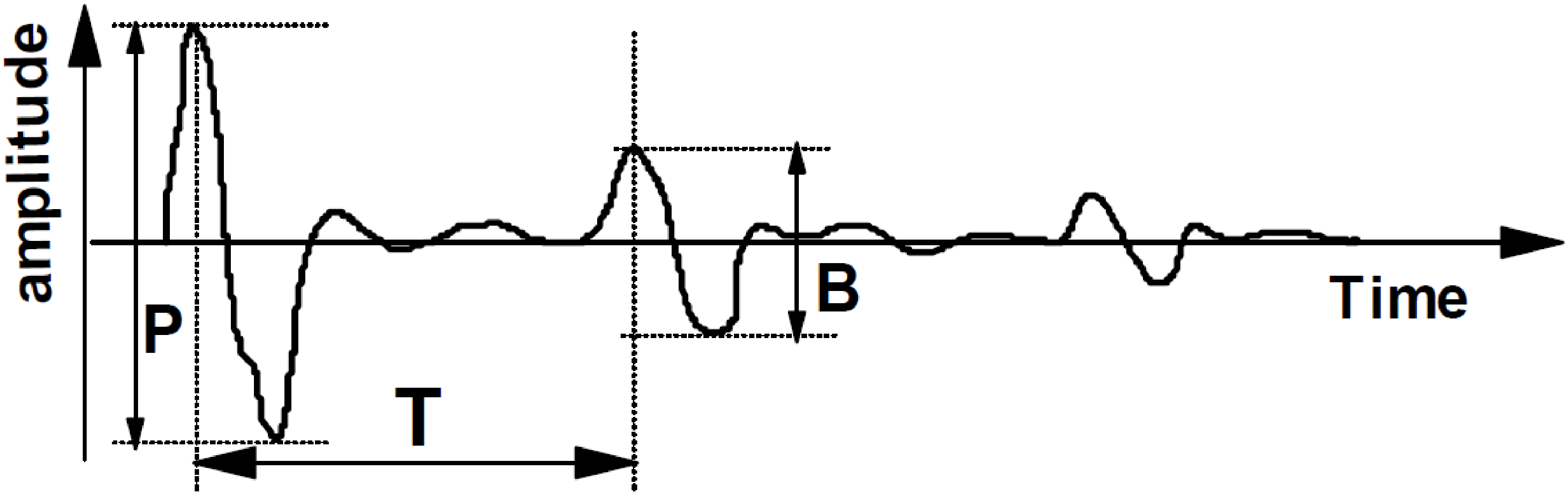

Primary to bubble ratio: P/B
Bubble time period: T

P/B-ratio is frequency-dependent!

Some empirical relations:

Nooteboom, 1978 – bubble time period: $T \propto \dfrac{P^{1/3}V^{1/3}}{P_h^{5/6}}$

Nooteboom, 1978 – Amplitude: $A \sim P^{2/3}$

NN – Amplitude: $A \sim V^{1/3}$

Experimental tank experiment used in Jan Langhammer's PhD thesis:

a)

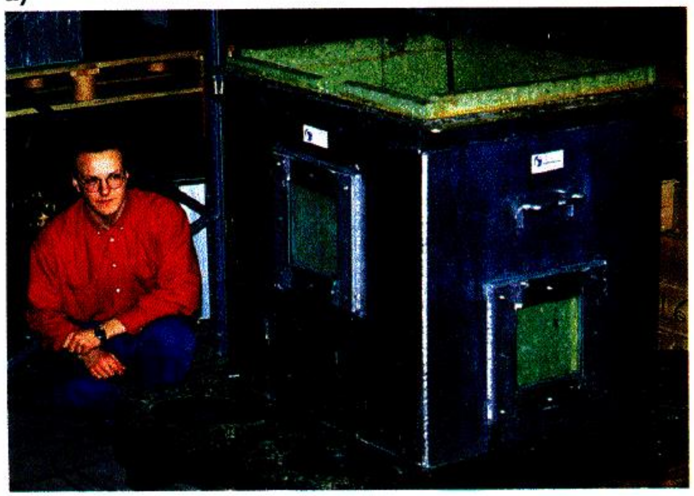

b)

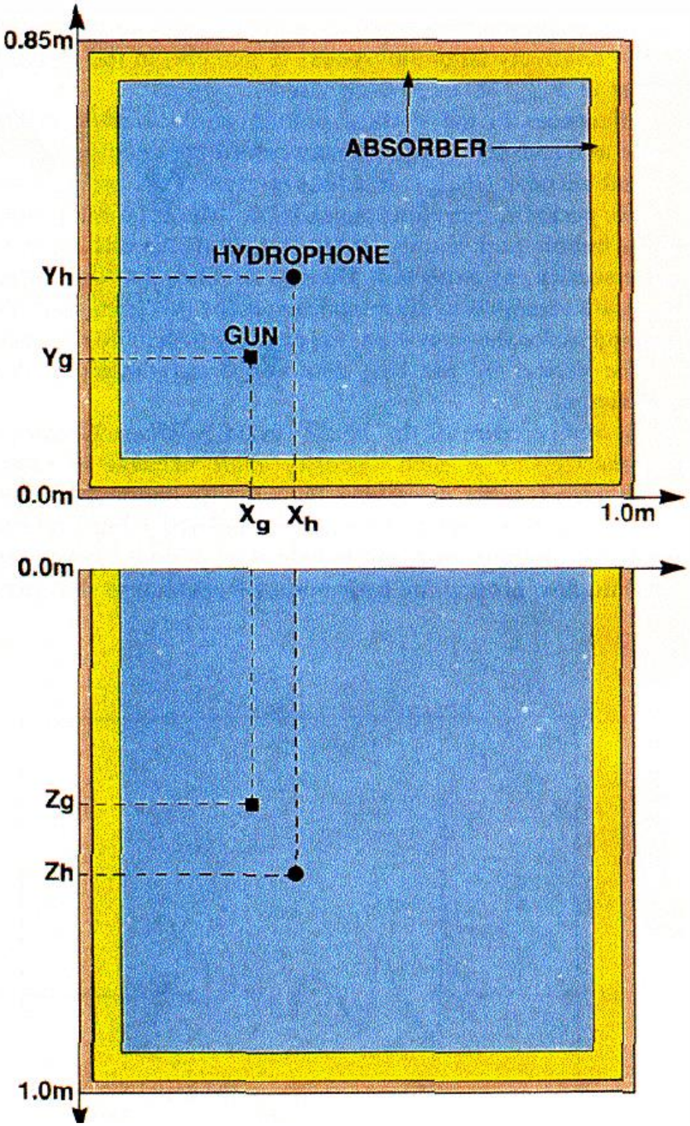

Filming of a small air gun in a water tank

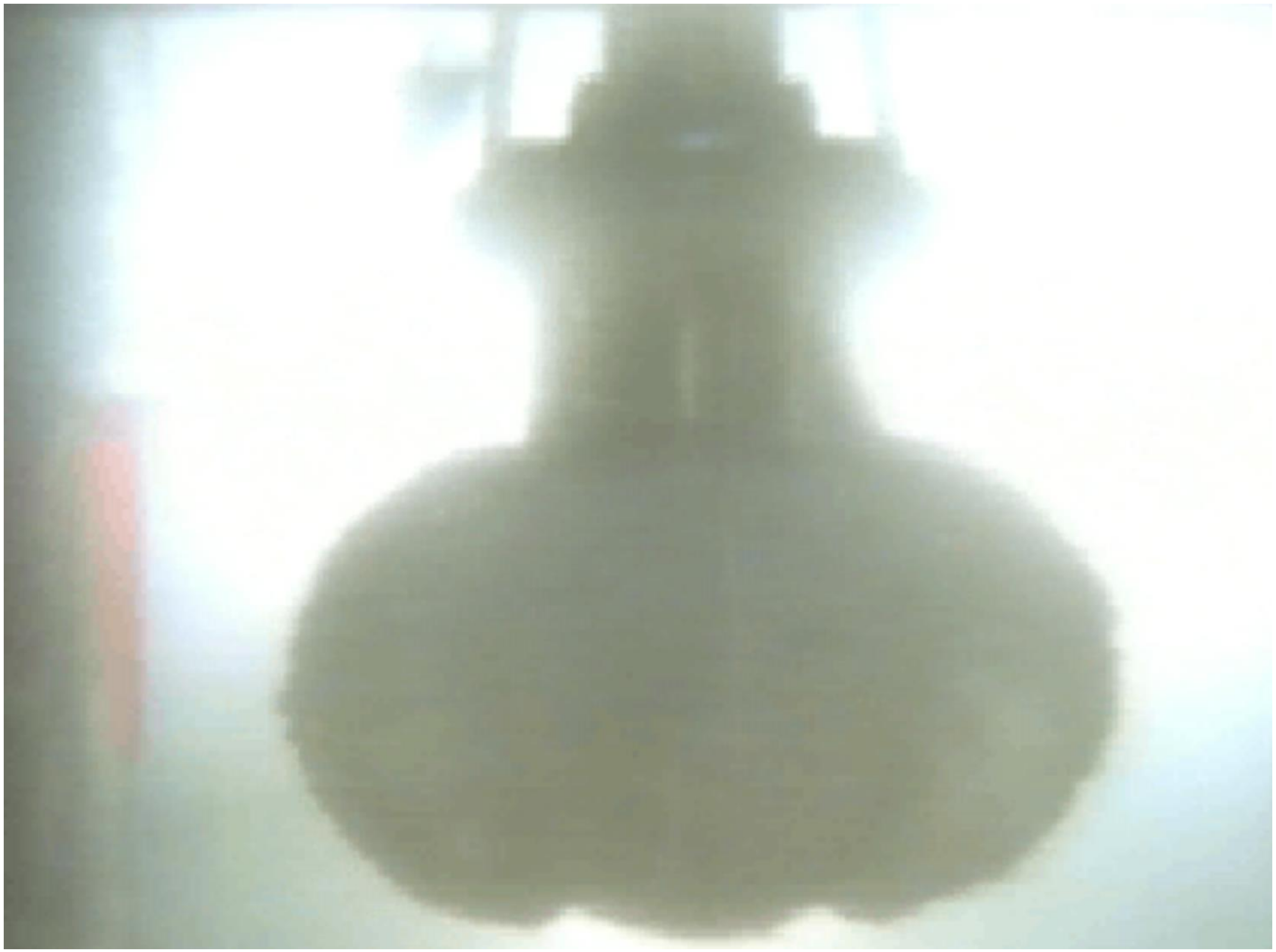

Jan Langhammer and Martin Landrø, 1991

Snapshots from above

Langhammer and Landrø, Geophysical Prospecting, 1996

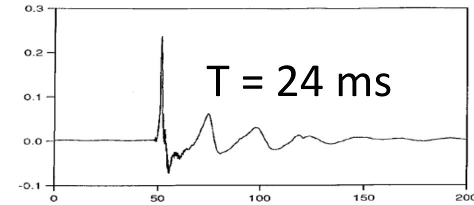

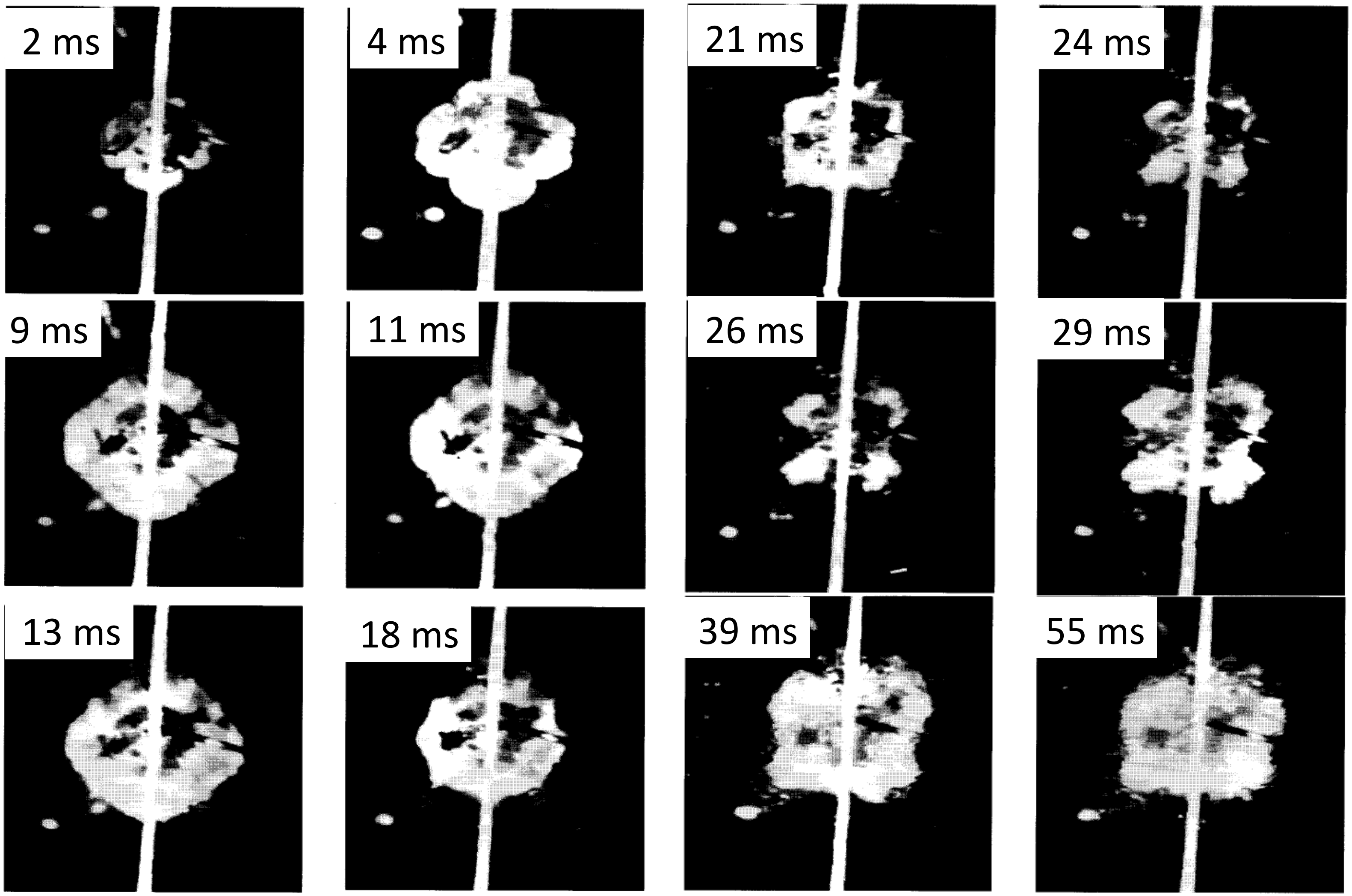

Notice the 45 degree rotation of the bubble system between primary and bubble

Upward movement of the bubble

$$U_{\mathrm{d}} = \frac{2g}{R^3}\int_0^t R^3 \mathrm{d}t,$$

Herring, 1941; Taylor, 1942

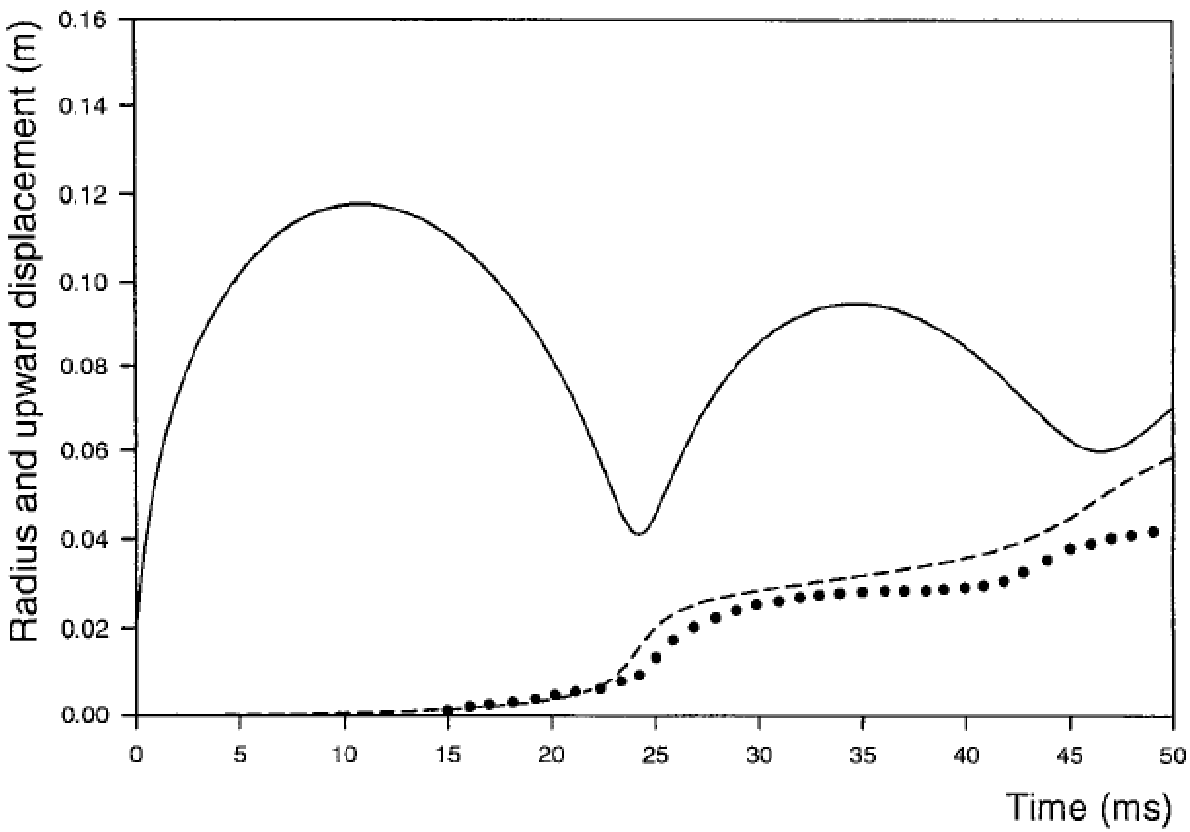

Figure 6. Modelled bubble radius (solid line) and modelled upward displacement (dashed line). The dots mark the upward displacement of the bubble centre estimated from high-speed filming.

Langhammer and Landrø, Geophysical Prospecting, 1996

Comparing near-filed measurements in a tank with free field

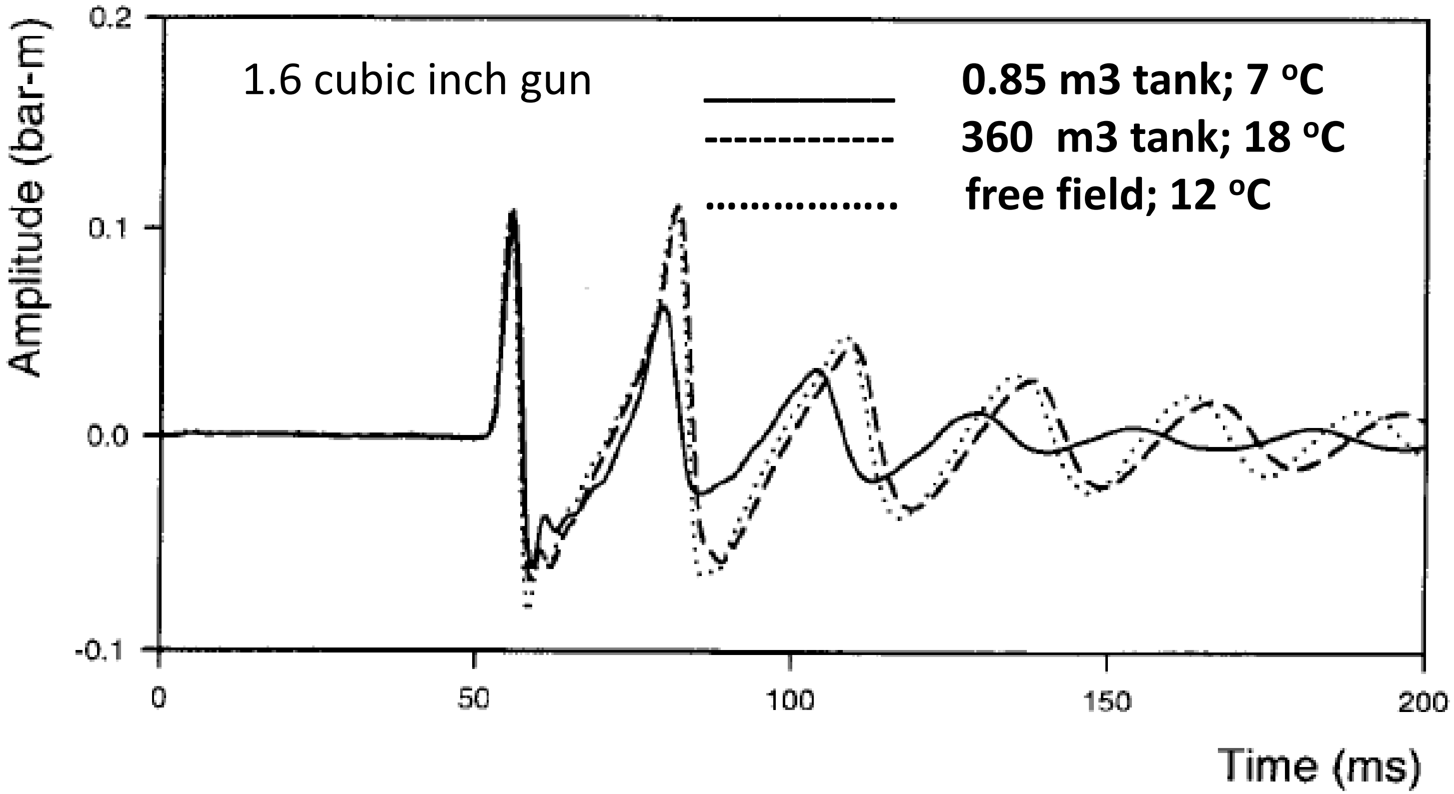

The difference between the big tank and the free field is probably a temperature effect

The bubble time period is shorter for the tank experiment - however, the deviation is too big to be explained by temperature ??

Experimental study of viscosity effects on air-gun signatures

Jan Langhammer* and Martin Landro‡

Geophysics, 1993, 58, 1801-1808

Bornhorst and Hatsopoulos (1967):

$$\ddot{R} = \frac{P_a - P_\infty}{R\rho} - \frac{3}{2}\frac{\dot{R}^2}{R} - \frac{2\sigma}{R^2\rho} - \frac{4\mu\dot{R}}{R^2\rho}$$

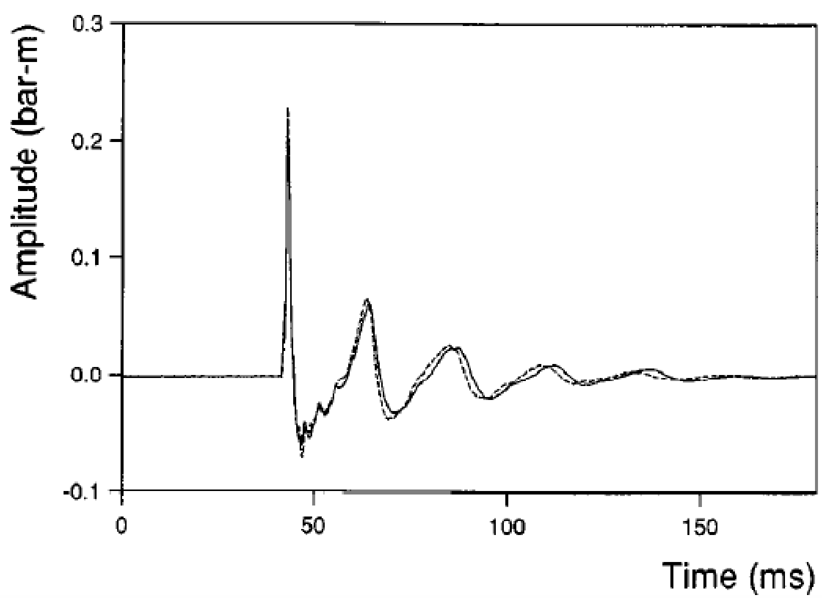

FIG. 3. Unfiltered signatures when the gun was fired in a liquid with viscosities of 6 centipoise (solid line) and 489 centipoise (dashed line).

a)

b)

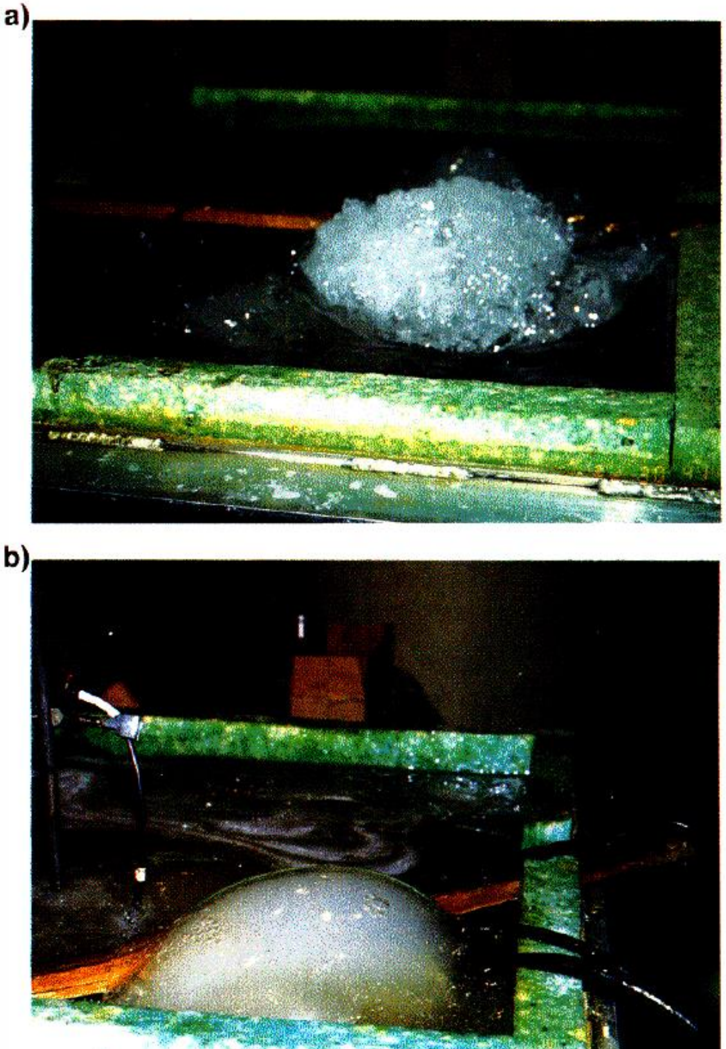

P/B-ratio and bubble time period decrease with increasing viscosity

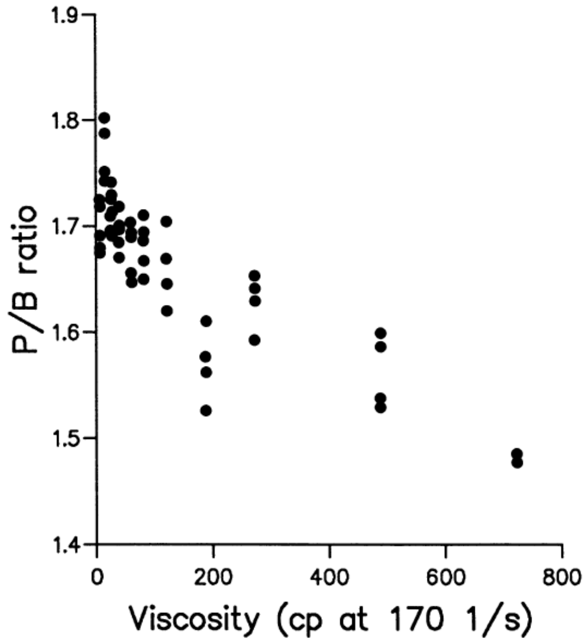

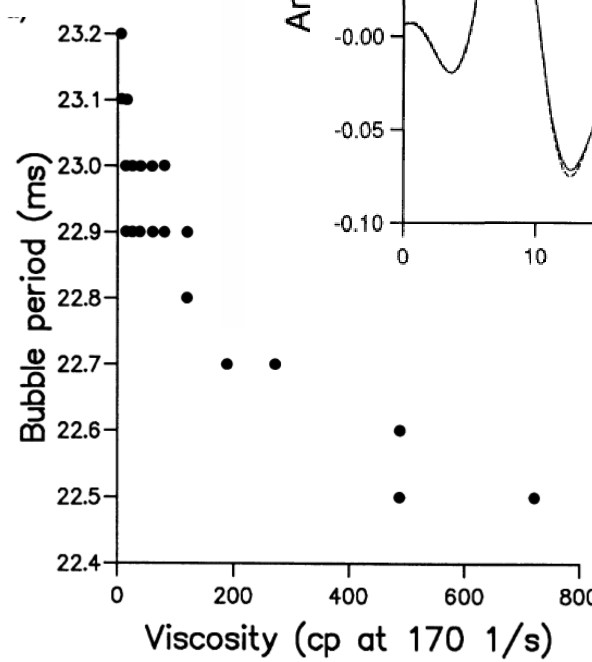

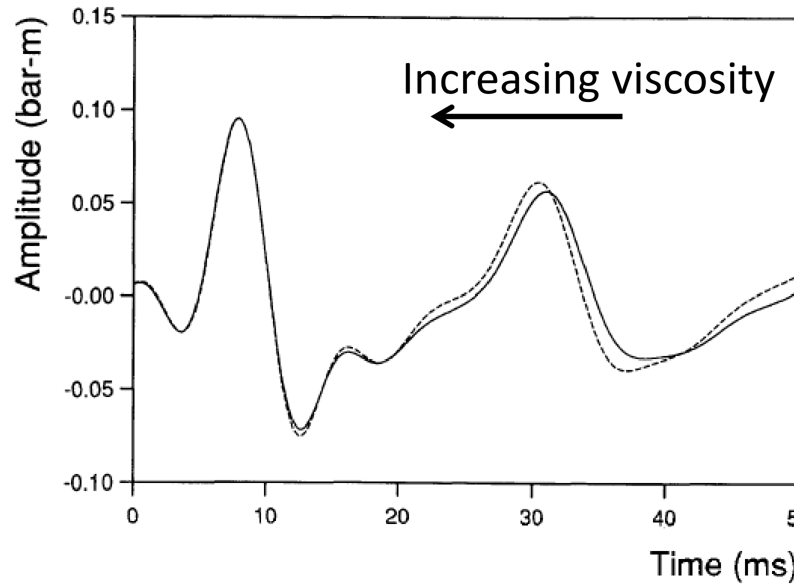

Viscosity is NOT the main energy loss mechanism for air gun bubble damping

TEMPERATURE EFFECTS ON AIRGUN SIGNATURES[1]

JAN LANGHAMMER[2,3] and MARTIN LANDRØ[3]

Geophysical Prospecting **41,** 737–750, 1993

Schrage, 1953 proposed the following mass transfer formula (water vapour across the bubble wall)

$$\dot{n} = \sigma \sqrt{\frac{1}{2\pi R_g M_w}} \left(\frac{p_{sv}(T_\infty)}{\sqrt{T_\infty}} - \frac{p_v(T_b)}{\sqrt{T_b}} \right) A,$$

n = mol of evaporated or condensed water
Psv = Saturated water pressure
Pv = partial pressure of vapour in the bubble
A = Area of bubble surface

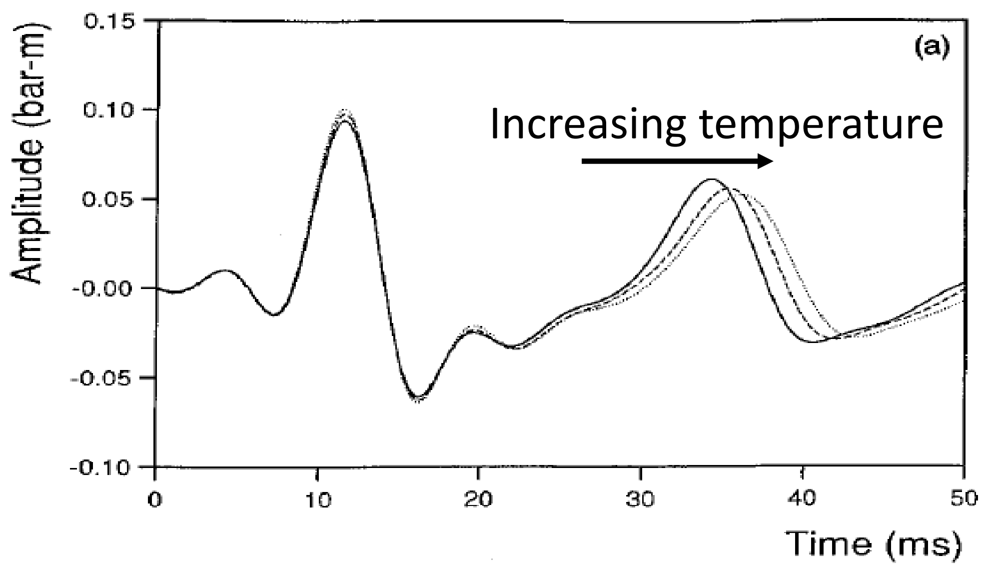

Measured near-field signatures for 5 (solid) 29 (dashed) and 44 (dotted) centigrades water temperature

Bubble period and P/B-ratio increases with increasing temperature

Bubble time period and P/B-ratio increases with water temperature

0.6 % change in P/B-ratio per centigrade

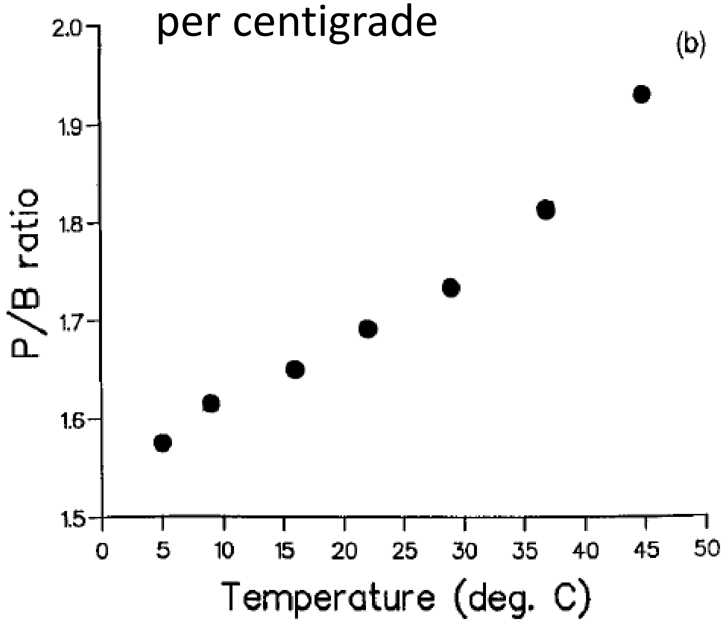

0.2 % change in bubble period per centigrade

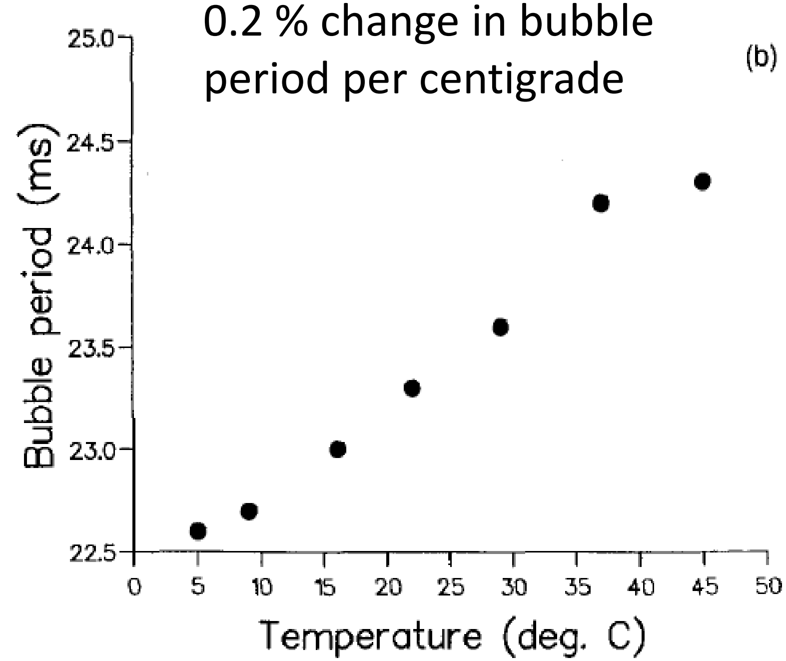

Methods to improve the source signature

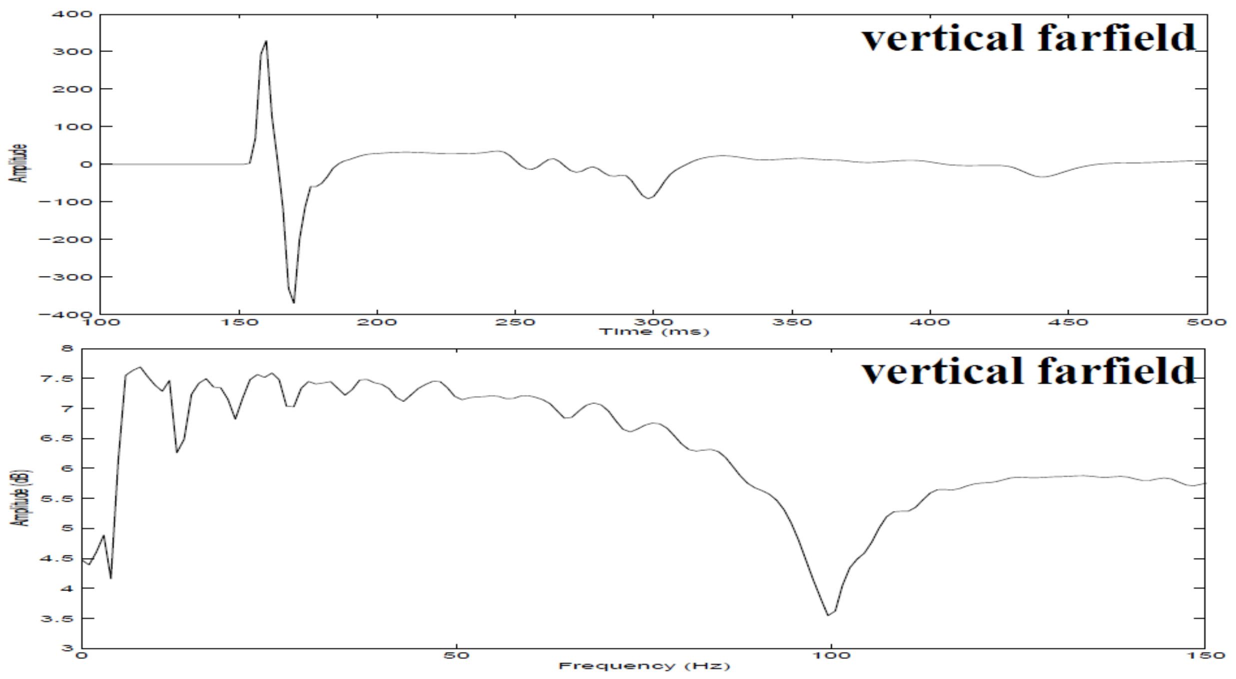

Improving the Primary to Bubble ratio: Guns with varying volumes

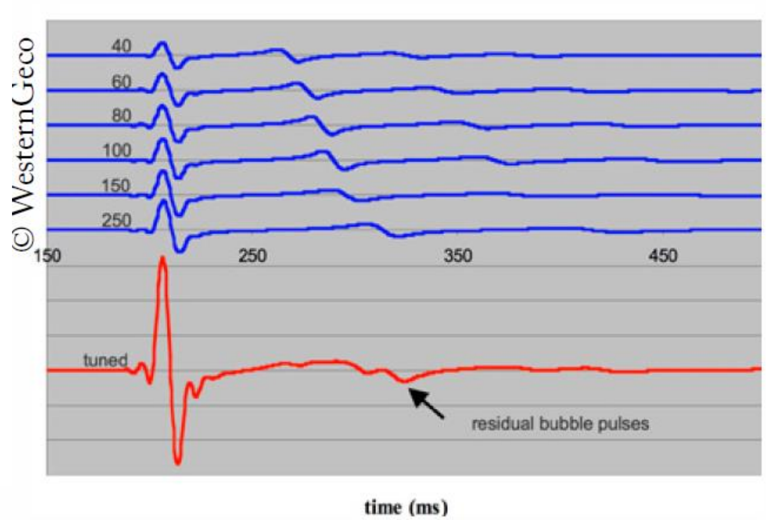

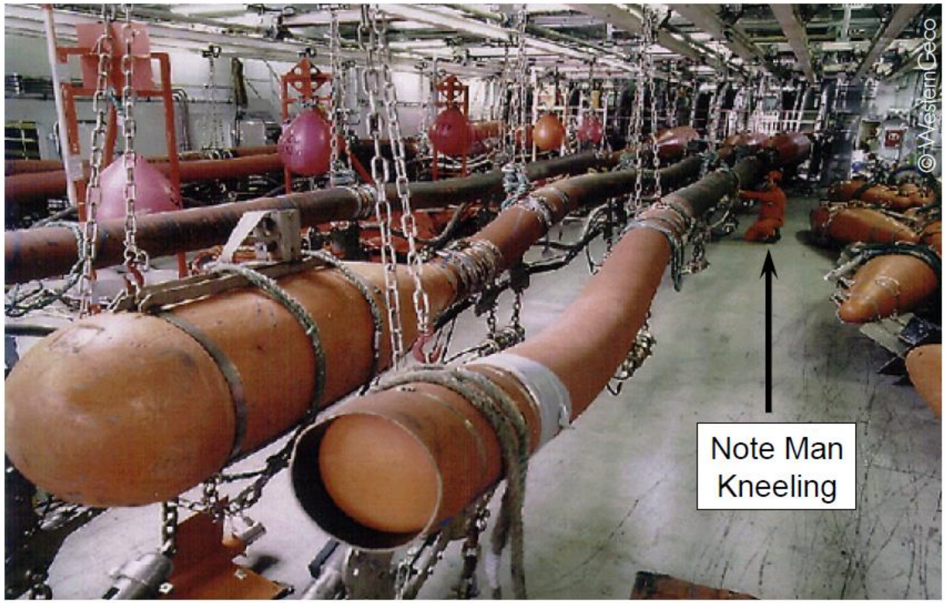

Part of an air-gun array onboard a vessel.

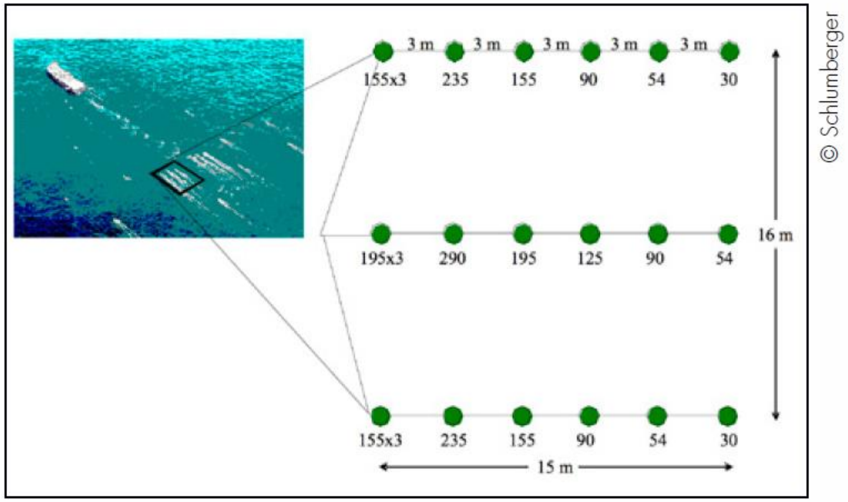

Seismic vessel towing two air-gun arrays at 6 m depth. One array, consisting of three strings with in total 24 guns, is sketched in plan view. It measures 15 m x 16 m (inline x cross-line). The numbers are gun volumes in in^3. The total volume is 3,397 in^3.

Modeling of GI gun signatures,

Landrø, 1992, Geophysical Prospecting, **40**, 721-747.

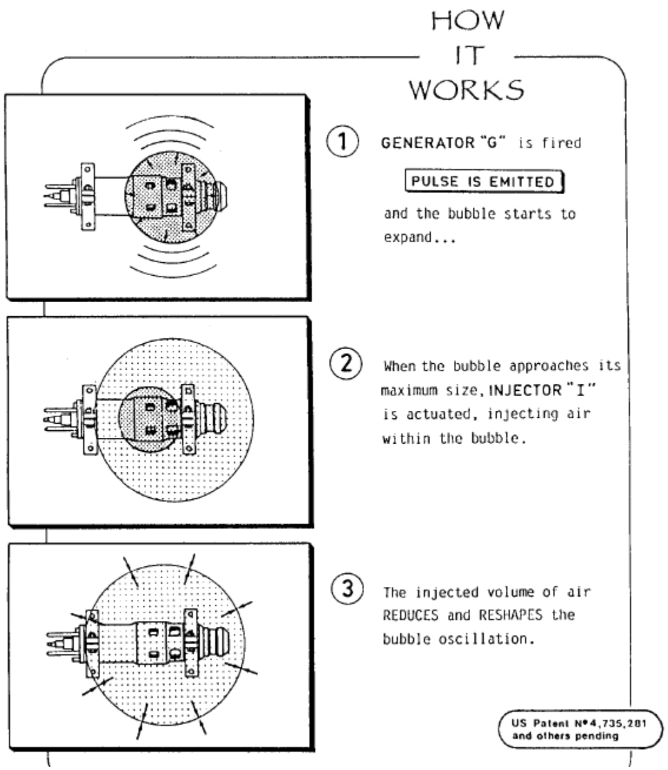

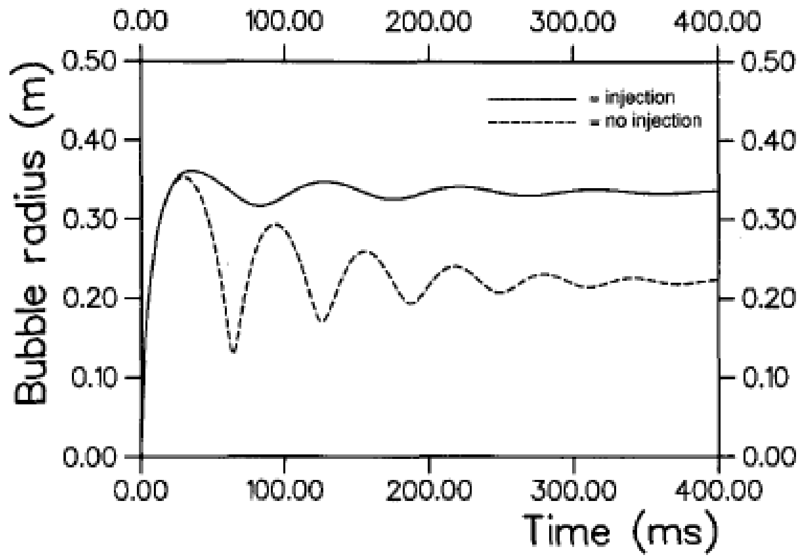

Need a lot of air:

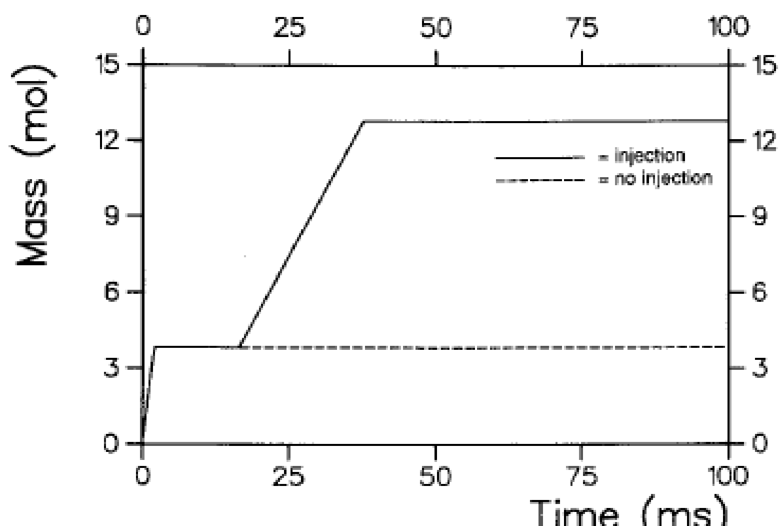

Use modeling to optimize the P/B-ratio with respect to injection start time, injection volume and injection period

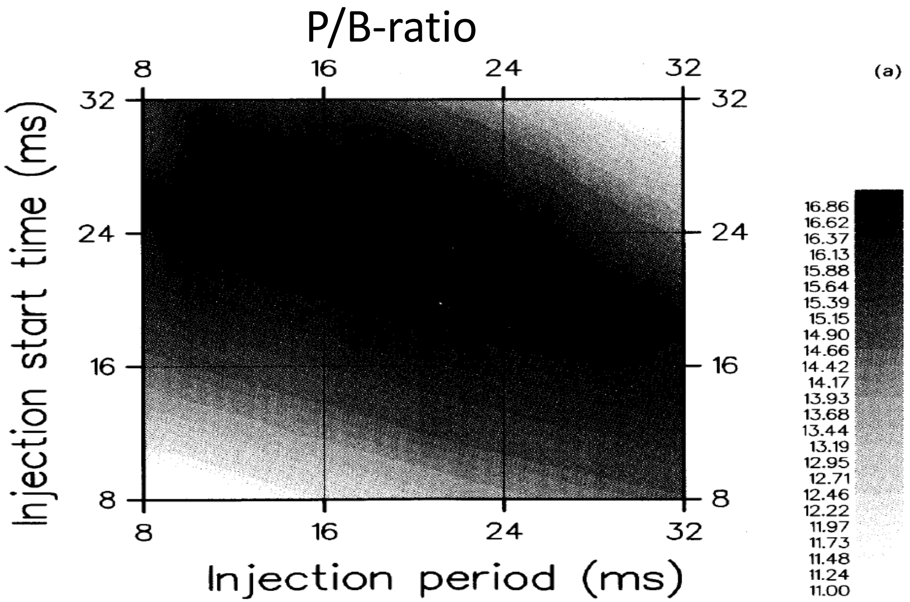

Comparing measured and modeled farfield signatures:

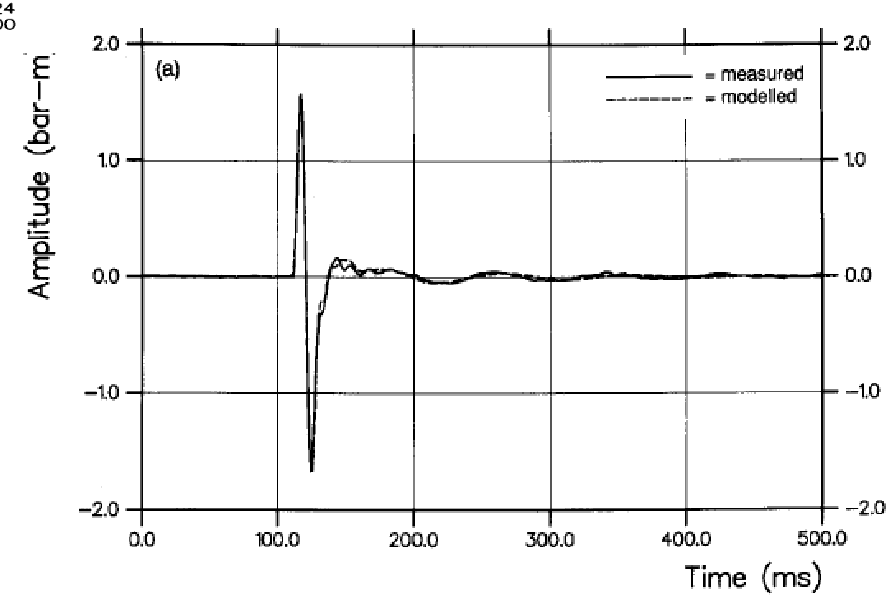

Clustered airguns : Improved primary to bubble ratio

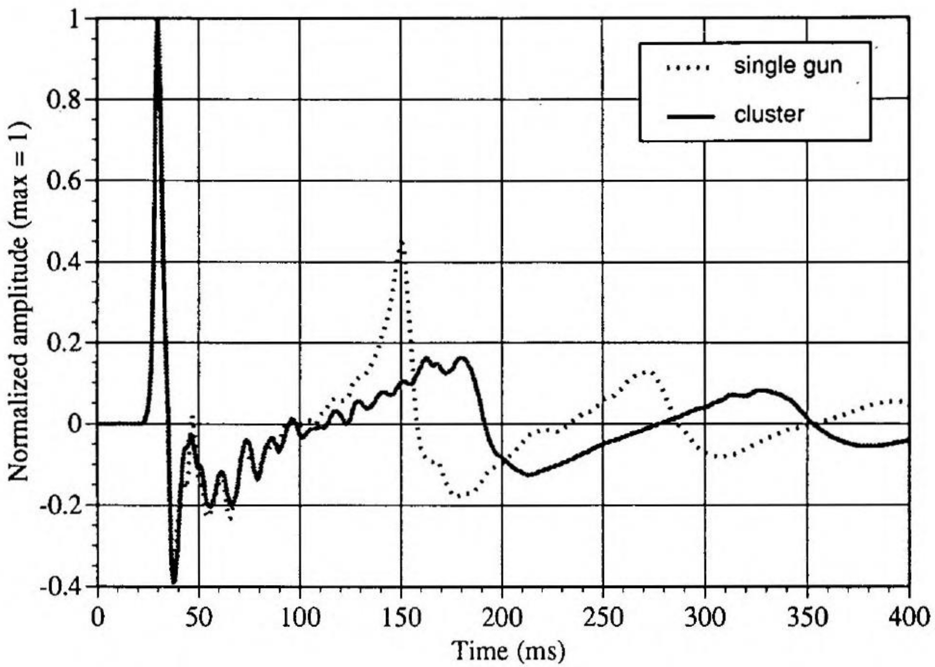

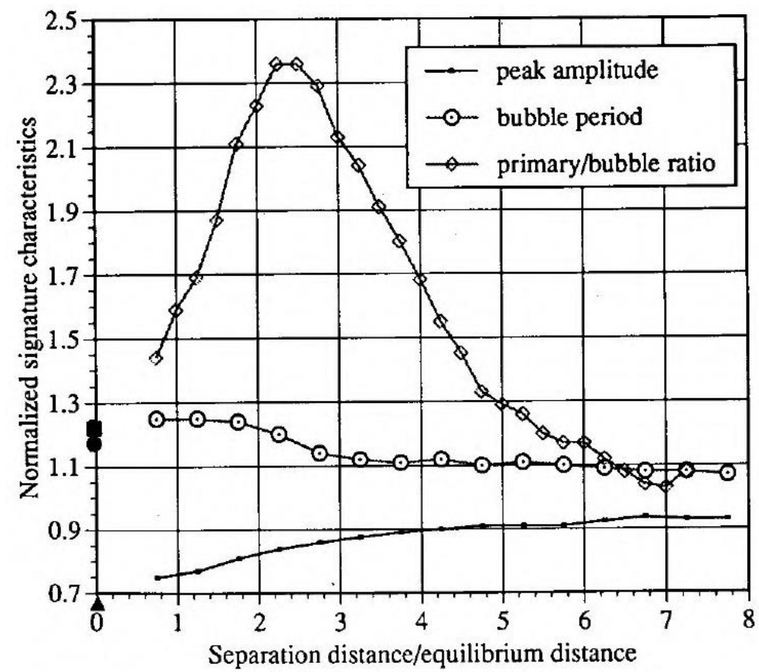

Strandenes and Vaage, First Break 1992

The equilibrium distance: $$R_{\mathrm{EQ}} = R_0 \left(\frac{P}{P_\infty}\right)^{1/3\gamma}$$

Example of a three-gun cluster

This figure compares the peak amplitudes of far-field measurements for three-, two- and single-gun clusters.

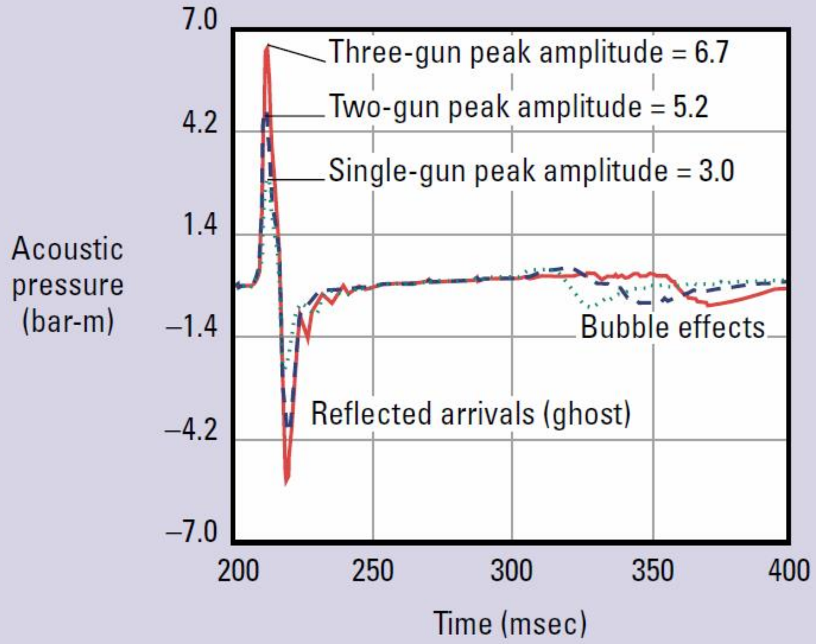

The three-gun cluster source can be used for many types of surveys.

These plots show the peak amplitudes and frequency spectra from far-field measurements made on a three-gun cluster fired at 2000 psi.

Source: Schlumberger

8-gun cluster

The frequency spectrum of the geophone data in the salt sheet shows that the dual ITAGA 16-gun tuned array provided a usable bandwidth of 5 to 100 Hz.

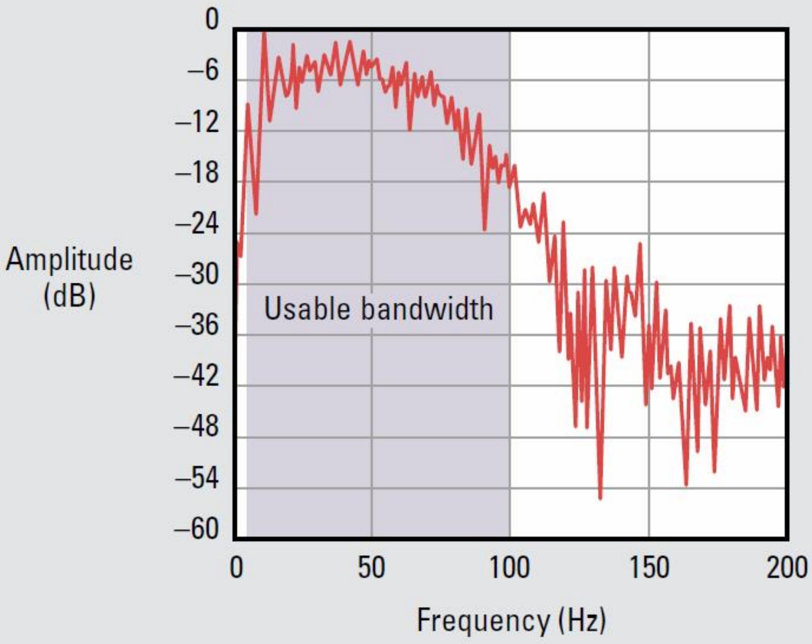

The ITAGA source provides optimal results in deep wells, ensuring good signal penetration over a large frequency bandwidth.

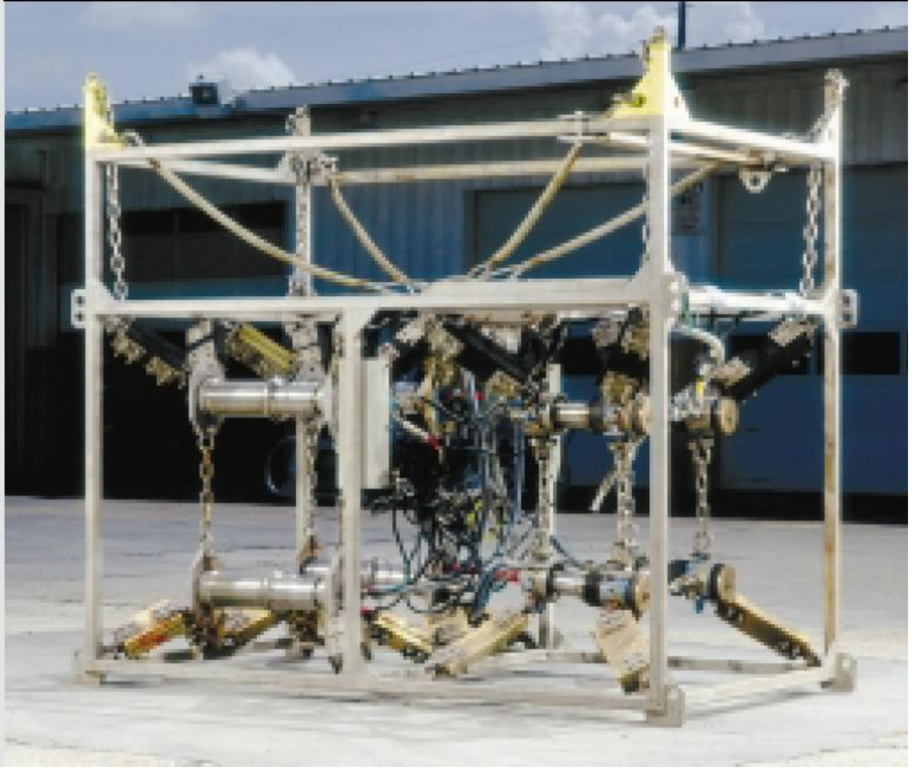

Source: Schlumberger

Far-field measurements of the 3-gun cluster for various depths

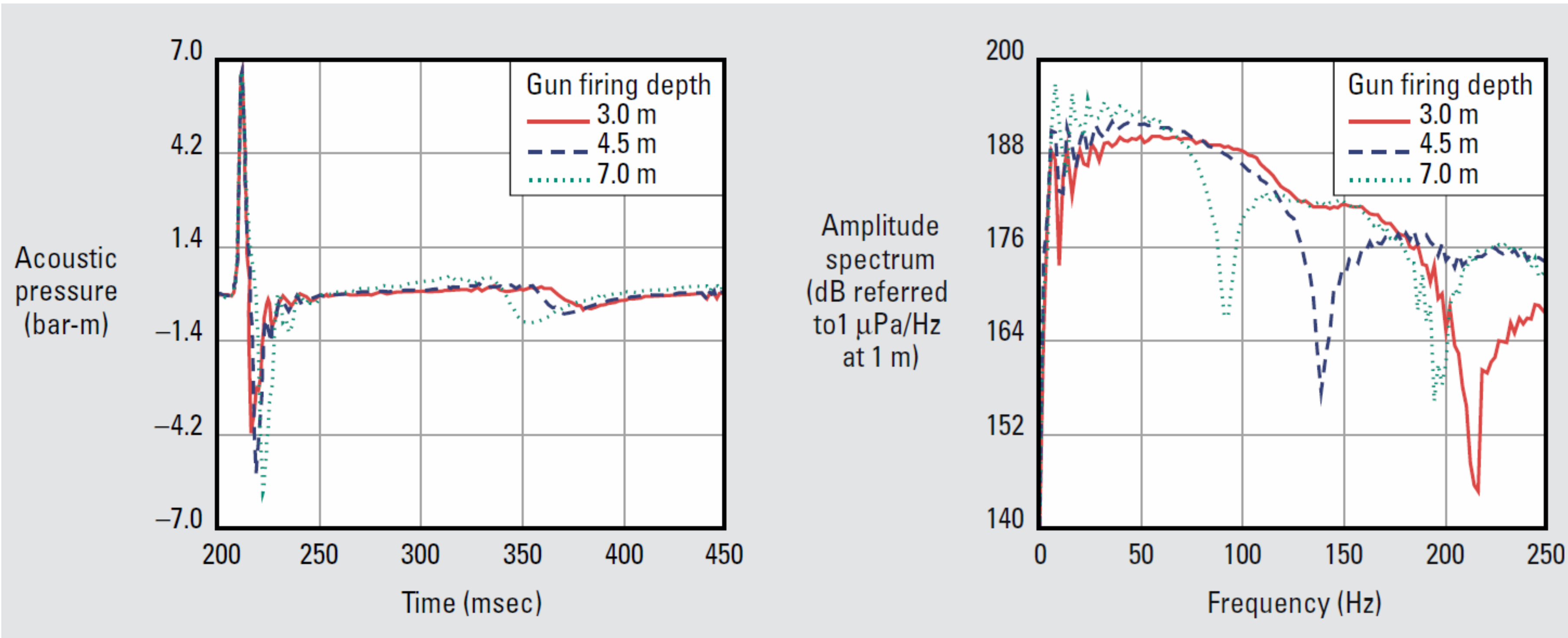

Source: Schlumberger

- Bubble time period decreases with increasing depth
- Ghost notch decreases with increasing depth
- More low frequencies (between 10-70 Hz) for deeper sources

A G-gun cluster

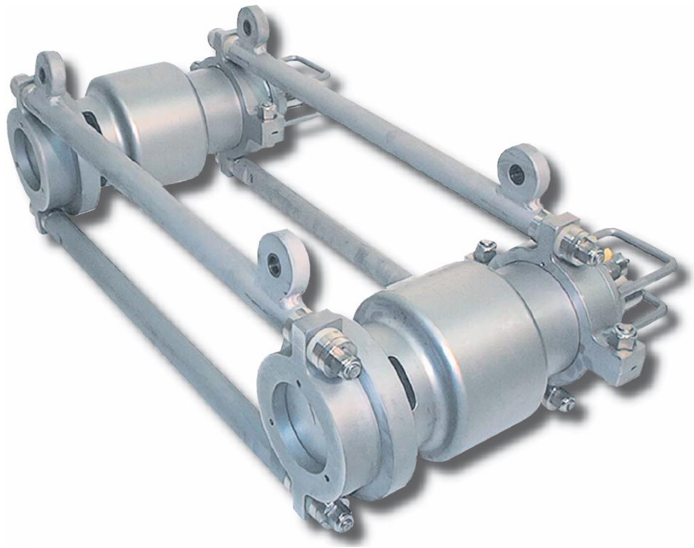

Source depth 5 m and 2000 psi

IGNATURE AND SPECTRUM

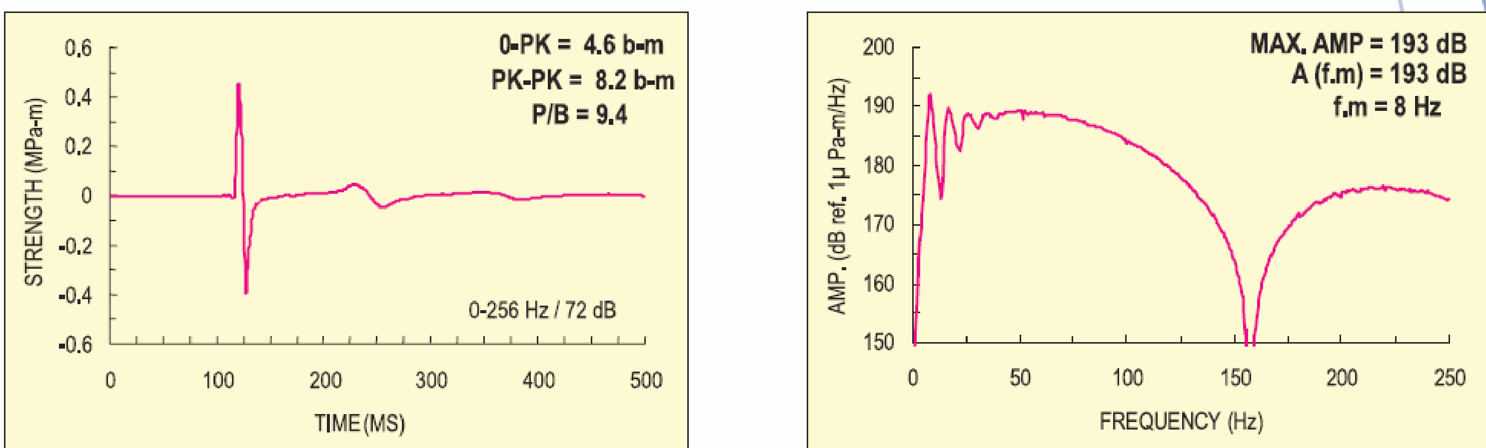

2 * G. GUN in Parallel Cluster / 300 in^3

Source: Sercel

Low frequency and large G-gun sources

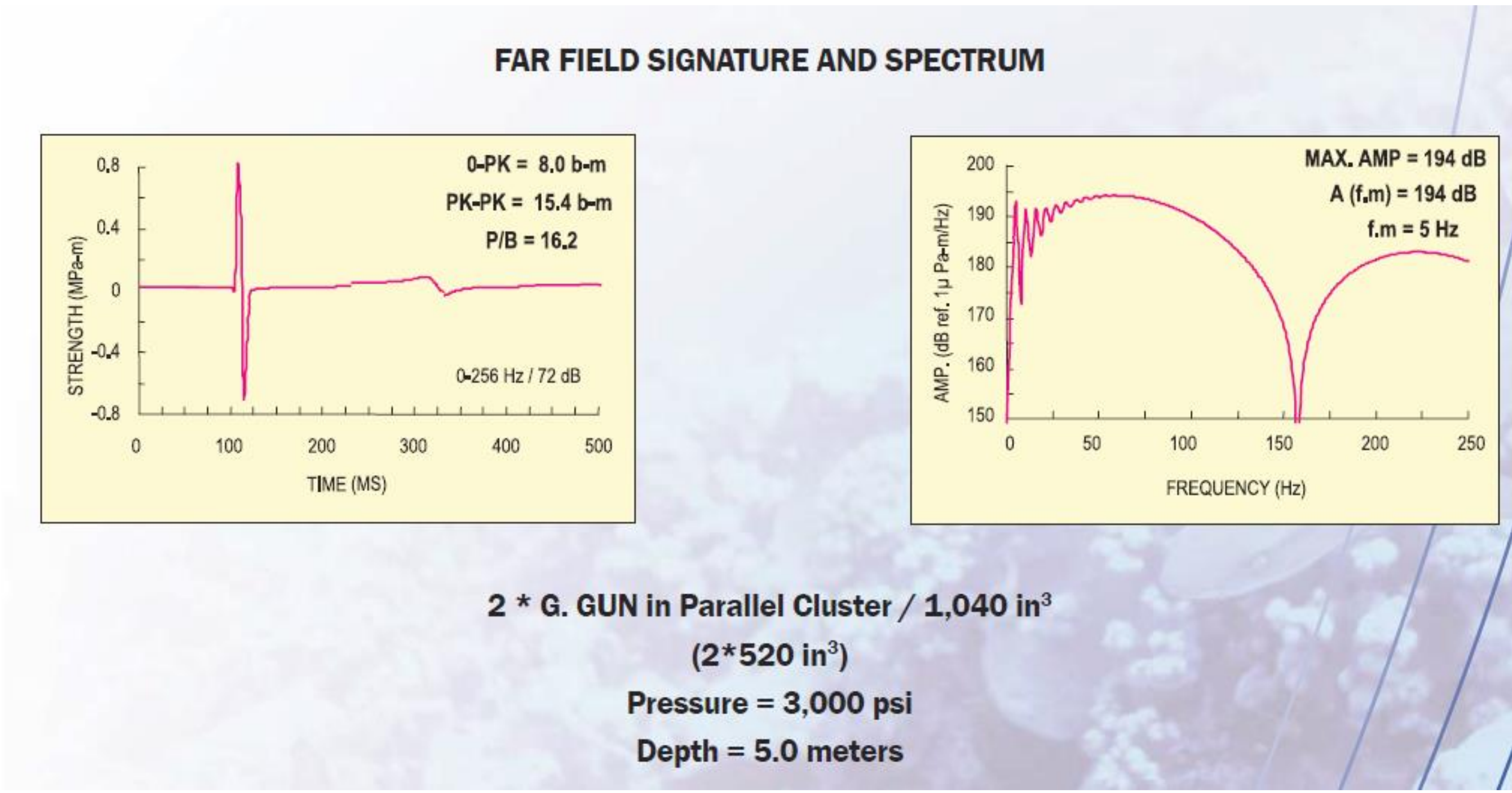

Source: Sercel

Rattray’s PhD thesis (Caltech, 1951)

Collapse of a cavity in the vicinity of a wall ⬄ a two-gun cluster

$$R = \sum_{n=0}^{\infty} R_n(t) P_n(\cos\theta) \qquad \nabla^2 \Phi(r,\theta,t) = 0,$$

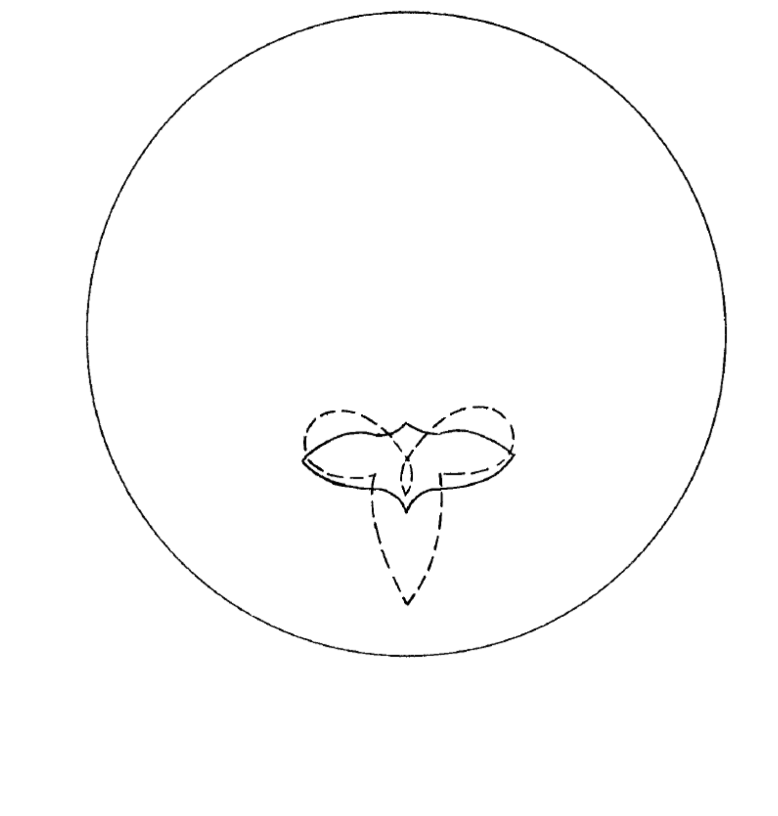

Estimated shape of cavity versus time: solid and dashed shapes represent two different approximations

Expanding in powers of h and considering coefficients of h^1, one obtains with the aid of equation (16)

$$\frac{dt^{(1)}}{dR_0} = \frac{R_0^2 \cdot \frac{1}{2} R_0}{\Phi_0^{(0)}}$$

Thus

$$\tau^{(1)} = \int_1^0 \frac{1}{2} \frac{R_0^3}{\Phi_0^{(0)}} dR_0$$

$$= 0.41 \, \tau^{(0)}$$

The time of collapse is therefore

$$\tau = .915(1 + 0.41 h) + O(h^2). \qquad (17)$$

Another solution (from Rattray's thesis) for tranlational motion of bubble

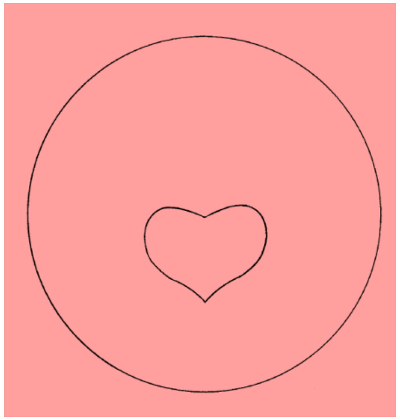

..no wonder why we love science

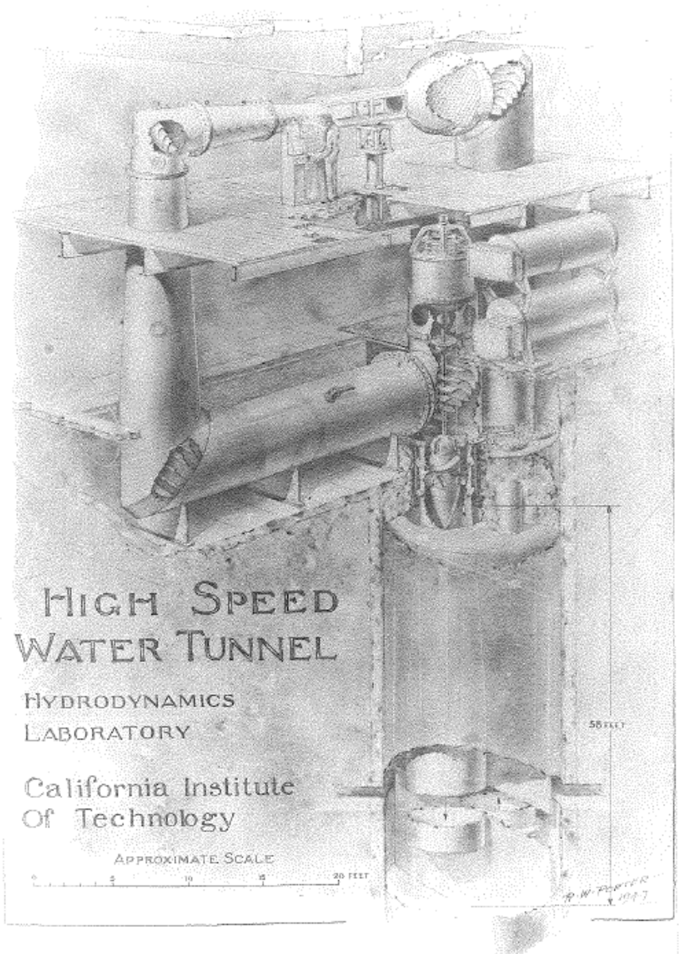

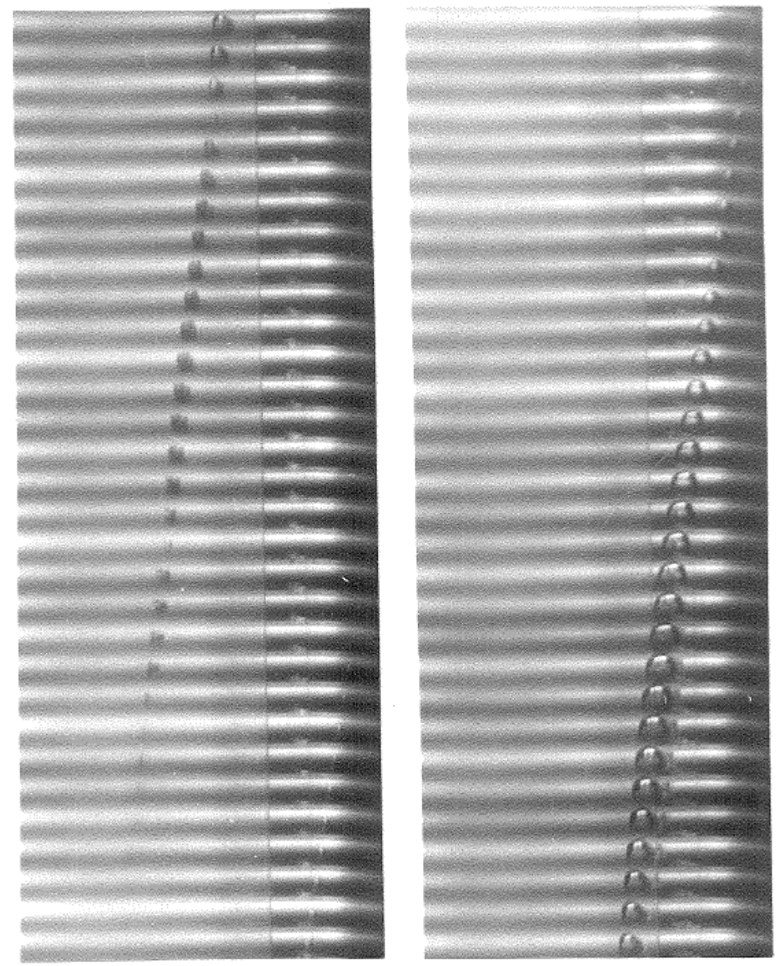

Fig. 3 - Motion of cavitation bubble as observed by Knapp and Hollander (11).

Simple expression for the bubble-time period of two clustered air guns

GEOPHYSICS, VOL. 77, NO. 1 (JANUARY-FEBRUARY 2012); P. A1–A3,

Daniel Barker[1] and Martin Landrø[1]

Strandenes and Vaage (1991) introduced the equilibrium radius: $$R_{EQ} = R_0 \left(\frac{P}{P_\infty}\right)^{1/3\gamma}$$

Rayleigh found in 1917: $$T_0 = 0.915 R_0 \sqrt{\frac{\rho}{P}}$$

Rattray found in 1951 that the collapse time for a cavity close to a wall is $$T = T_0 (1 + 0.41 \frac{R}{2b})$$

Barker and Landrø (2012) suggested to replace R with R_{EQ} $$\frac{T_{\text{cluster}}}{T_{\text{single}}} = 1 + 0.41 \frac{R_{EQ}}{2b}$$

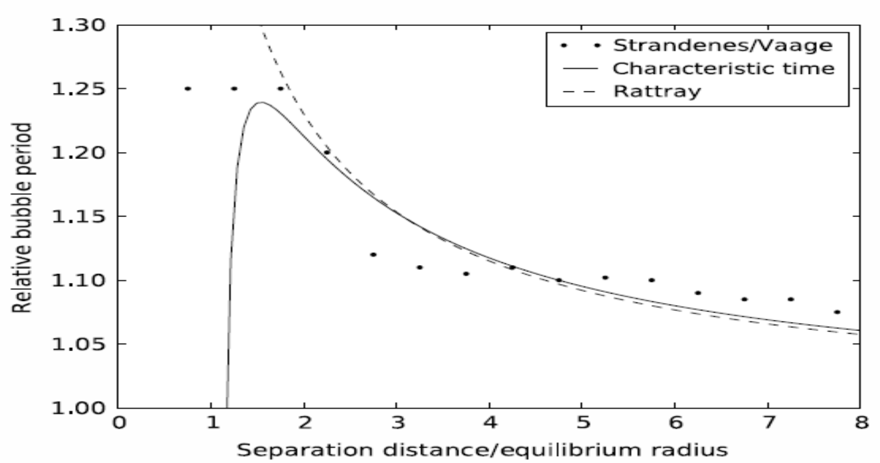

Barker and Landrø (2012) found the following expression for the cluster bubble time period:

where we have used the parameter $\kappa = 2b/R_{\mathrm{EQ}}$ to simplify the expression. Dividing by the charateristic time of a single gun, we get the ratio

$$\frac{T_{\mathrm{Cluster}}}{T_{\mathrm{Single}}} = \frac{1}{2}\sqrt{\frac{4\kappa + 4 - \ln\left(\frac{\kappa-1}{\kappa+1}\right)}{\kappa} + \frac{2}{1-\kappa^2}}, \qquad \kappa \geq 2.$$

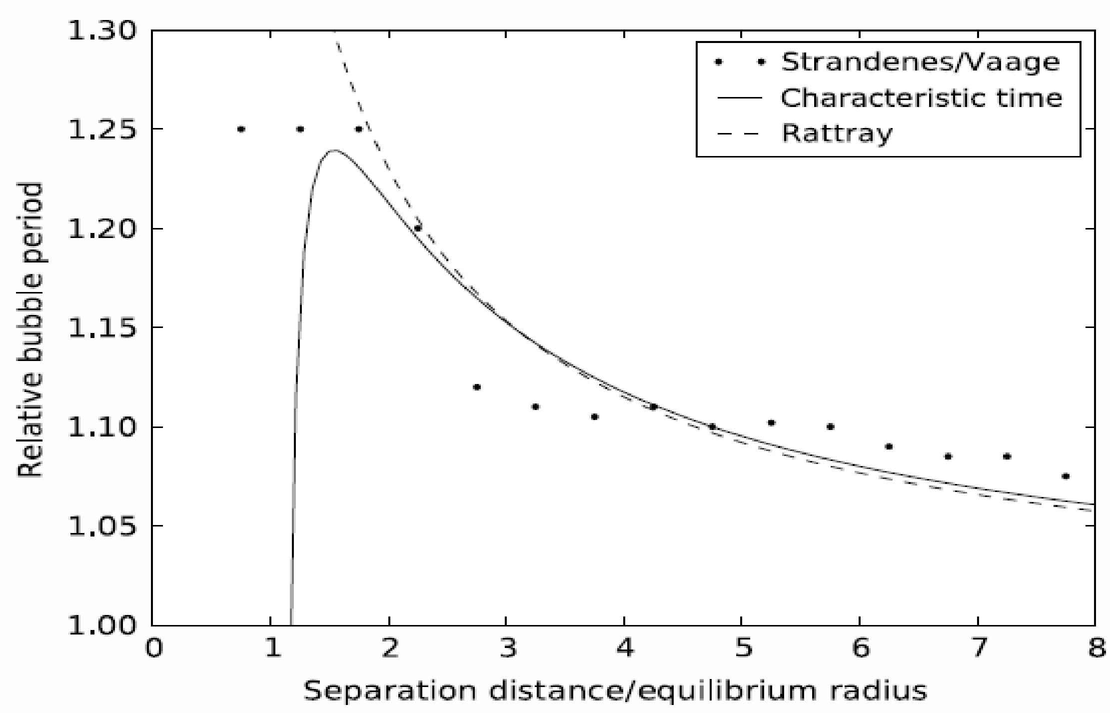

Clustered air guns – important to include the water motion

Barker and Landrø, 2013: Use equipotential surfaces to account for clustering effects (submitted to Geophysics)

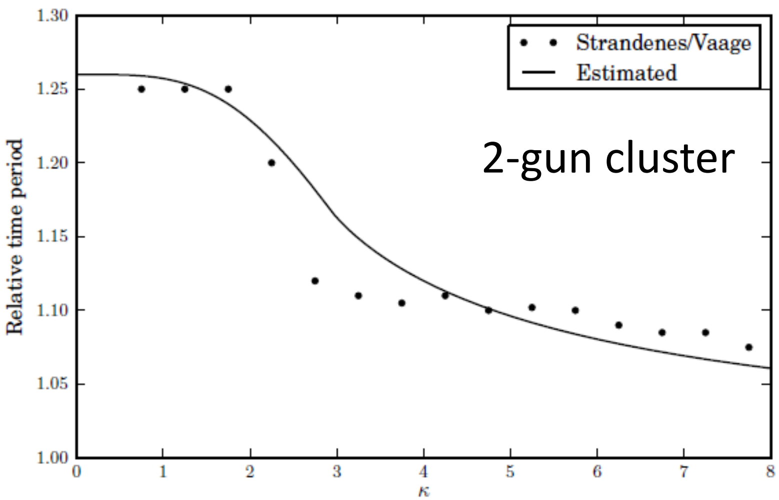

Model the bubble time period by this technique, further work is needed to adapt this modeling approach also for amplitudes

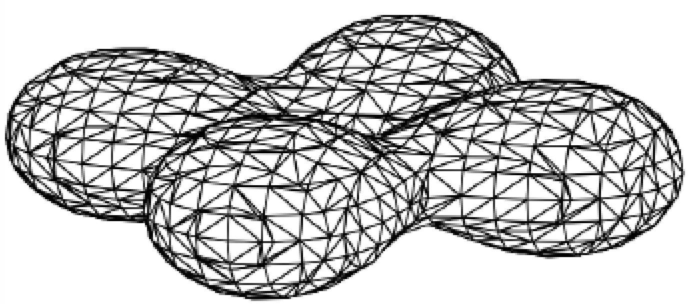

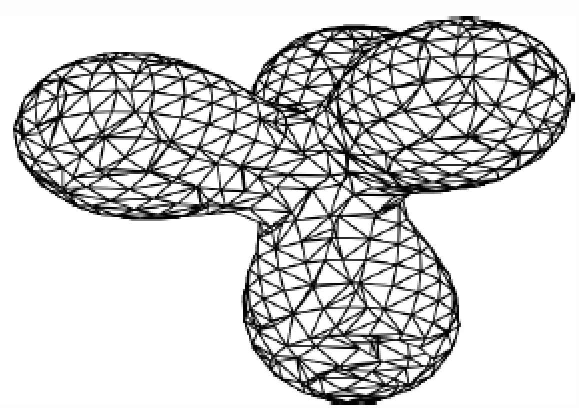

Estimating bubble time periods for inline and triangle 3-gun clusters

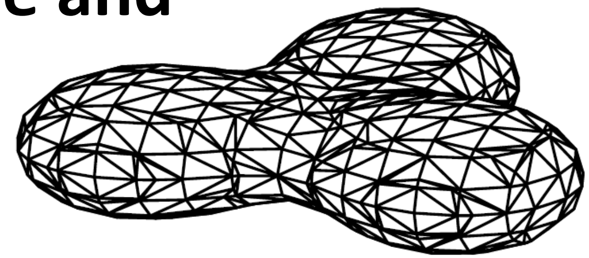

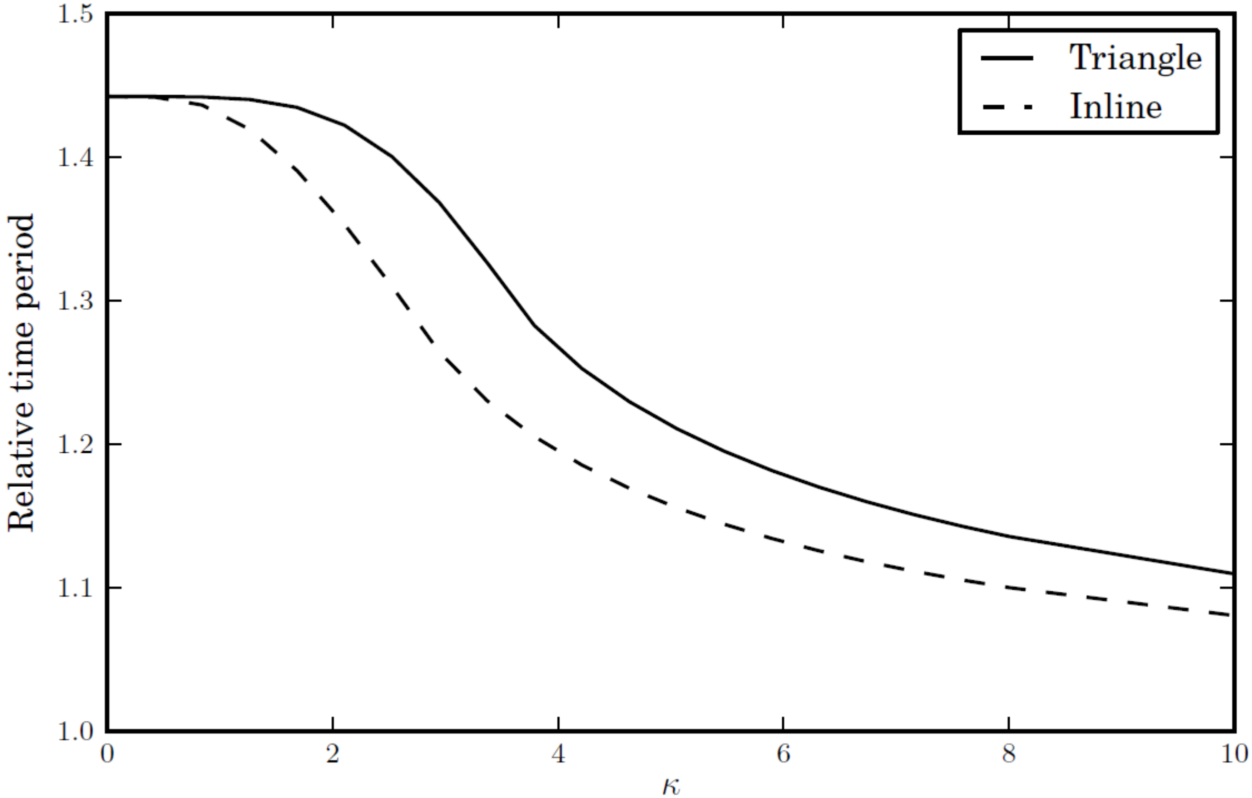

Triangle configuration seems to be more effective since bubble time increase starts earlier as separation distance decreases

Calculating the bubble period for n-gun clusters in a circle

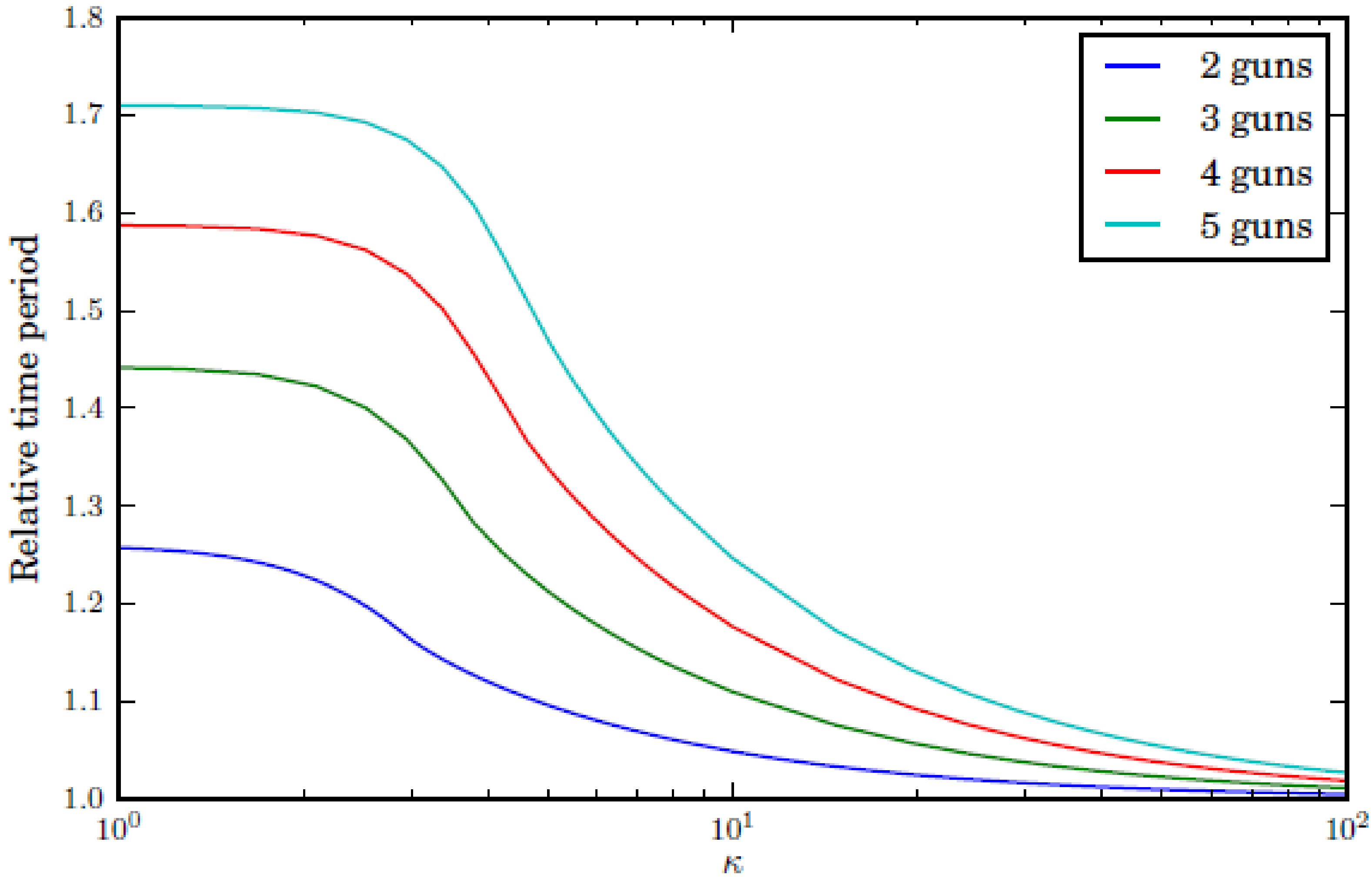

Barker and Landrø, 2013

Air gun bubble damping by a screen, *Langhammer et al., Geophysics 1995*

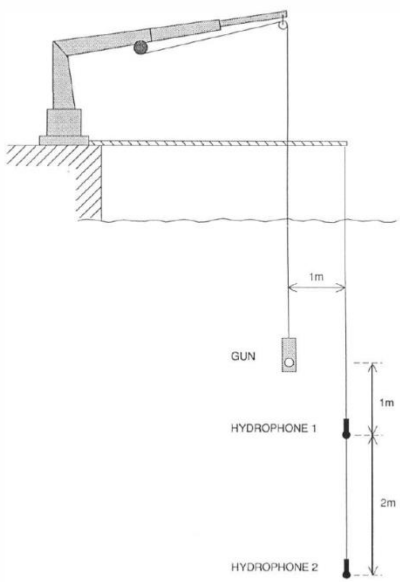

FIG. 5. Experimental configuration of hydrophone array and air gun.

screen, we observed the same tendency of an increasing primary-to-bubble ratio with an increasing screen length, at both 3-m and 5-m water depths.

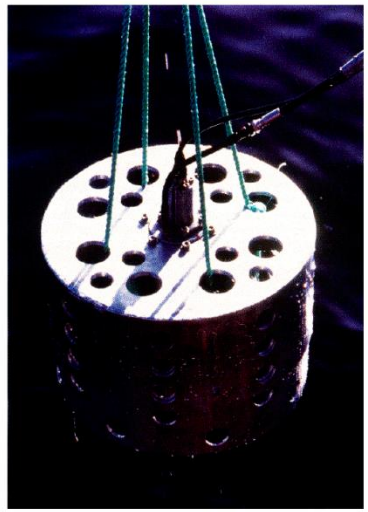

FIG. 6. The 28-cm radius screen mounted on the gun.

The bubble oscillations are damped significantly

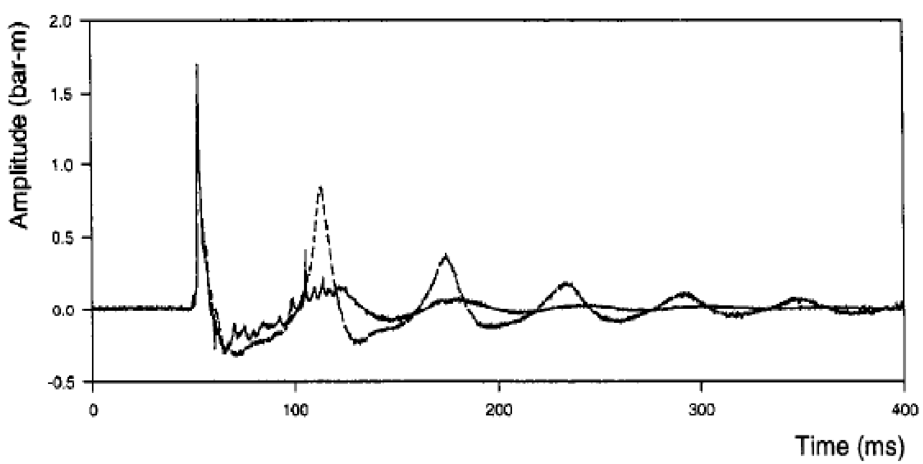

Notice: More low frequencies

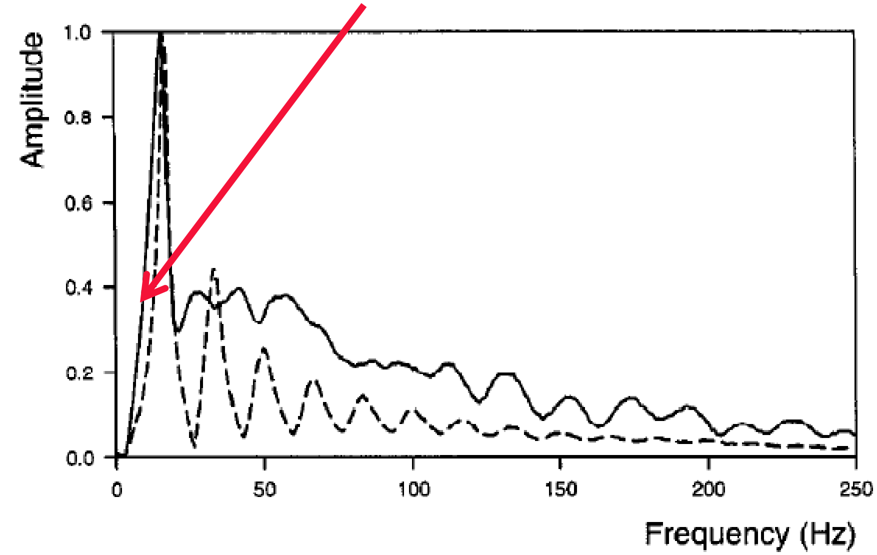

Damping of secondary bubble oscillations for towed air guns,

Landrø et al., Geophysics, 1997

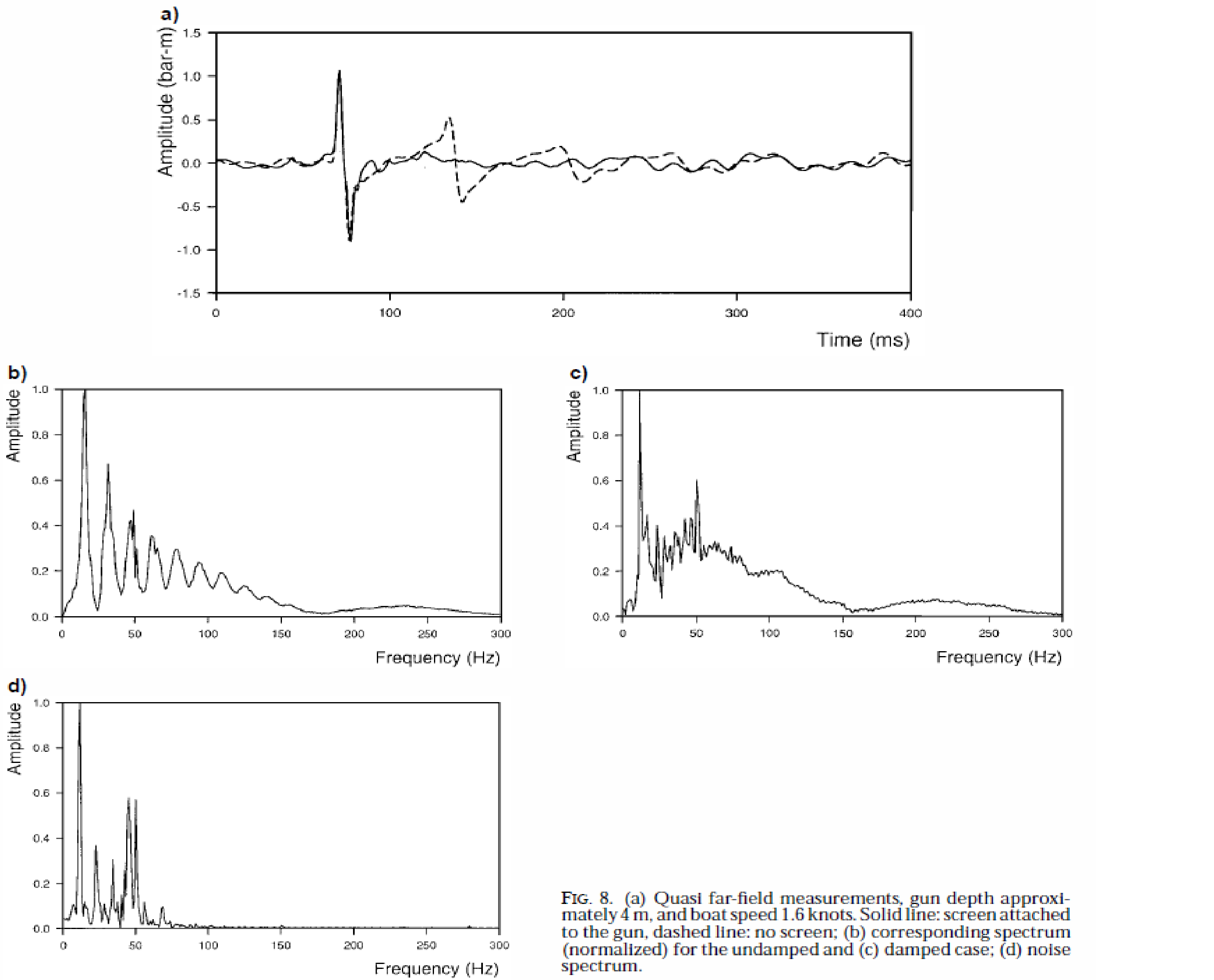

FIG. 8. (a) Quasi far-field measurements, gun depth approximately 4 m, and boat speed 1.6 knots. Solid line: screen attached to the gun, dashed line: no screen; (b) corresponding spectrum (normalized) for the undamped and (c) damped case; (d) noise spectrum.

Modeling of water gun signatures

Landrø et al., 1993, Geophysics 58, 101-109.

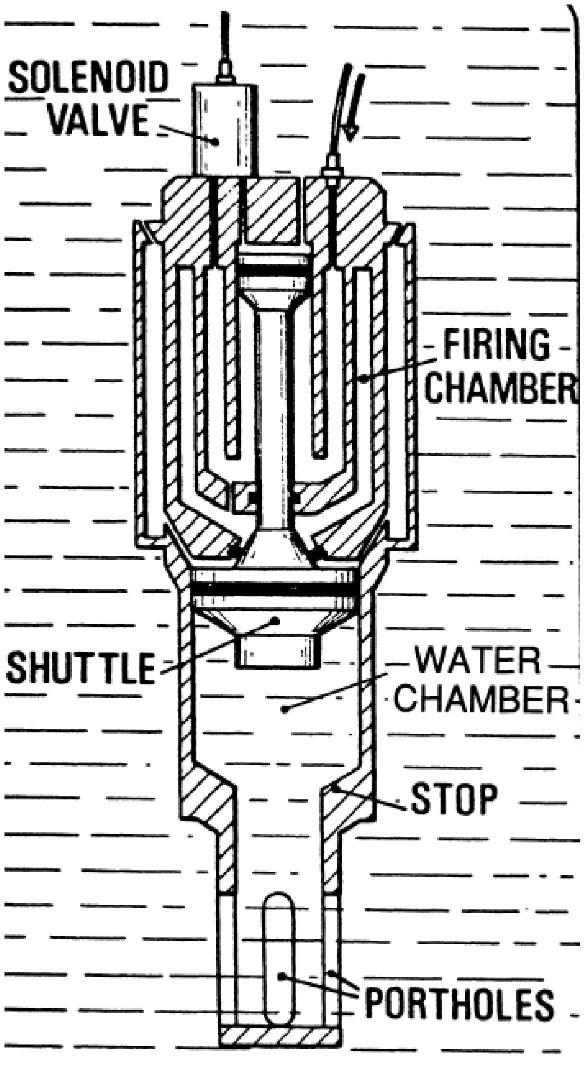

Measured and modeled nearfield S80 signatures

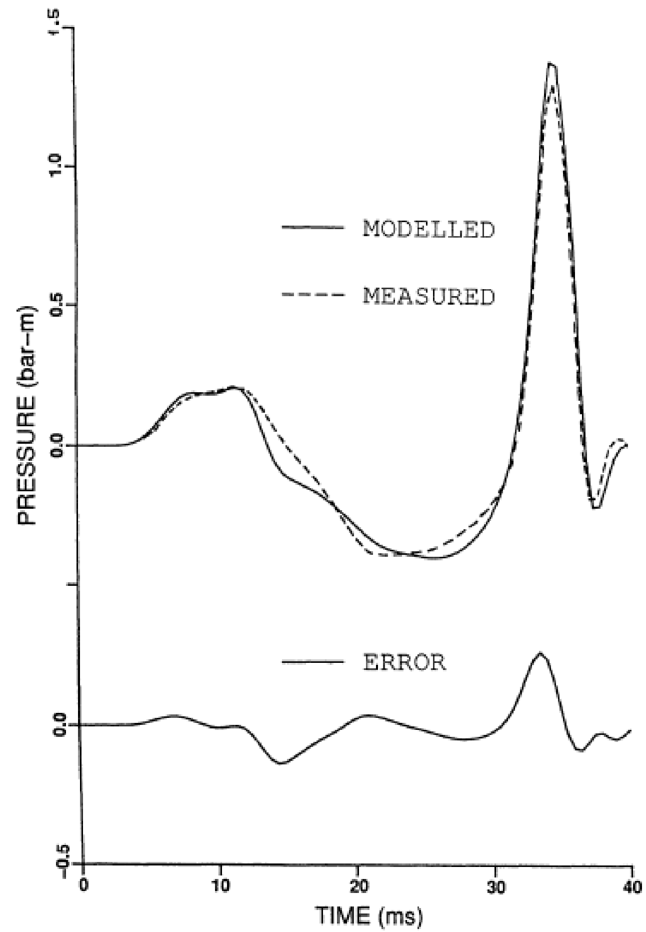

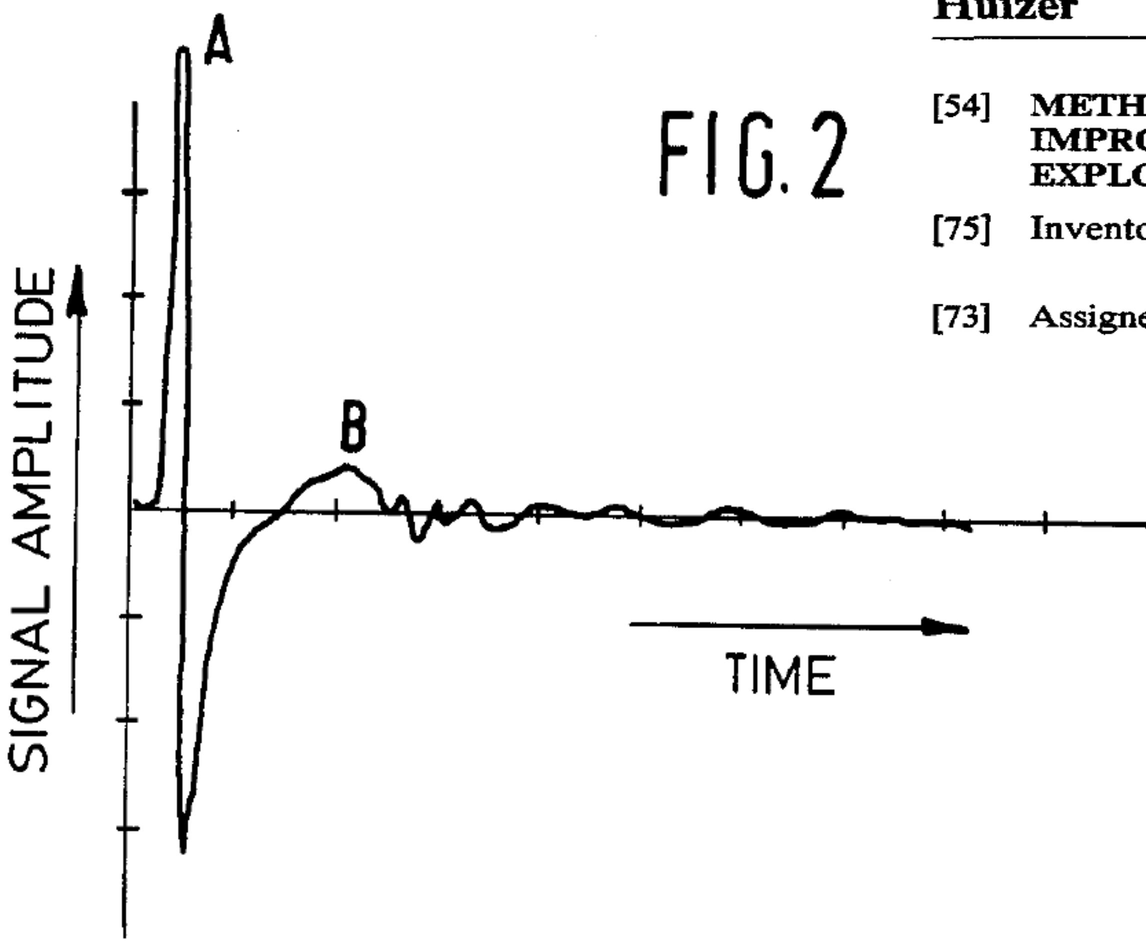

FIG. 2

United States Patent [19]

Huizer

[54] **METHOD AND APPARATUS FOR SIGNAL IMPROVEMENT IN MARINE SEISMIC EXPLORATION**

[75] Inventor: **Willem Huizer**, Rijswijk, Netherlands

[73] Assignee: **Shell Oil Company**, Houston, Tex.

By towing one subarray at 7.5 m depth and the other at 5 m depth, and using firing time delays, the P/B –ratio was improved from 5.6 to 9.5.

Estimating the source signature

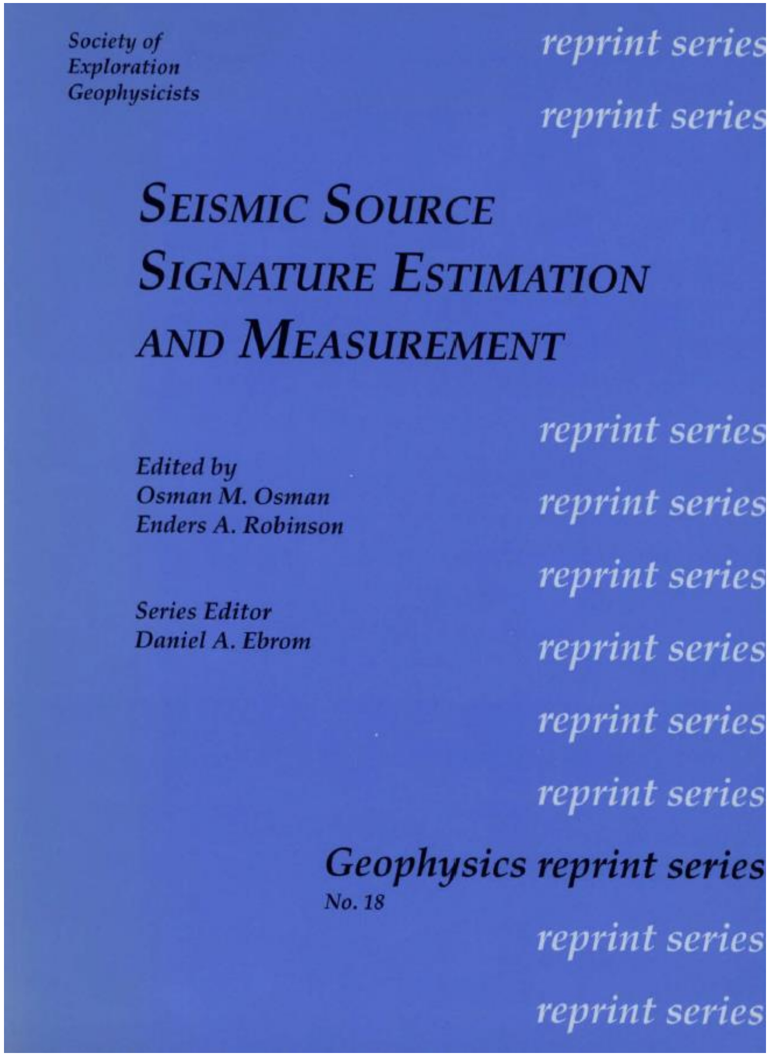

Estimating the source signature

Ziolkowski, Parkes, Hatton and Haugland, 1982, The signature of an air-gun array: Computation from near-field measurements including interactions, Geophysics, 47, 1413-1421.

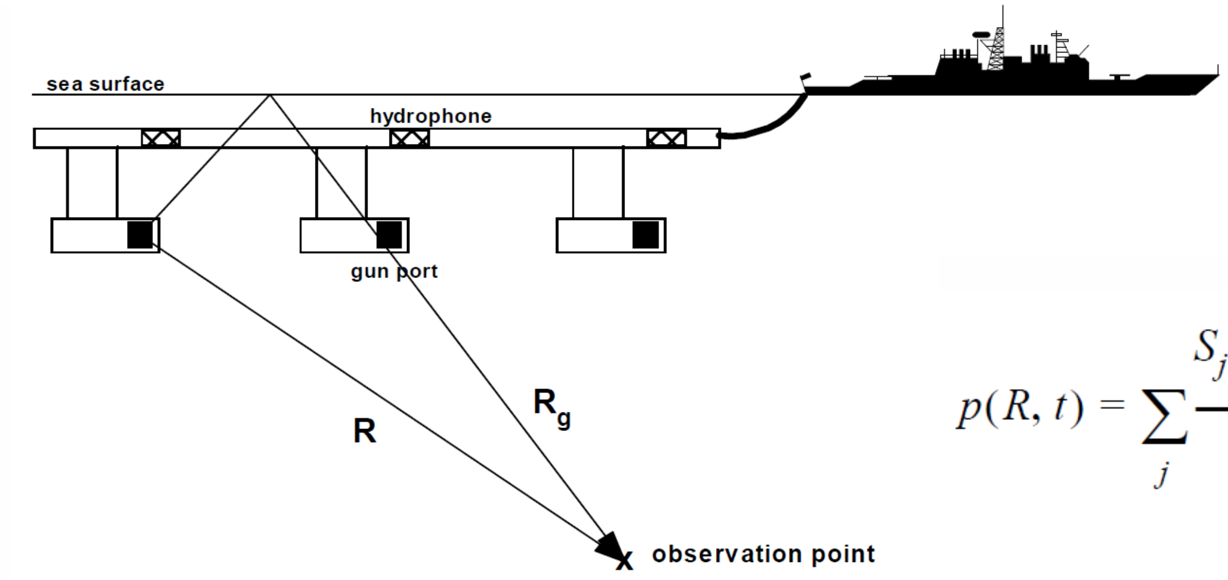

$$p(R,t) = \sum_j \frac{S_j\left(t - \frac{R_j}{c}\right)}{R_j} + \beta \frac{S_j\left(t - \frac{R_j^g}{c}\right)}{R_j^g}$$

For N sources we get N equations like the one above, and then we solve for S_j from the N measured near-field measurements (p_n)

Farfield test experiment of near-field to far-field extrapolation, Landrø, Vaage and Strandenes, 1991, First Break, 9, 375-385.

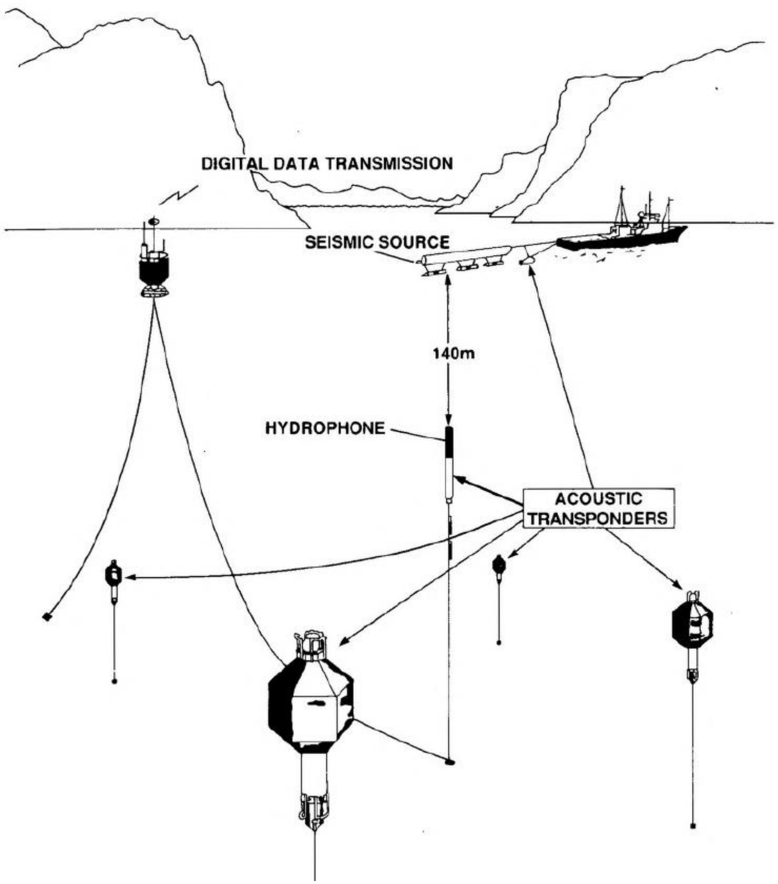

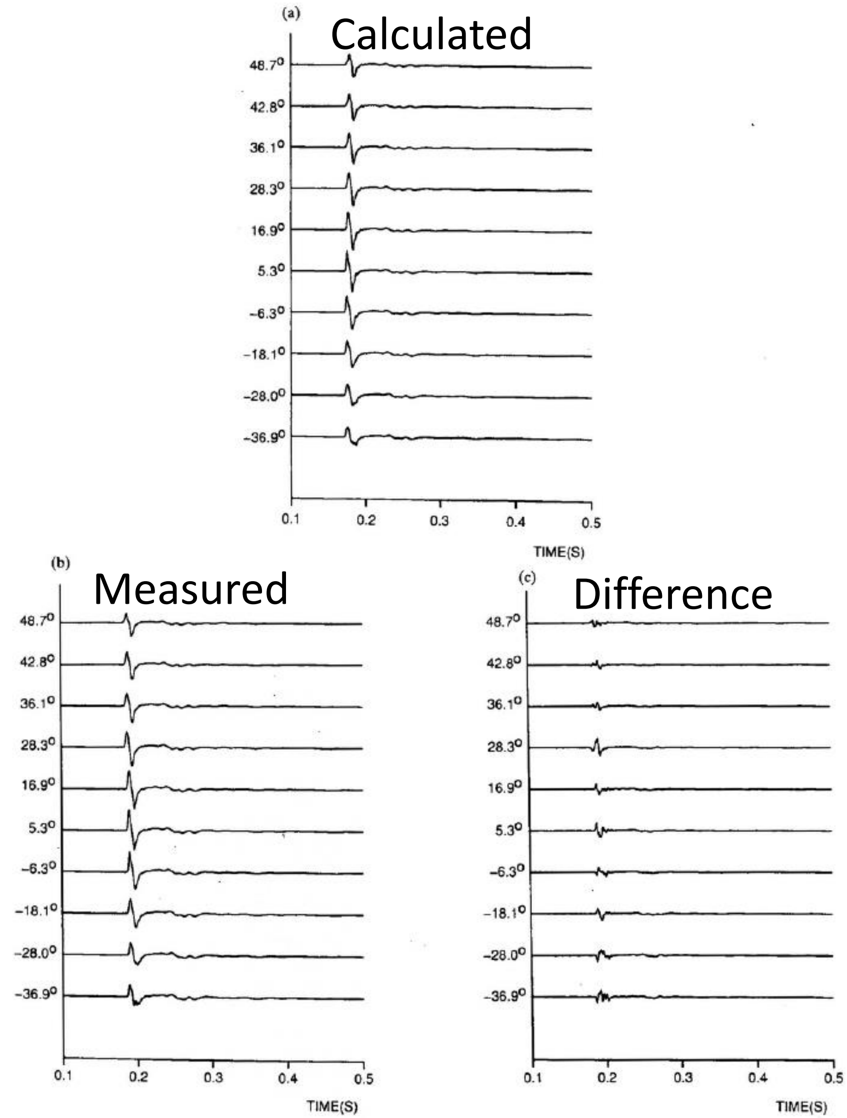

However, for compact air gun arrays we found instabilities:

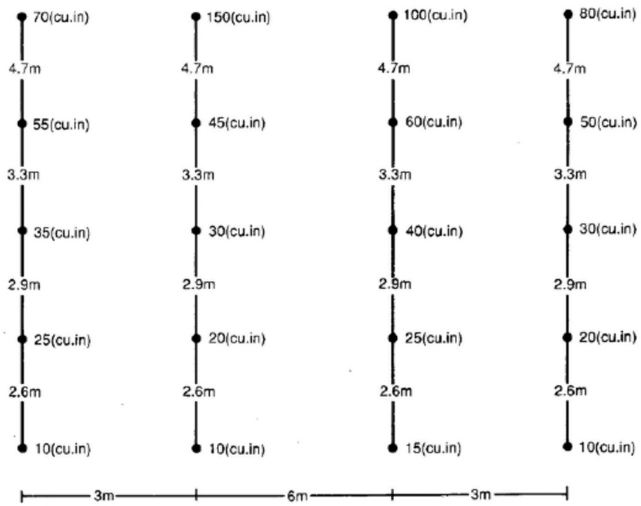

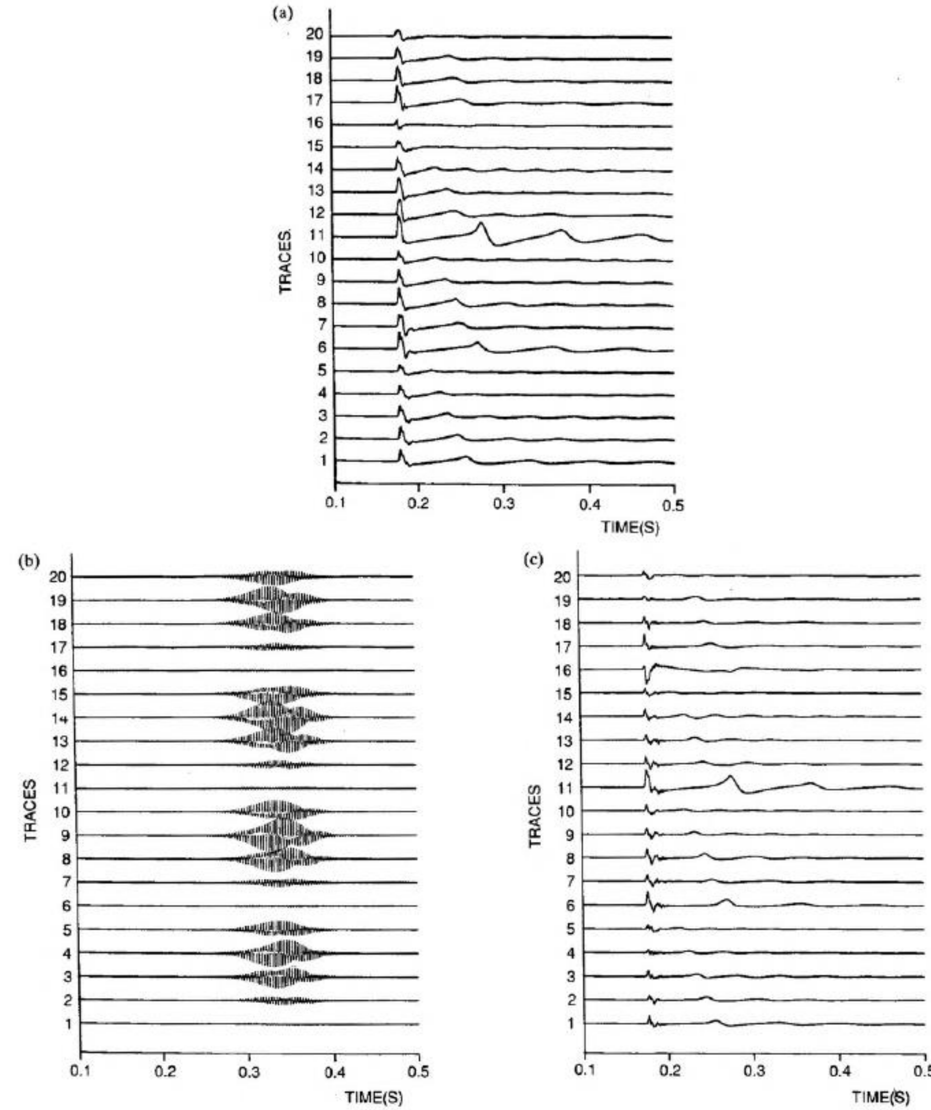

Plausible cause: We use a linear theory for measurements that are made close to each gun, and especially the ghost effect is hard to model correct assuming linearity

Reduce this effect by measuring farther away from the sources =>

The ministreamer inversion method: Landrø and Sollie, 1992, Geophysics, **57**, 1633-1640: Source signature determination by inversion

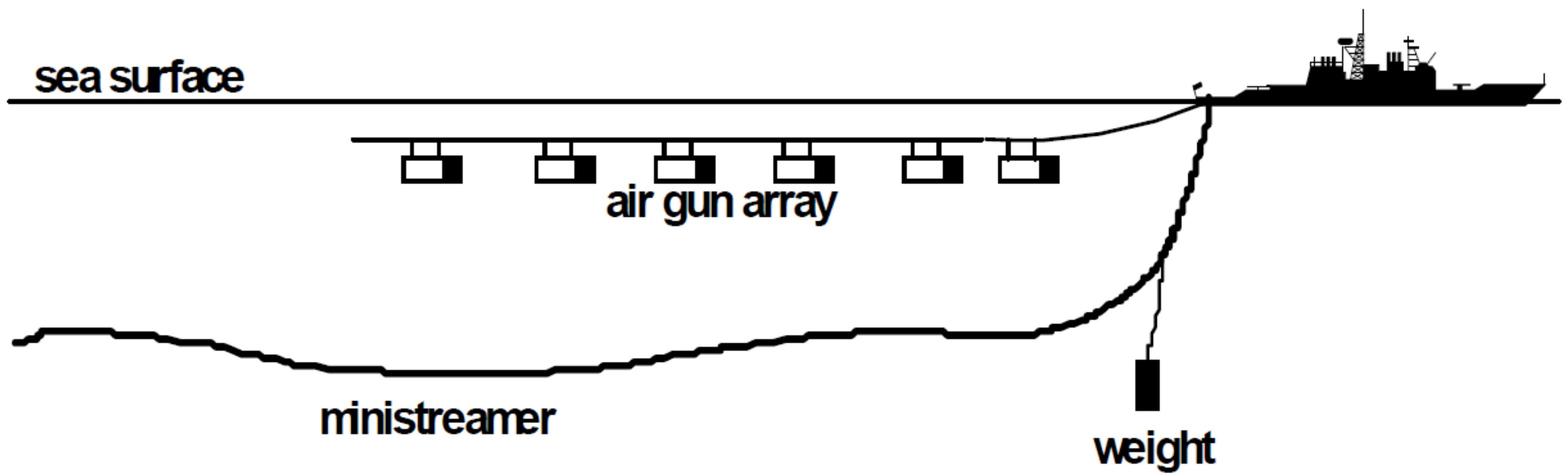

Modified Kirkwood-Bethe equation:

$$R\ddot{R}\left(1-\frac{\dot{R}}{C}\right)+\frac{3}{2}\dot{R}^{2}\left(1-\frac{\dot{R}}{3C}\right)=H\left(1+\frac{\dot{R}}{C}\right)+R\frac{\dot{H}}{C}\left(1-\frac{\dot{R}}{C}\right)-\alpha\dot{R}+\beta\dot{R}^{2}$$

Measure quasi-farfield signatures at a ministreamer below the source array, and invert for α β

Geophysical Prospecting, 1998, 46, 353–389

An experimental comparison of three direct methods of marine source signature estimation

Robert Laws,[2] Martin Landrø[3] and Lasse Amundsen[3]

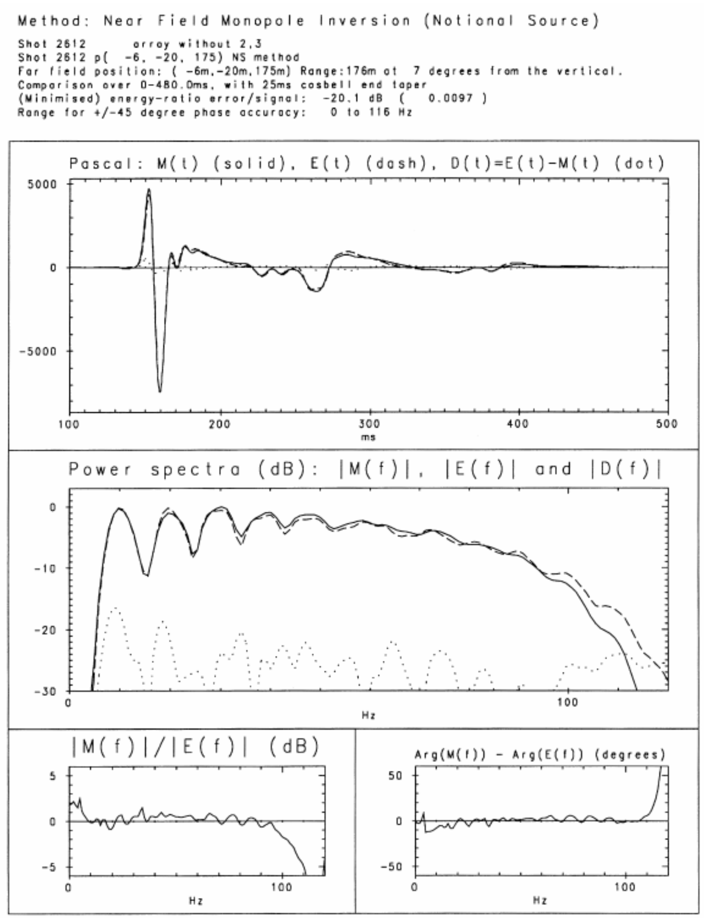

Figure 3. Near-vertical (7° off) signature of a 854 cu.in. string of single airguns.

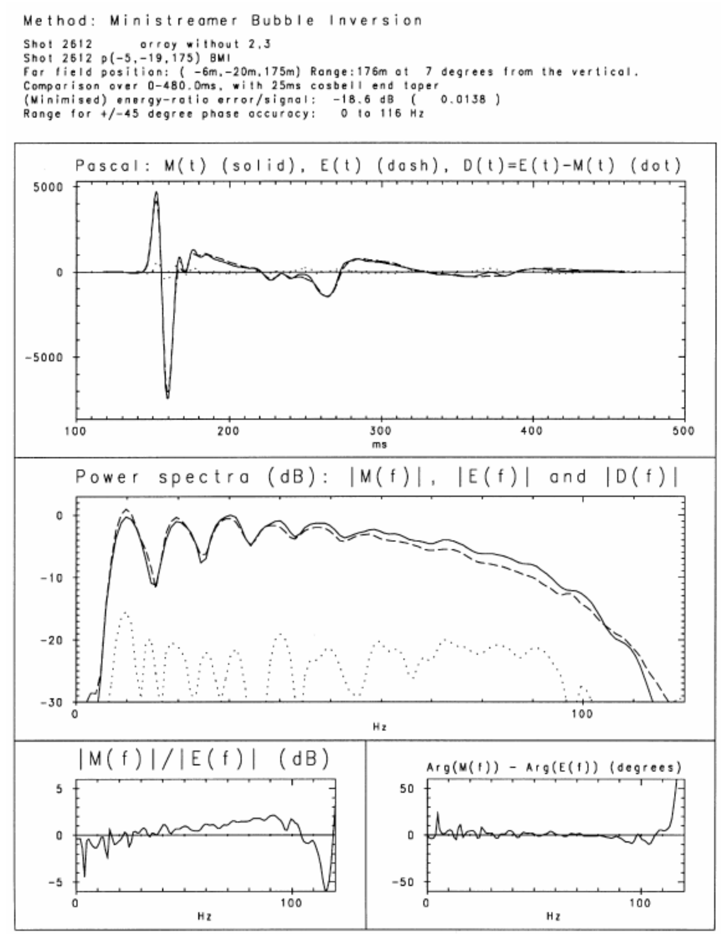

Figure 13. MBI: Near-vertical (7° off) signature of a 854 cu.in. string of single airguns.

Summary of all tests

Table 2. Error-energy (3.5–110 Hz bandwidth) expressed as a percentage of the total received energy for a variety of test conditions for each of the three methods. The 854 cu.in. array does not include a cluster but the 1244 cu.in. array does. The specified angle is the radiation angle aft of the vertical in the plane of the source string. Because of the overloading of the ministreamer there is no result from the MMI method for some tests. The experimental errors would lead to a residual error-energy of about 0.1%.

		Error-energy as % of signal energy		
Shot no.	Description	NS	MBI	MMI
0313	Single 155 cu.in. gun	4.0	2.7	4.7
1312	2*195 cu.in. cluster	3.8	6.0	3.2
1513	3*195 cu.in. cluster	7.2	2.6	2.5
2612	854 cu.in. near vertical	0.9	1.3	No result
2613	854 cu.in. 15°	1.0	1.4	No result
2614	854 cu.in. 29°	0.7	1.3	No result
2615	854 cu.in. 40°	2.2	2.4	No result
2616	854 cu.in. 48°	4.3	2.1	No result
2617	854 cu.in. 54°	7.2	3.6	No result
2618	854 cu.in. 59°	3.7	3.1	No result
2619	854 cu.in. 63°	3.6	3.1	No result
2620	854 cu.in. 66°	2.7	4.0	No result
2621	854 cu.in. 69°	2.4	4.2	No result
2713	1244 cu.in. near vertical	1.4	1.2	No result
2714	1244 cu.in. 21°	1.1	1.4	No result
2715	1244 cu.in. 33°	1.2	1.7	No result
2716	1244 cu.in. 43°	3.6	3.2	No result
2717	1244 cu.in. 51°	7.5	2.0	No result
1012	Severe drop-out	1.3	5.2	No result
2514	Severe mis-synchronization	1.9	3.6	8.8

Average : 3.1 2.8

Source ghosts and directivity effects

The source ghost spectrum

$$s(t) = \frac{1}{R}p\left(t - \frac{R}{c}\right) - \frac{1}{R_g}p\left(t - \frac{R_g}{c}\right) \tag{2.13}$$

where c is the sound velocity in water, and $R_g = R + 2z_g$. Fourier transformation of equation 2.13 and assuming that $R_g \approx R$ in the denominator of the last term (but not in the exponent!) yields:

$$S(\omega) = \frac{1}{R}P(\omega)e^{-i\omega R/c}\left(1 - e^{-i2\omega\frac{z_g}{c}}\right) \tag{2.14}$$

Letting the source ghost spectrum be the last part of this equation (within the paranteses) means that the source ghost spectrum ($H(\omega)$) is

$$H(\omega) = 1 - e^{-i2\omega\frac{z_g}{c}} \tag{2.15}$$

The norm of this ghost spectrum is given as ($\omega = 2\pi f$)

$$|H(f)| = \left|2\sin\left(\frac{2\pi f z_g}{c}\right)\right| \tag{2.16}$$

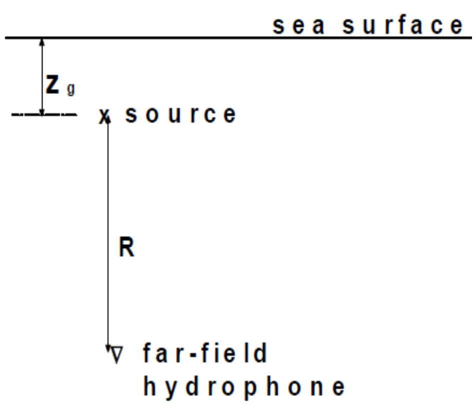

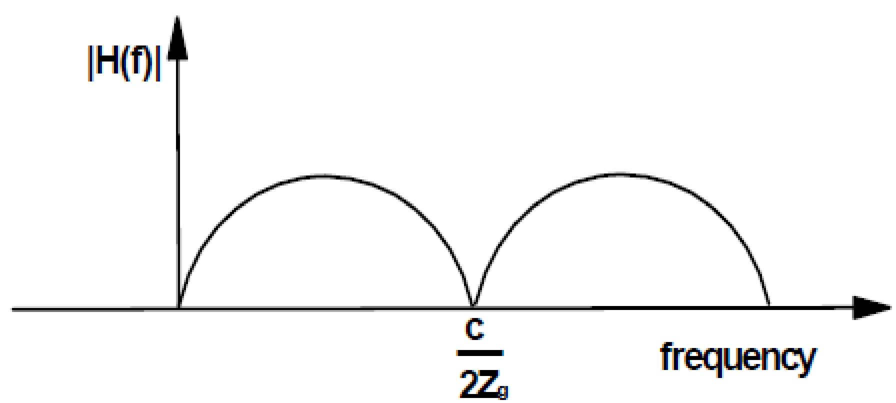

Angle dependency – ghost effect

$$|H(f)| = \left| 2\sin\frac{2\pi f z_g \cos\theta}{c} \right|$$

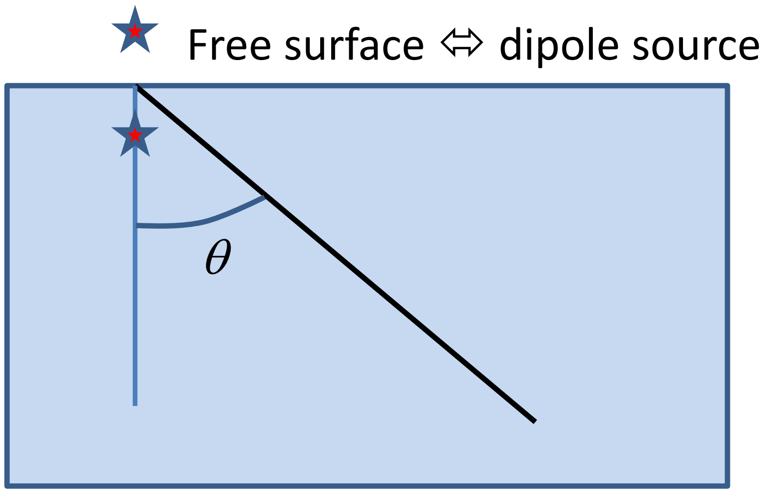

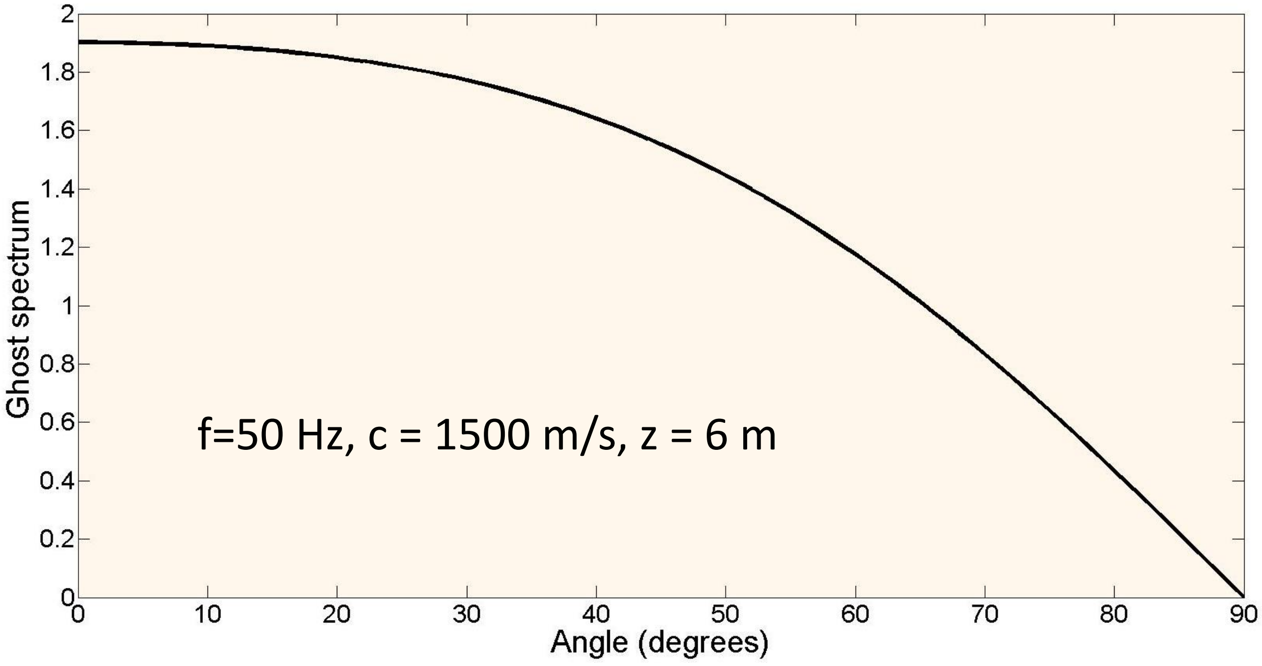

Typical source directivity plots

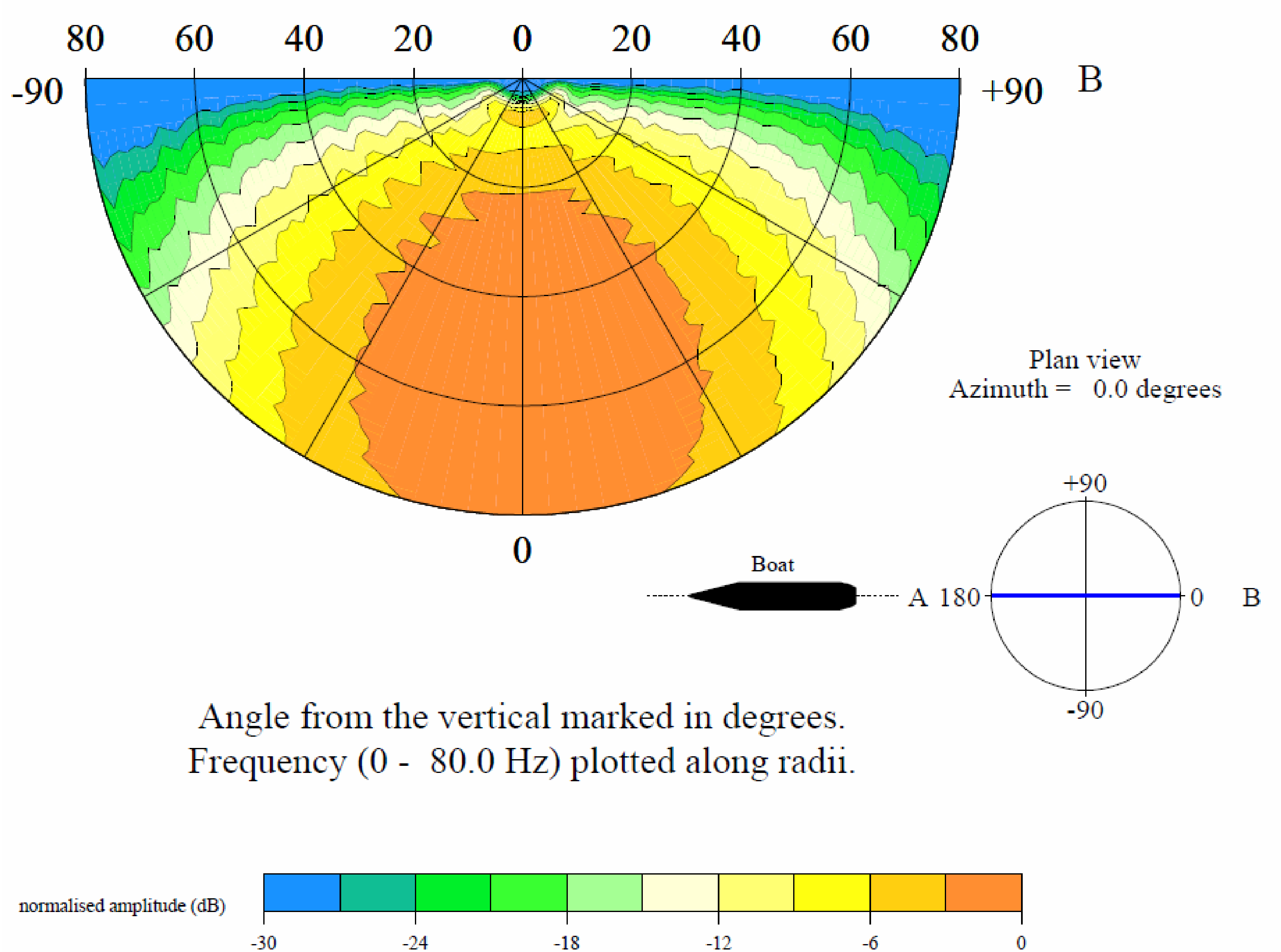

Source: PGS (Nucleus)

Amplitude variations with azimuth

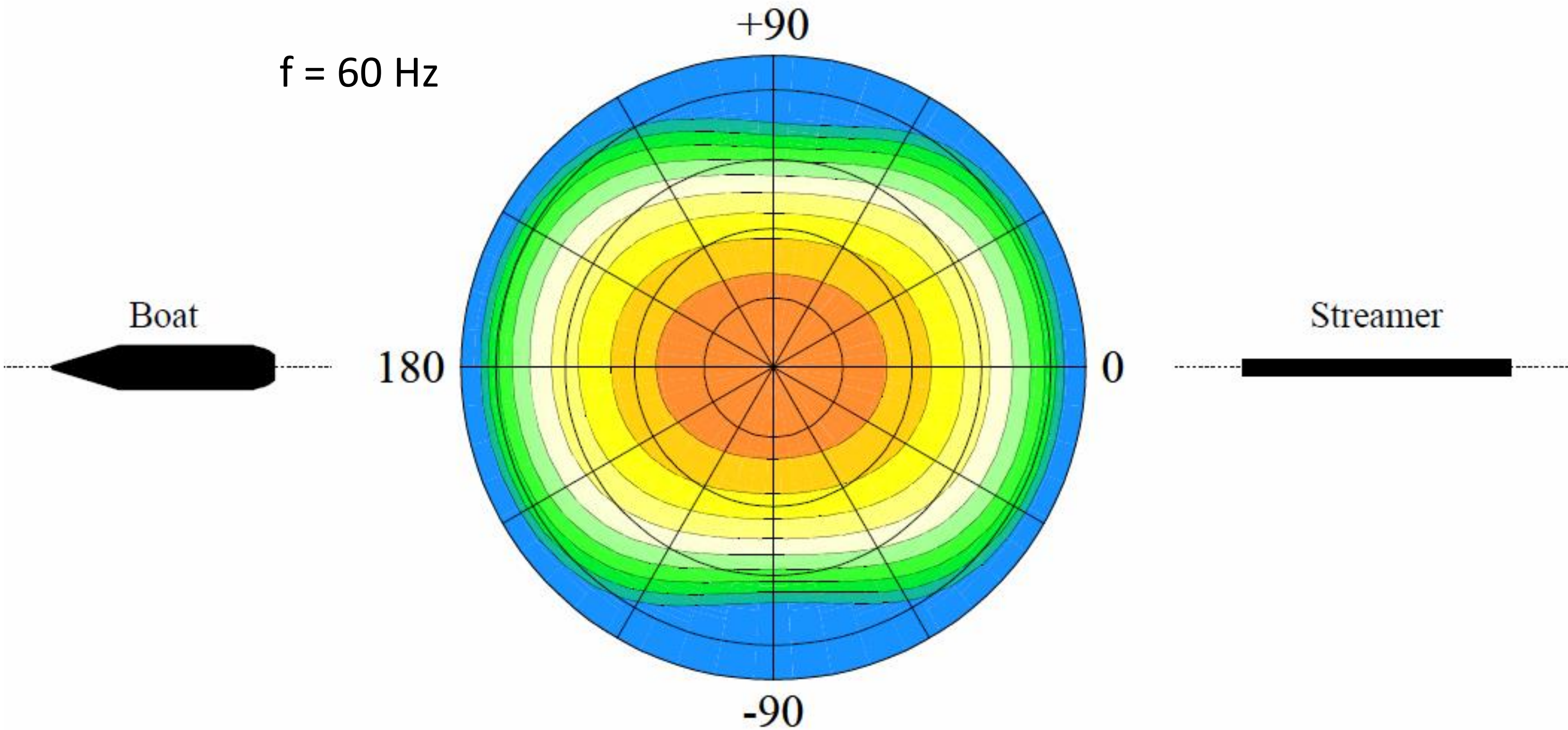

Source: PGS (Nucleus)

Superlong arrays are used to focus energy vertically

Array length L

Ghost effect

$$|\phi| = \frac{\sin\left(\dfrac{\pi f L \sin\theta}{C}\right)}{\left(\dfrac{\pi f L \sin\theta}{C}\right)} \sin\left(\frac{2\pi f z_s \cos\theta}{C}\right)$$

Hossein Mehdi Zadeh, PhD thesis, NTNU, 2011

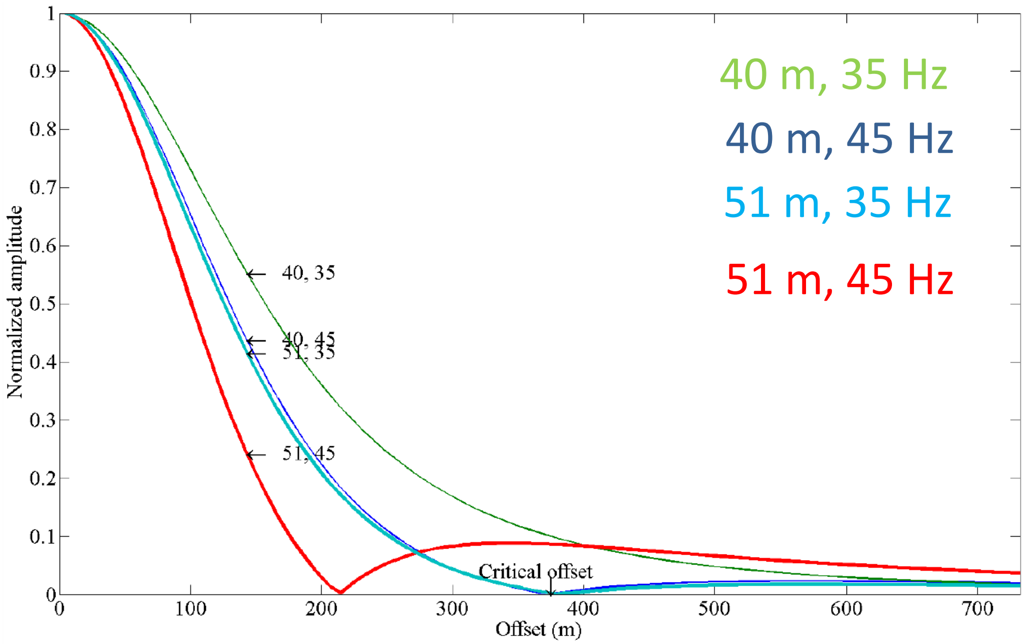

Finite difference modeling of single gun and long array (L)

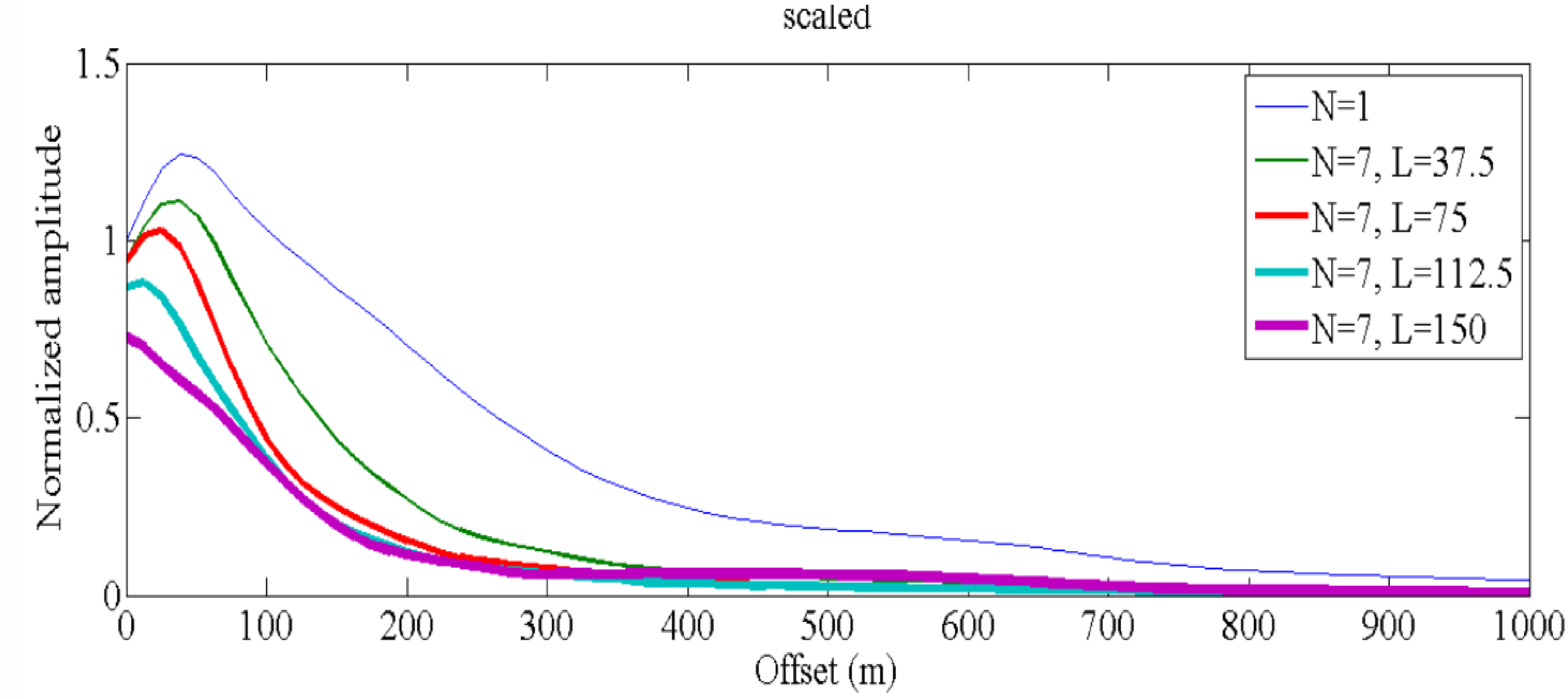

Source: H. M. Zadeh, PhD thesis, NTNU 2011

EXTENDED ARRAYS FOR MARINE SEISMIC ACQUISITION

GEOPHYSICS, VOL. 43, NO. 1 (FEBRUARY 1978)

J. H. LOFTHOUSE* AND G. T. BENNETT*

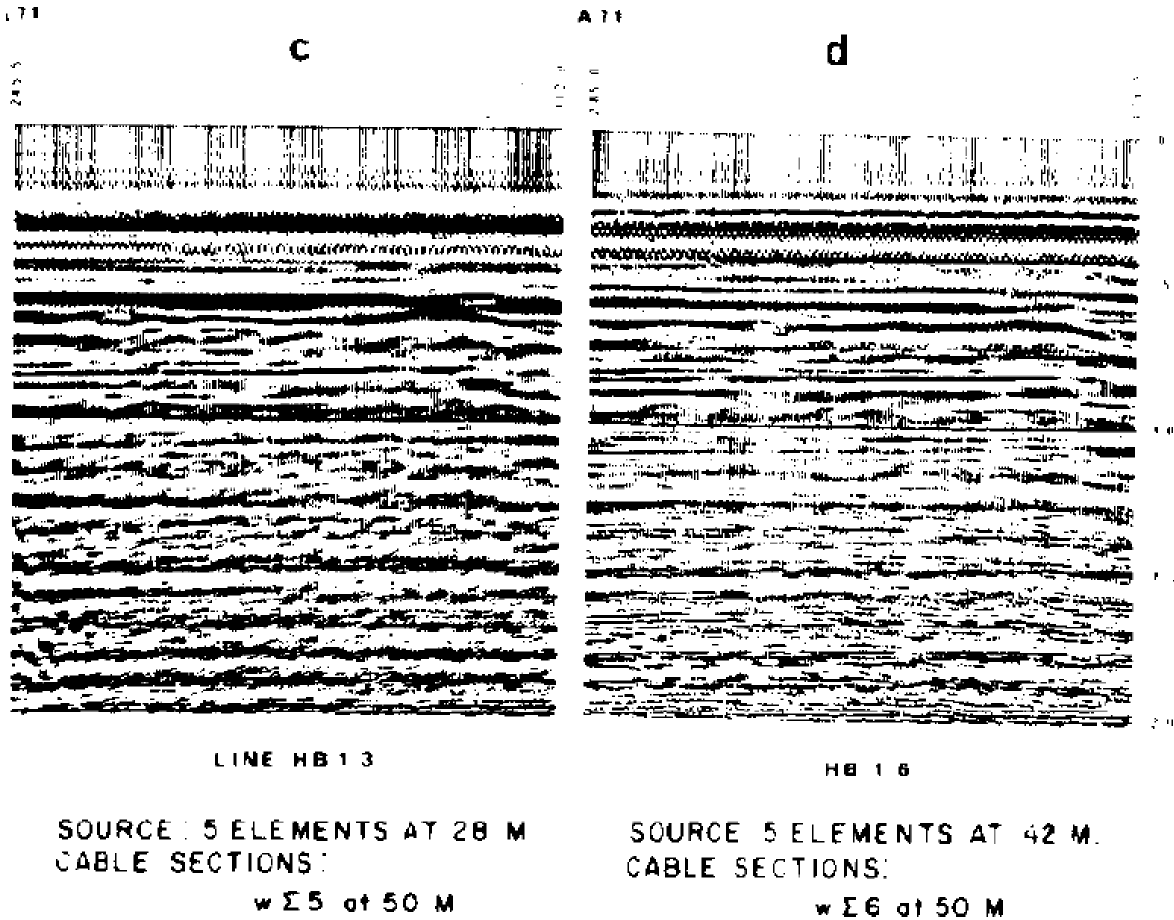

Superlong arrays are worse for shallow targets – improved for deeper

Vertical and directional far-field signatures & spectra

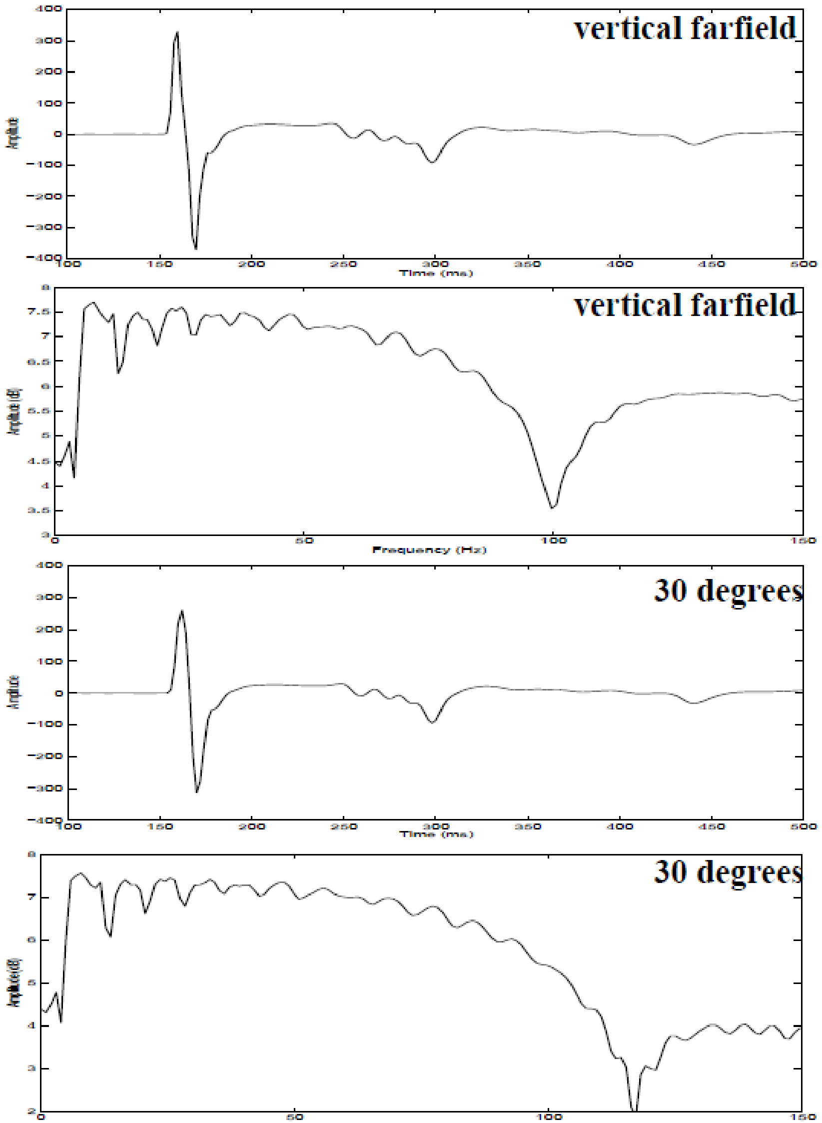

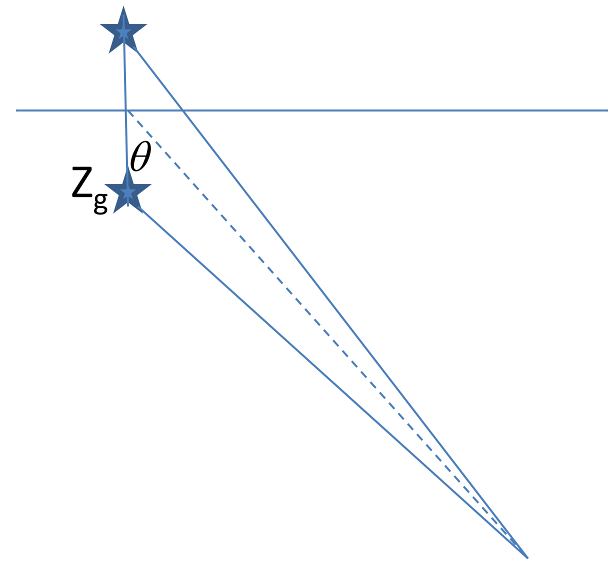

$$f_N = \frac{c}{2z_g \cos\theta}$$

Notch fequency increases with observation angle

PGS electrical marine vibrator, 2005

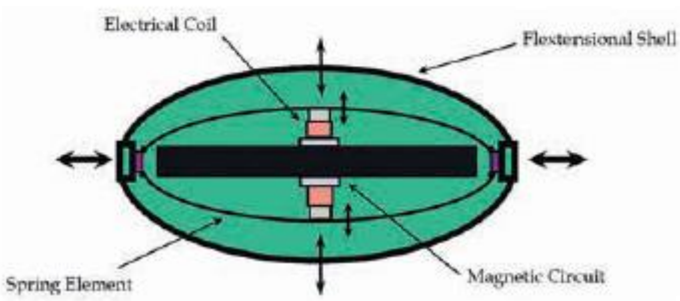

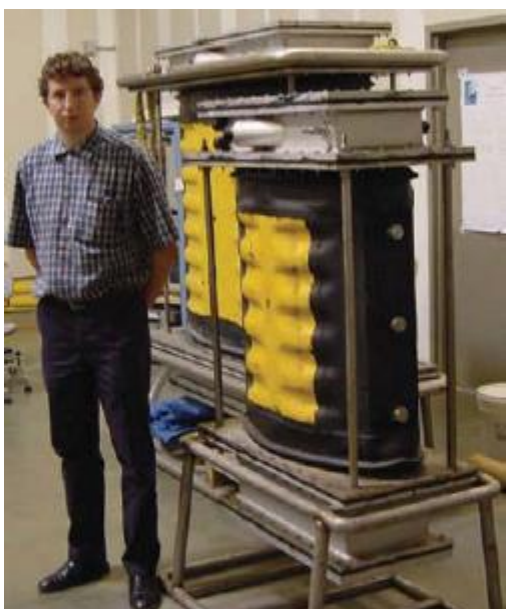

Figure 3: Triton and Subtone marine vibrators.

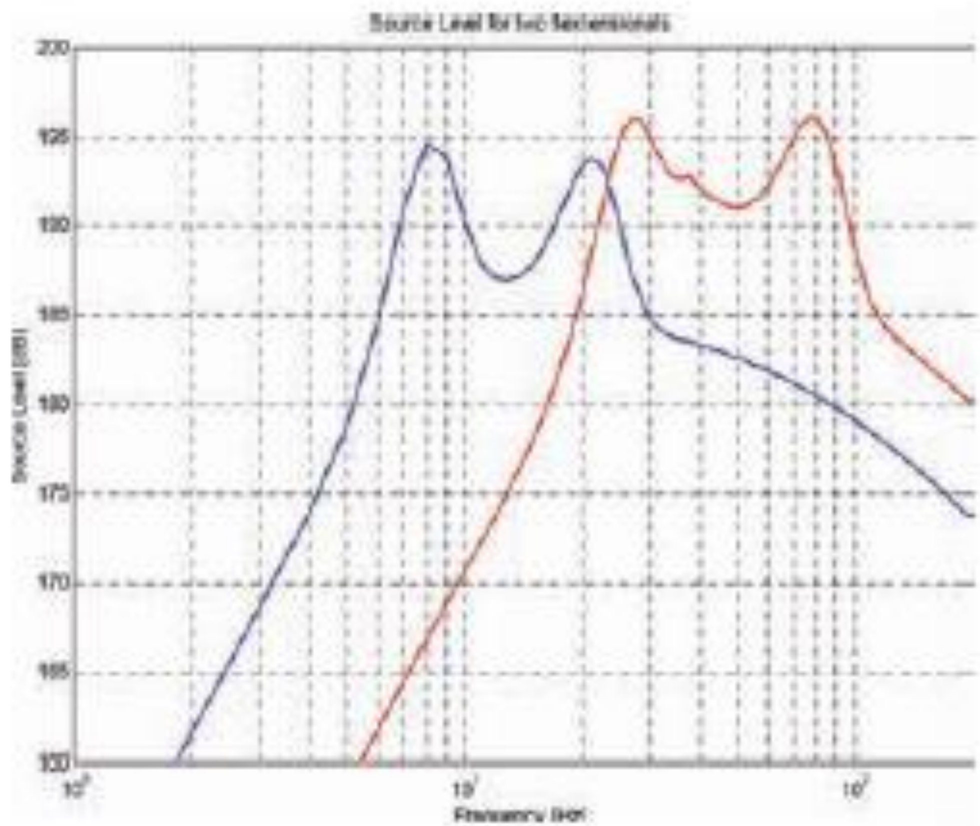

Figure 2: The combination of the amplitude spectra for the Subtone (low frequency) and Triton (high frequency) vibrator sources.

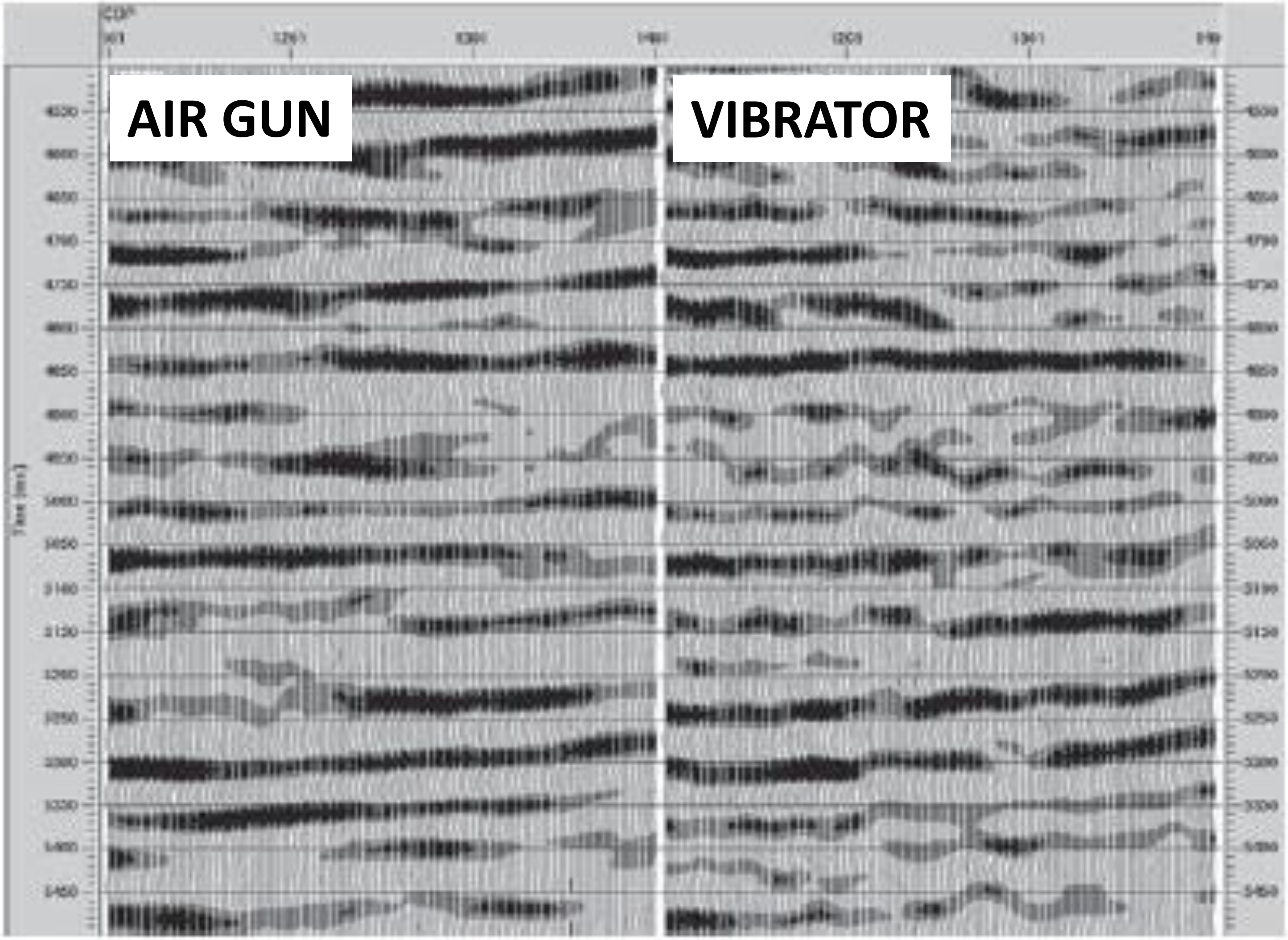

Figure 6: Migrated sections (deep) for an airgun source (left) and a marine vibrator source. The phase of the vibrator source section has been matched to the airgun data for comparison.

Source: PGS

Time slice comparison – vibrator versus dynamite

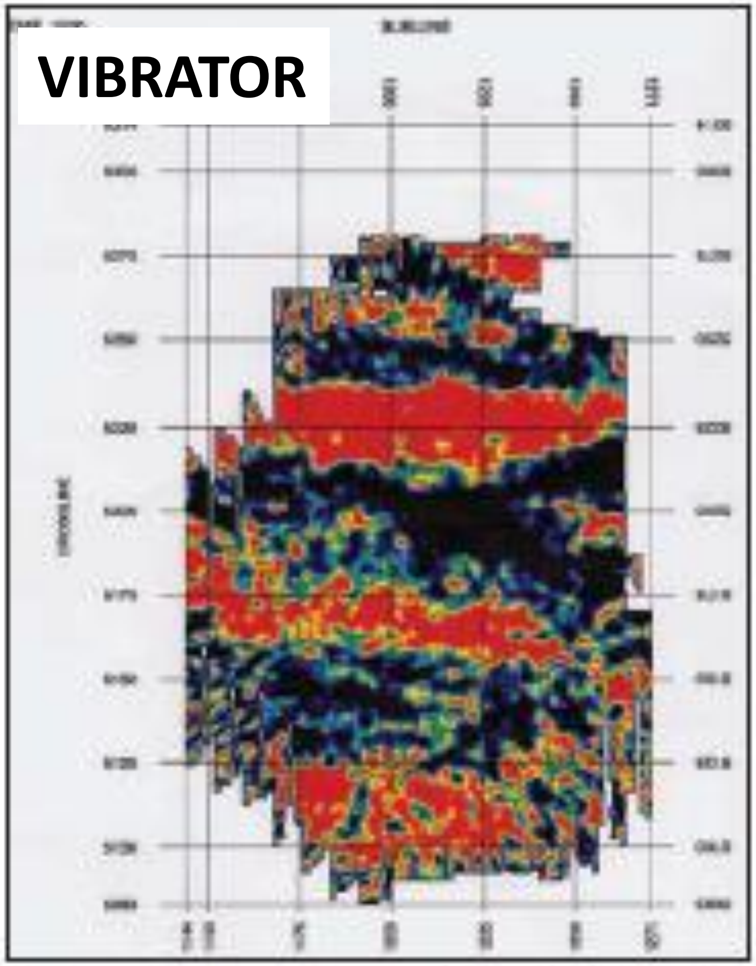

Figure 8: Time slice at 1.5 s TWT for the marine vibrator 3D migrated volume.

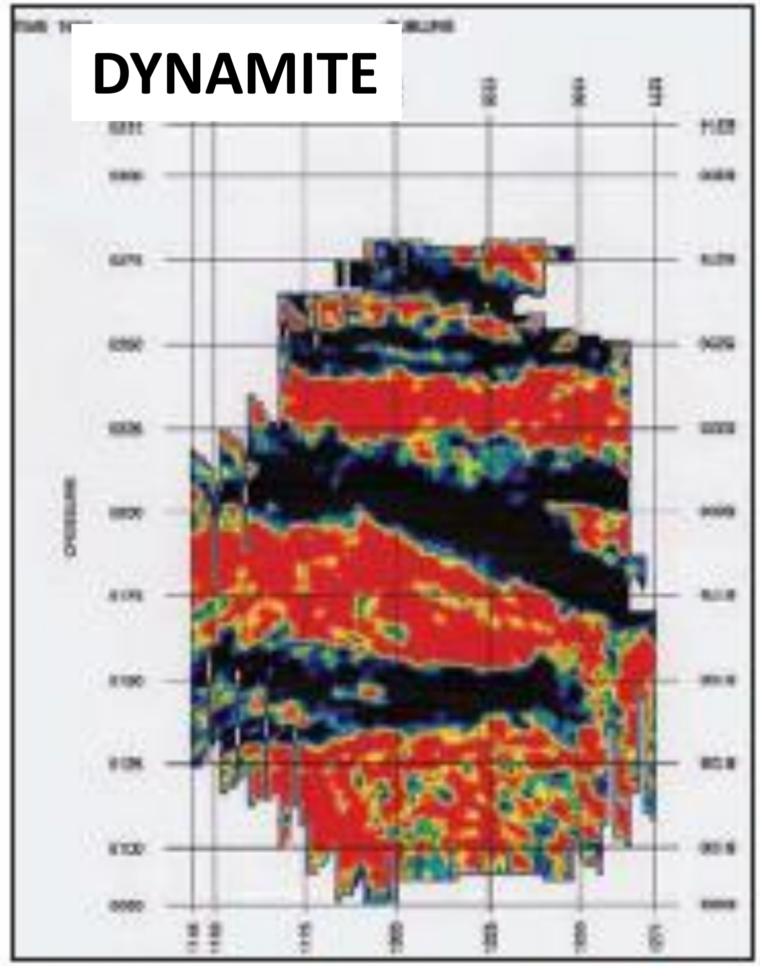

Figure 9: Time slice at 1.5 s TWT for the dynamite 3D migrated volume.

Source: PGS

Marine vibrators and the Doppler effect

Dragoset, Geophysics, 1988

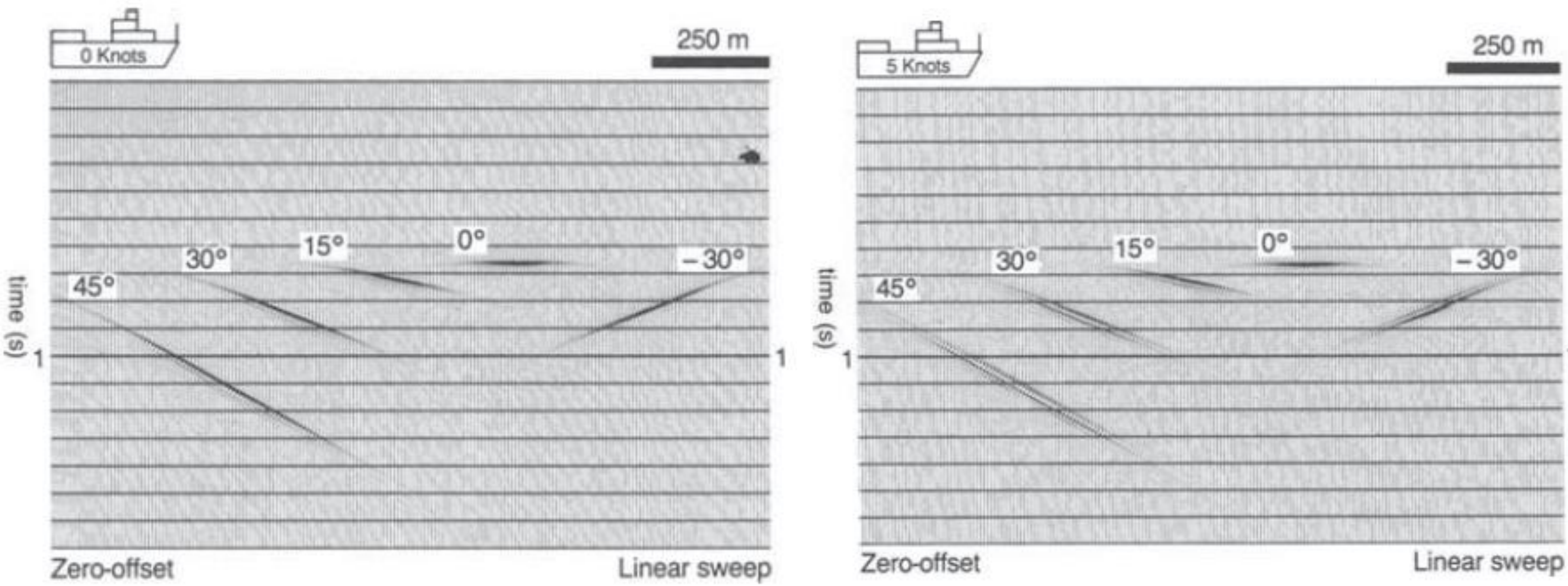

$$f_r = f_s(1 + \delta).$$

$$\delta = \mathbf{k} \cdot \mathbf{V}/V_p, \tag{4}$$

where **V** is the relative velocity of a source and receiver, **k** is a unit vector along the line joining the source and receiver, and V_p is the speed of sound in the medium.

Phase:

$$\phi(f) = 360°\delta T f^2/(f_2 - f_1).$$

Dragoset, Geophysics, 1988

Correcting for Doppler effect

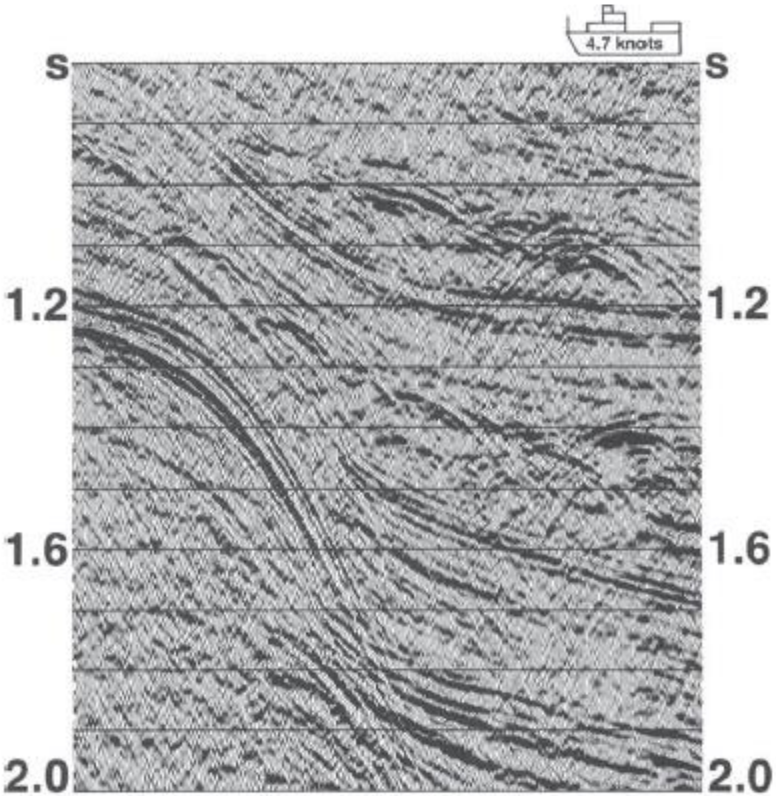

Before phase correction

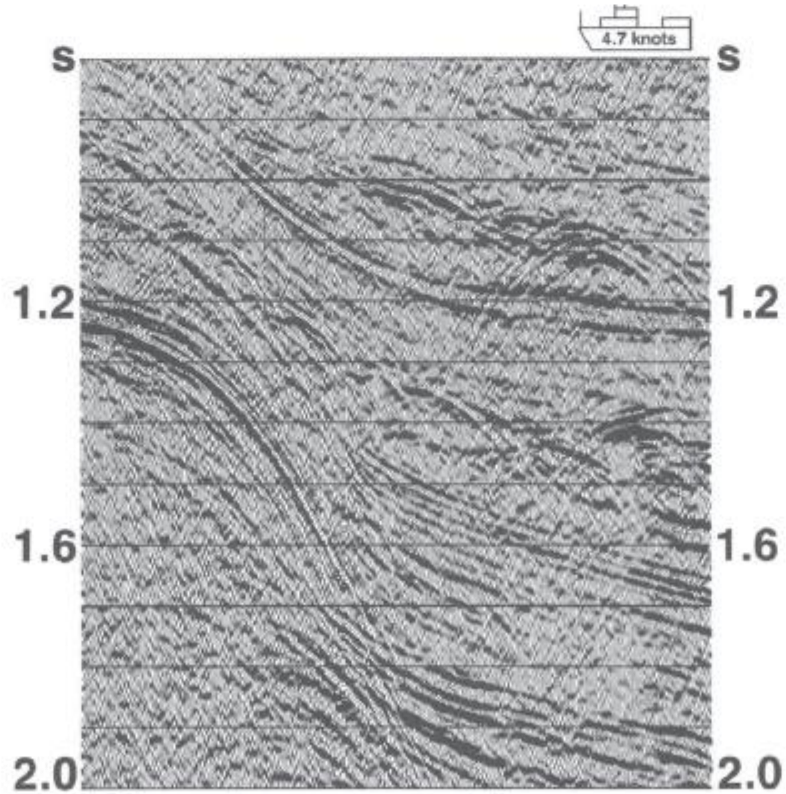

After phase correction

Dragoset, Geophysics, 1988

Comparing marine vibrator and air gun data

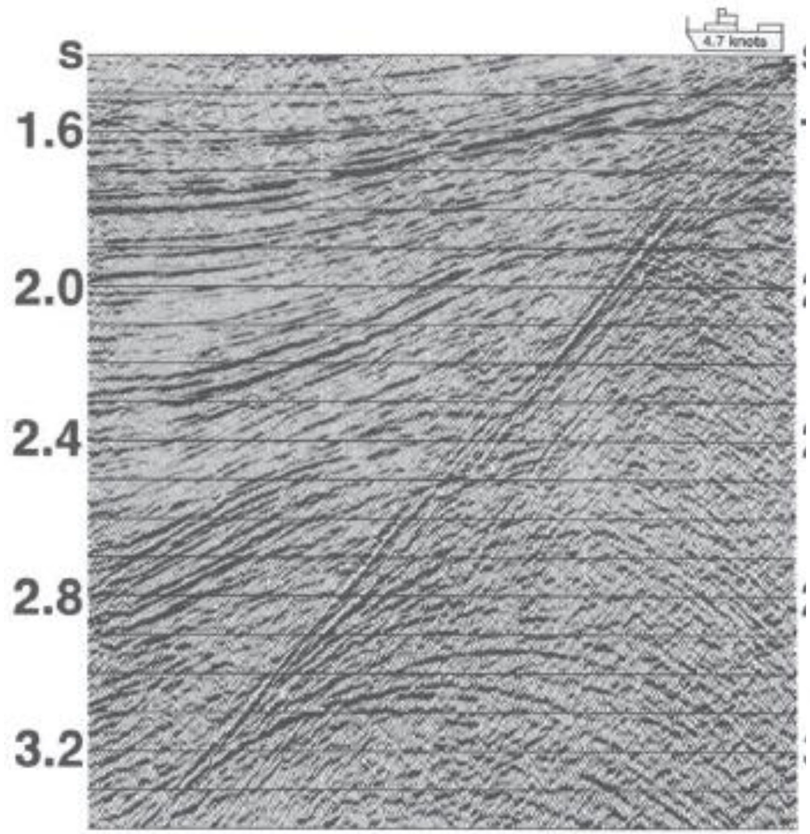

After phase correction

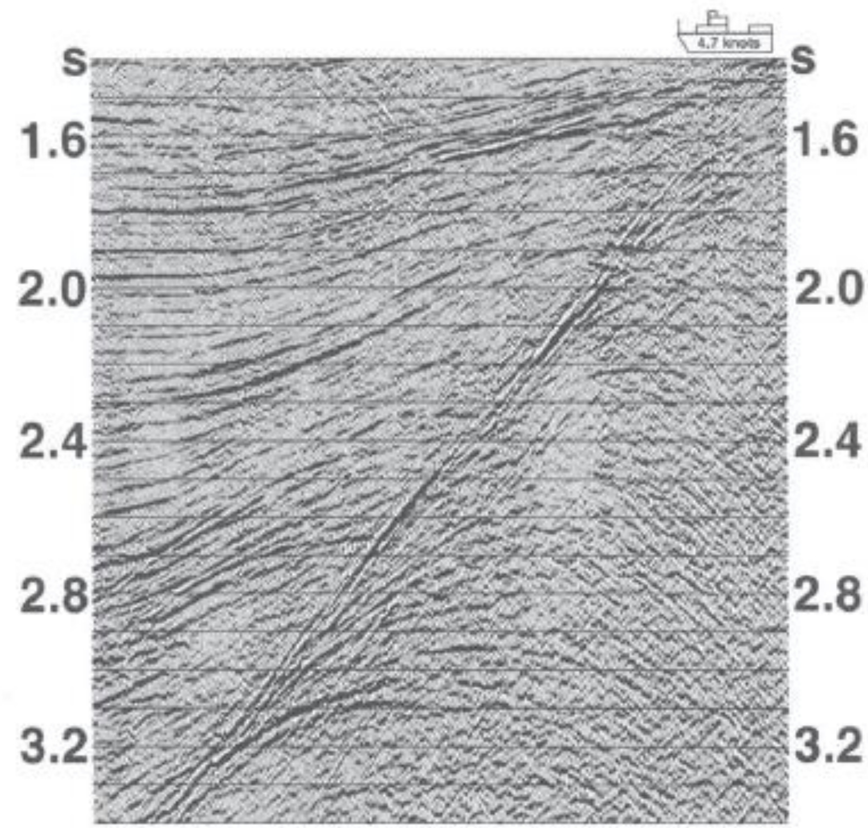

Air gun data

Dragoset, Geophysics, 1988

Low frequencies

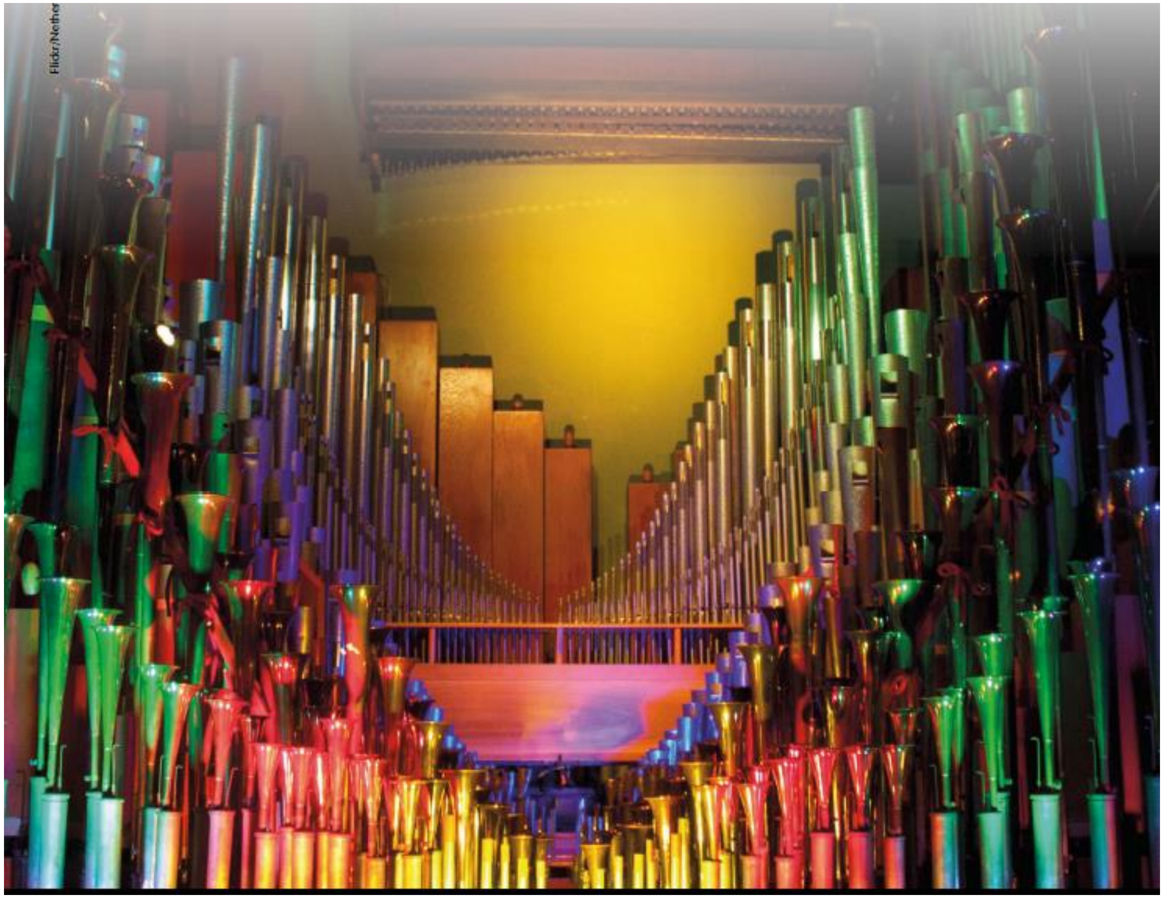

Why so difficult to make low frequency

- Free surface effect – strong for low frequency

- Limit on volume and pressure: $T \propto \dfrac{P^{1/3}V^{1/3}}{P_h^{5/6}}$

- Vibrators will be big as well

600 cubic inch (both), 6 m depth

Hopperstad et al. EAGE 2012

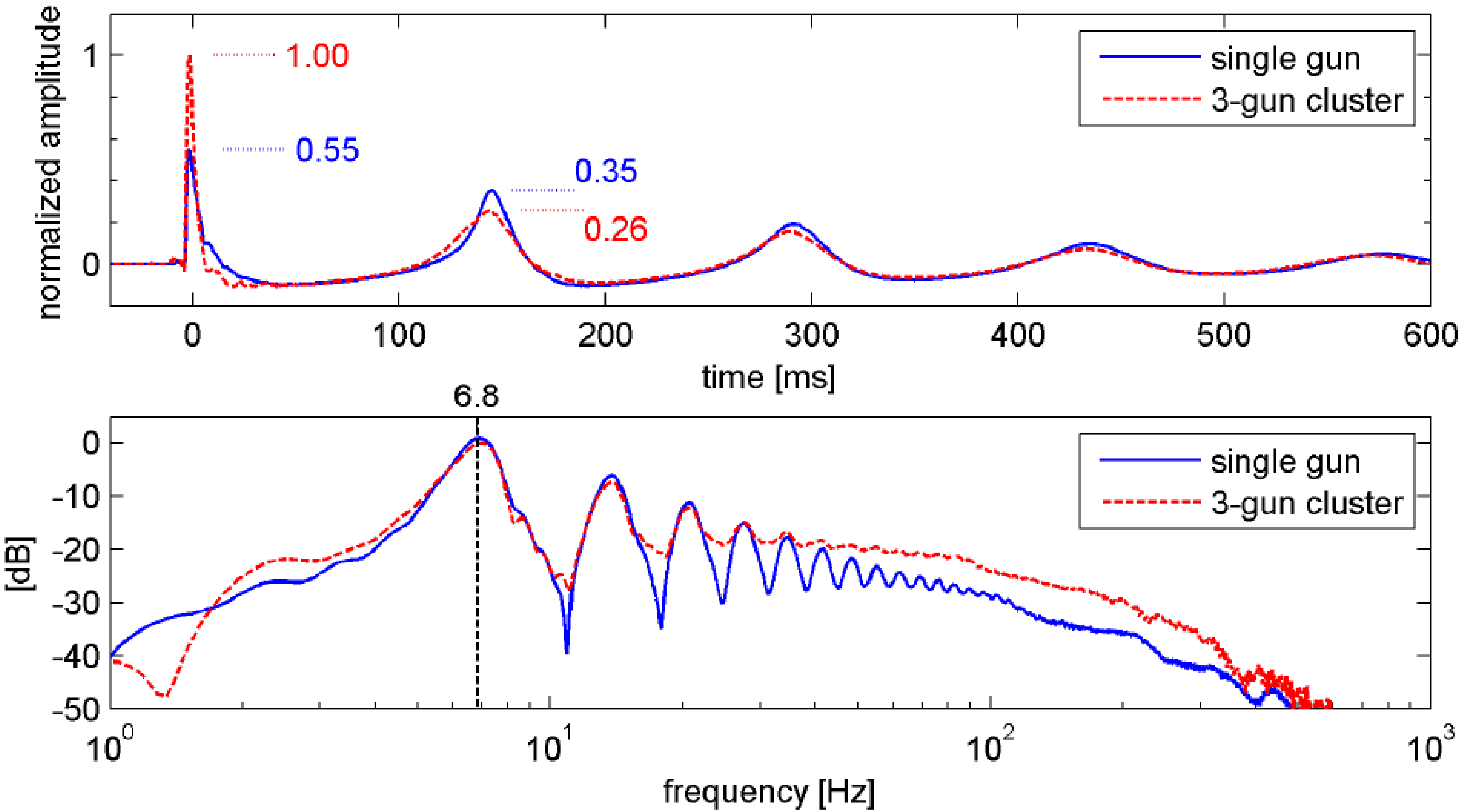

Near field measurements – note that 3-gun cluster gives slightly more energy around 2-4 Hz

Airgun hyperclusters, *Hopperstad et al. EAGE 2012*

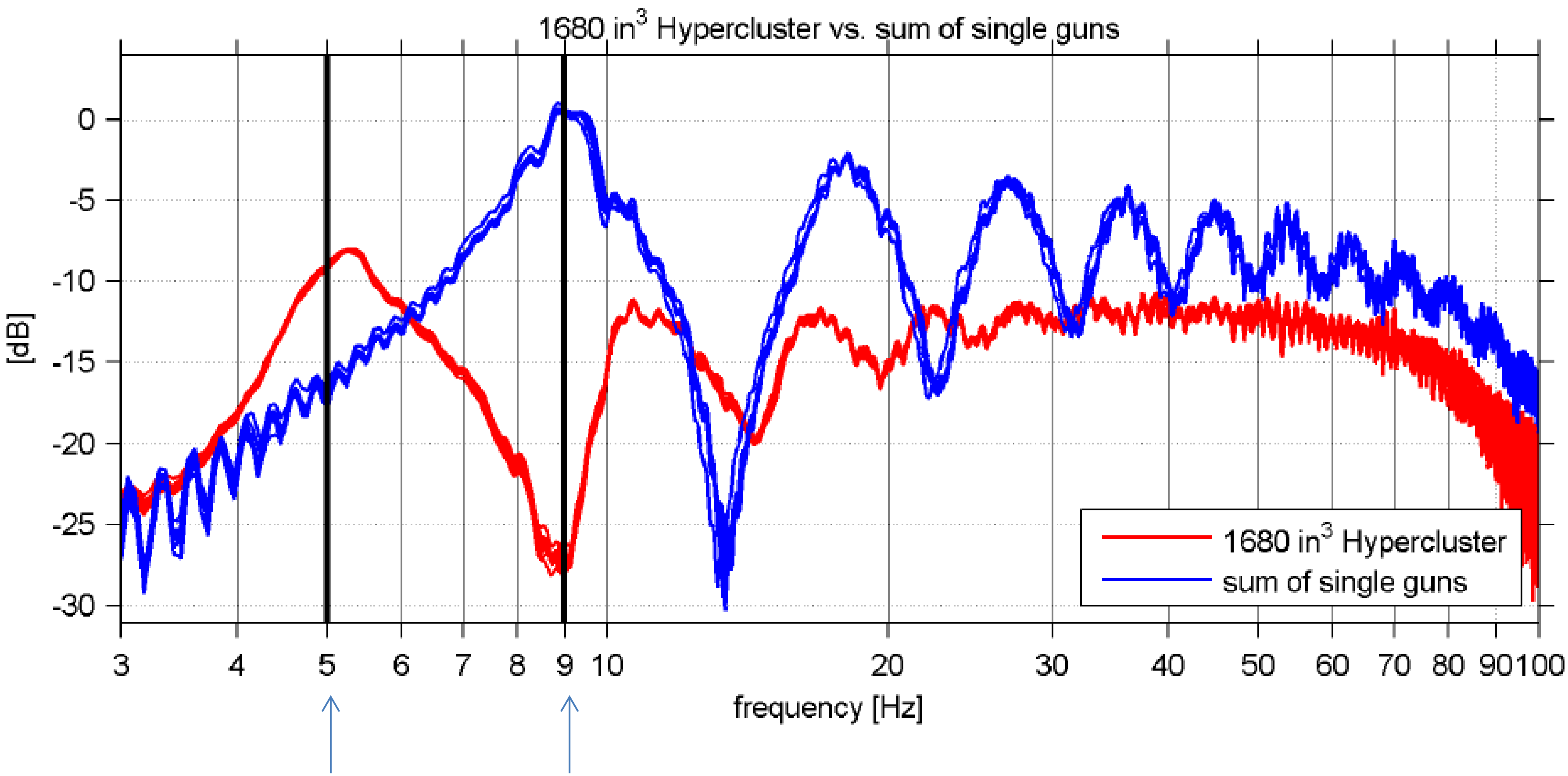

Theoretical bubble frequecies fit nicely with measured data

Gunnerus test –February 2009 Trondheimsfjorden

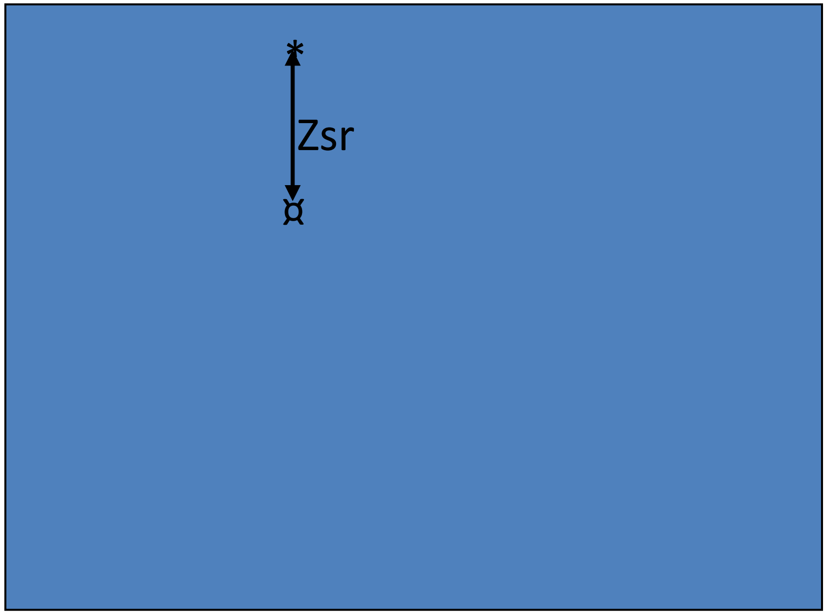

The source depth is varied from 3 to 40 m, and the distance between the source and the hydrophone is kept constant: Zsr = 20m. Water depth is ~300 m .

Source volume: 600 cubic inch Bolt
Firing pressure: 2000 psi

TC4047 hydrophone

Firing a 600 cubic inch air gun creates a big bubble:

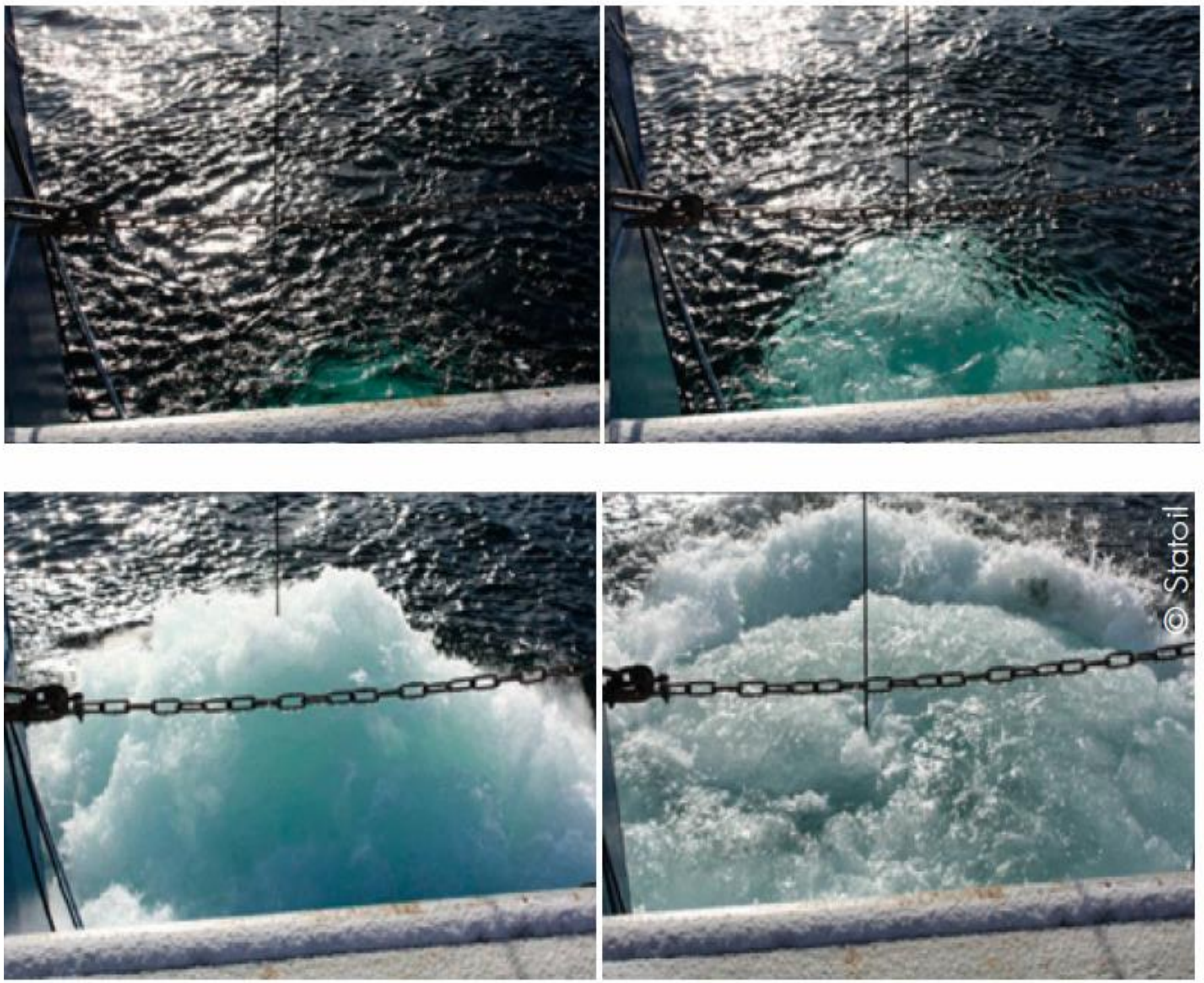

Bubble is not perfectly sperical

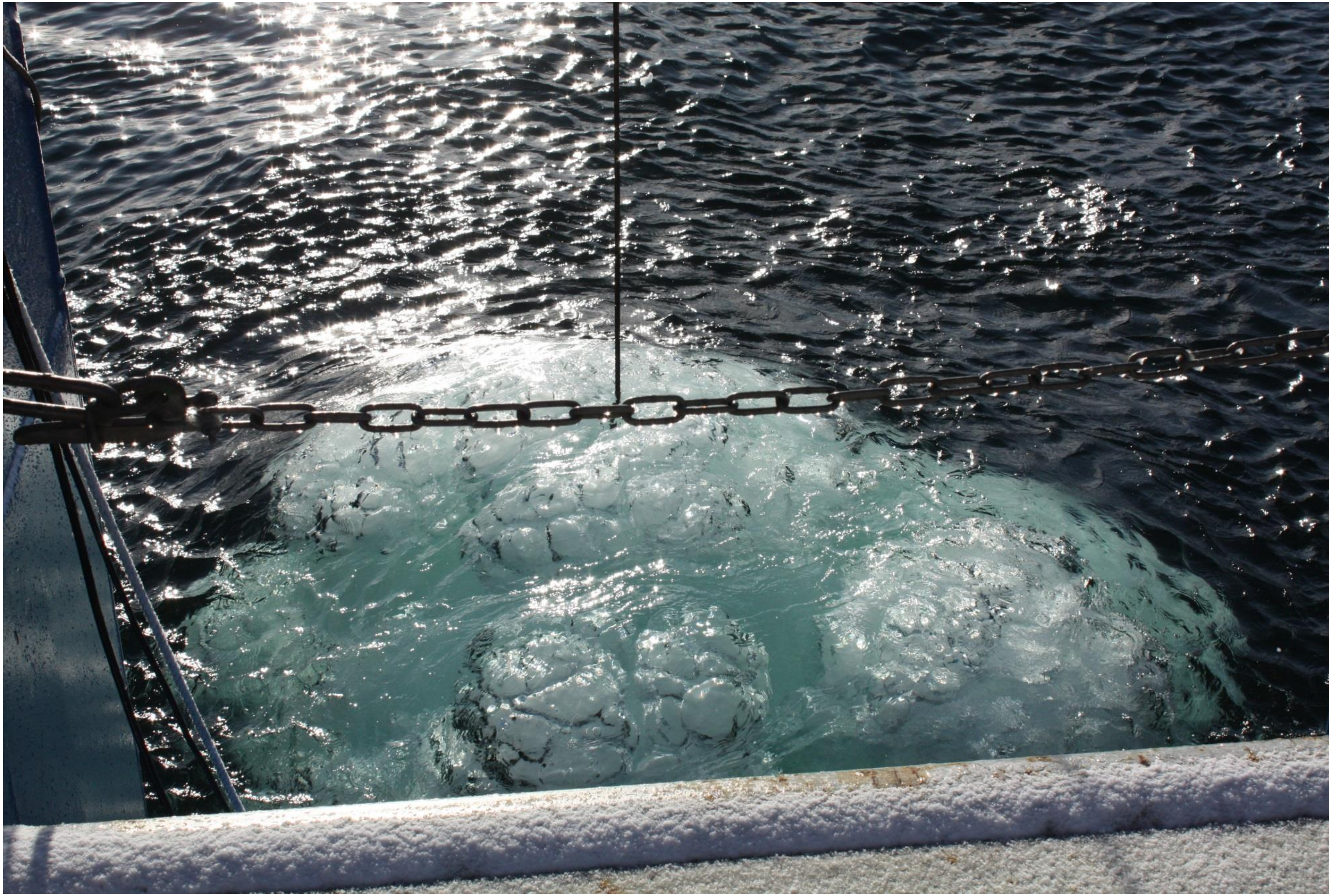

Band pass filtered (0-2-30-50 Hz) signatures

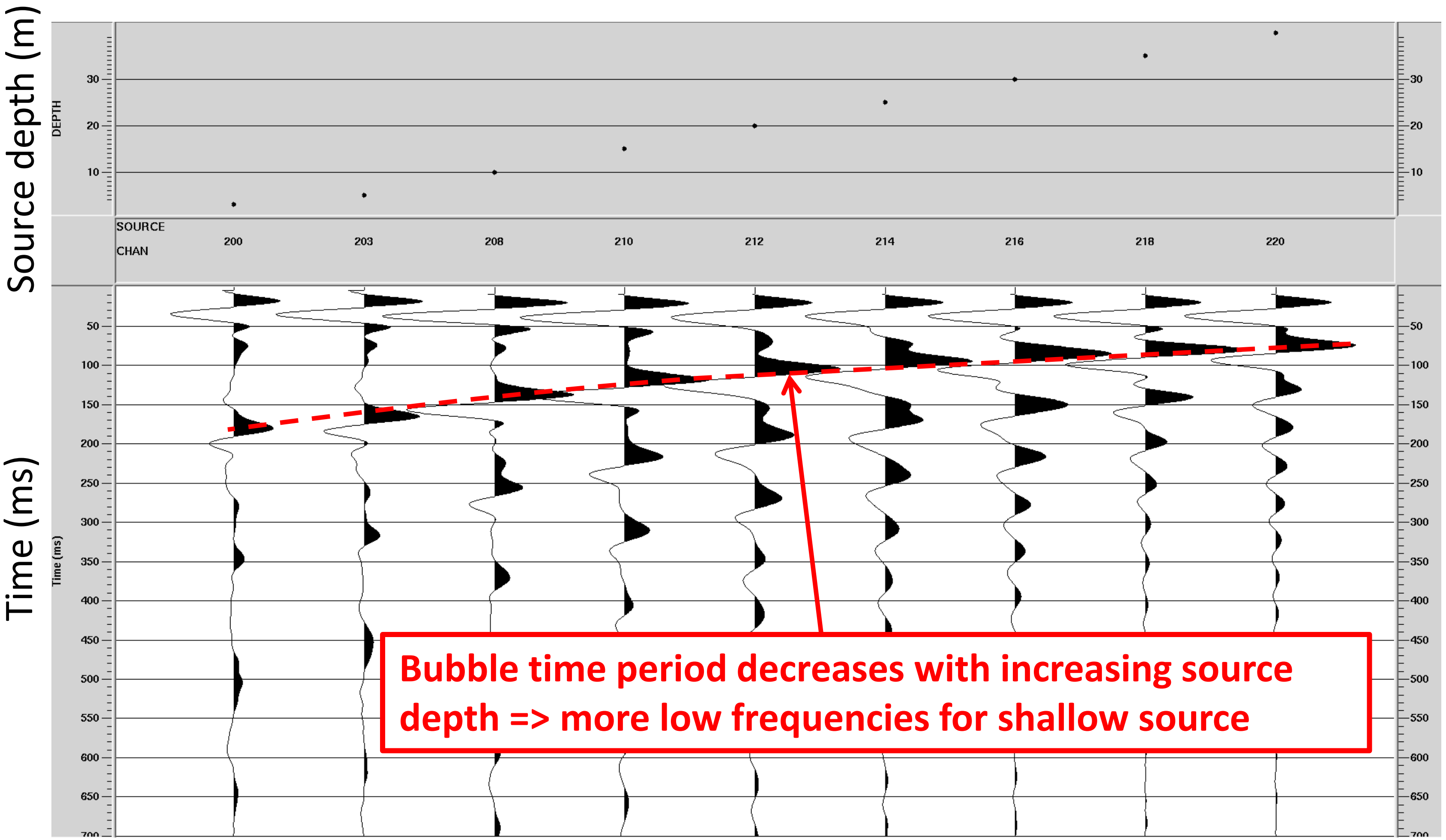

Notice: no damping between first and second bubble – then pronounced damping

Farfield spectra for various source depths

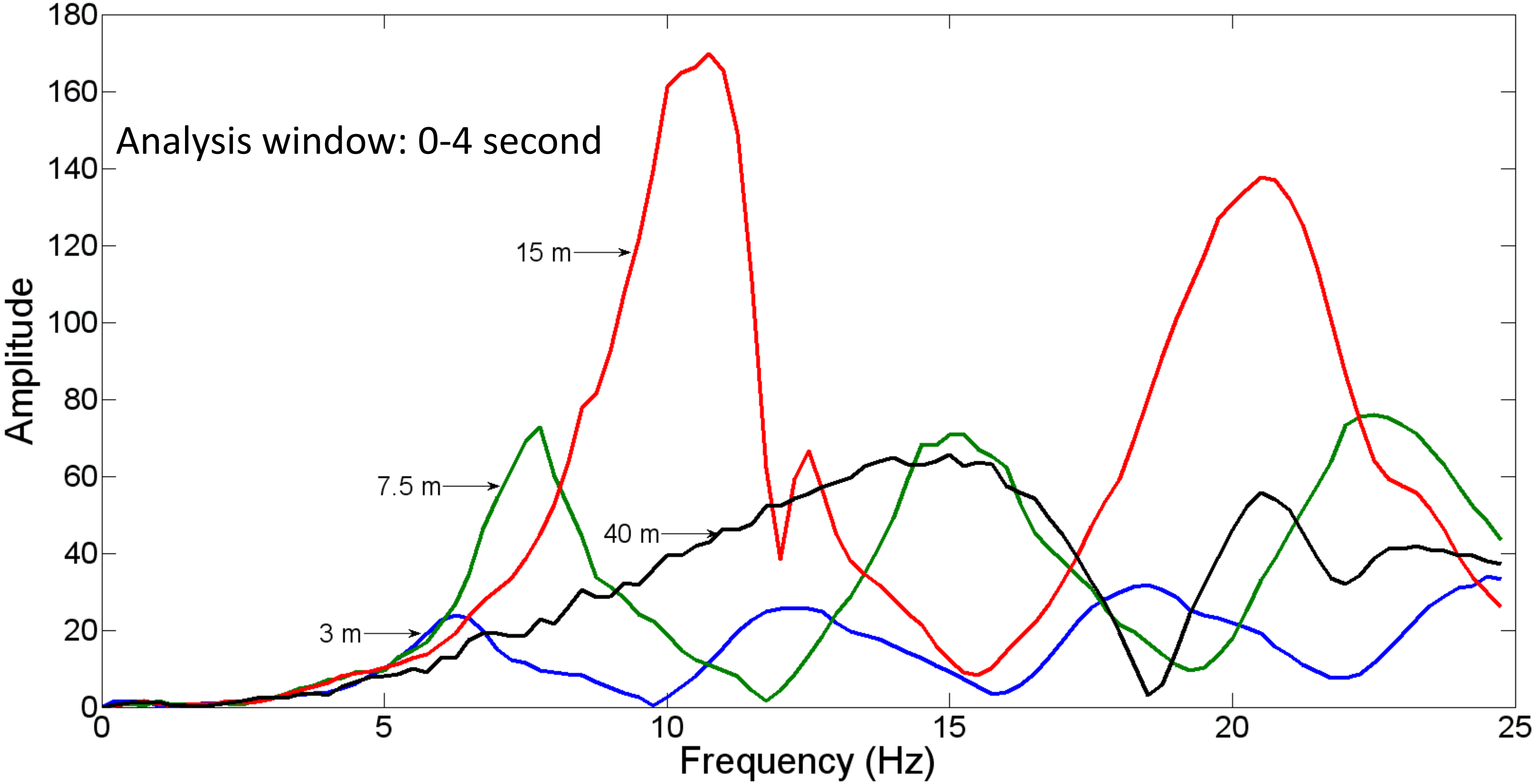

The data has been deghosted and THEN ghosted to estimate the farfield signature

Maxima occurs for f=n/(bubble time period), n=1,2,3..

Scaled farfield spectra for various source depths

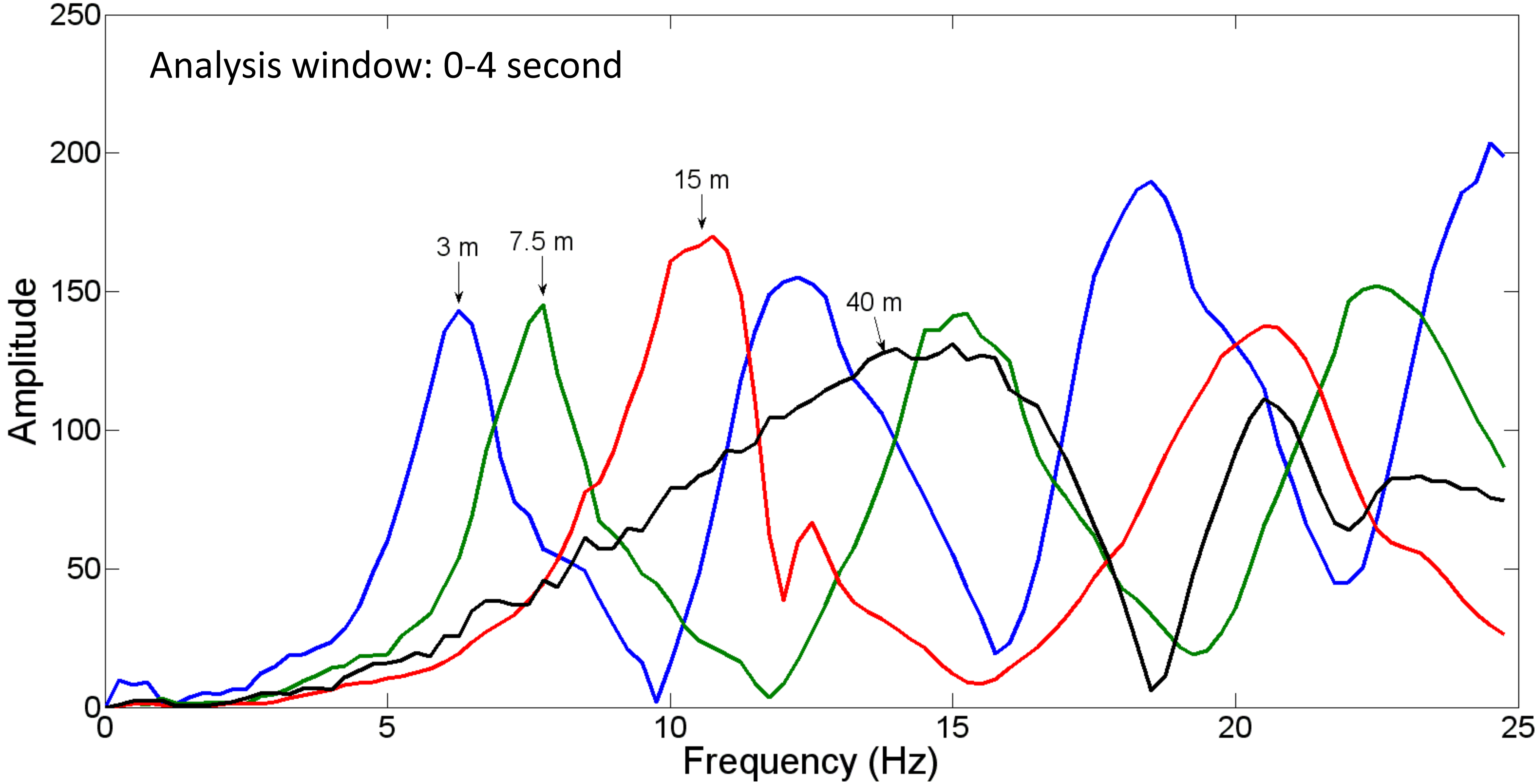

3 m: scaled by 6

7.5 m scaled by 2

15: no scaling

40 m : scaled by 2

Estimated notional source spectra for various source depths (0-4 s)

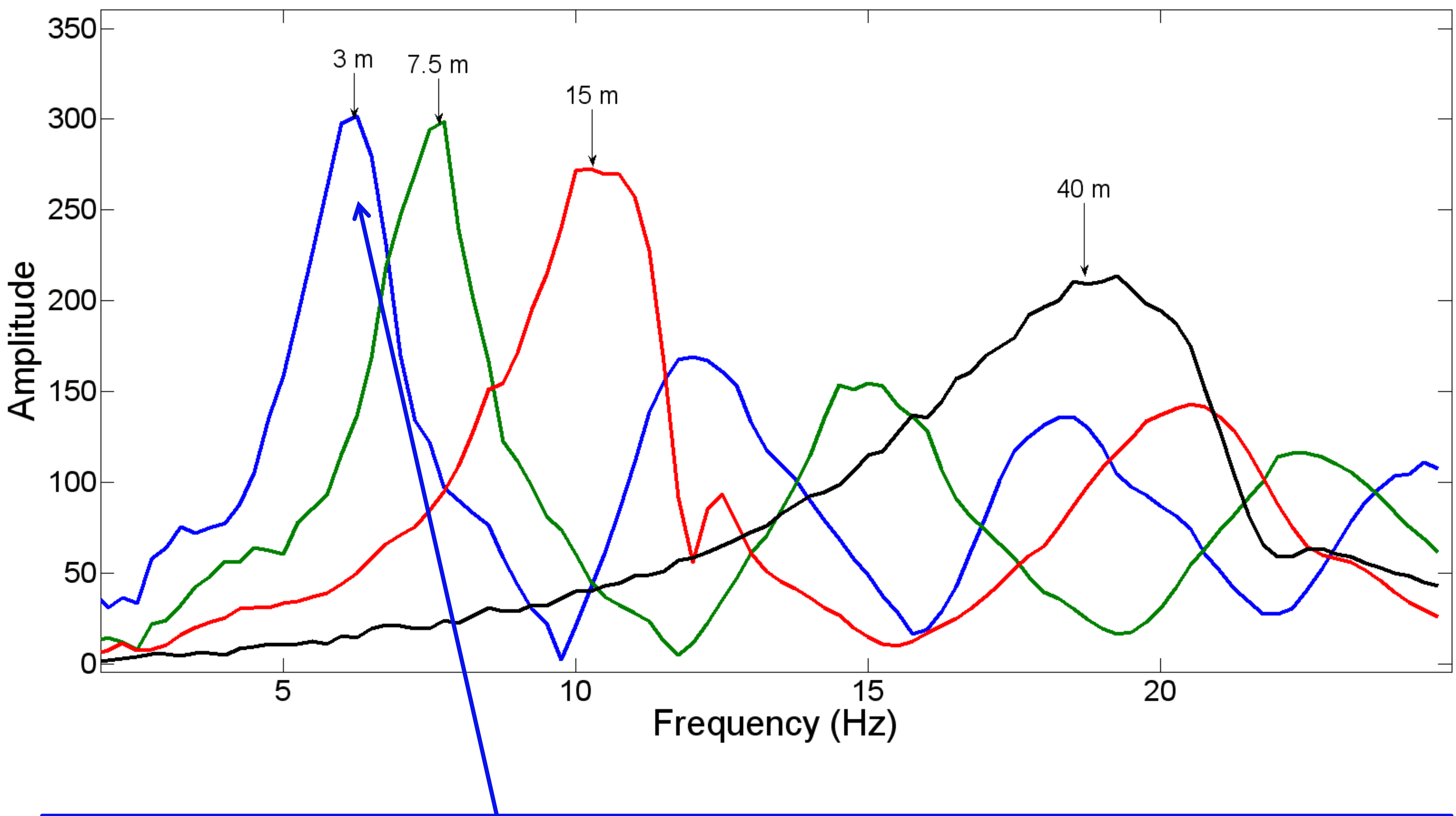

Bubble time period for 3 m source depth = 0.16 s => f = 1/0.16 Hz = 6.25 Hz